

4C Model description



Petra Lasch-Born¹, Felicitas Suckow¹, Franz-W. Badeck², Jörg Schaber³, Harald Bugmann⁴, Cornelia Fürstenau⁵, Martin Gutsch¹, Chris Kollas⁶, Christopher P. O. Reyer¹

1 *Potsdam Institute for Climate Impact Research,
P.O. Box 601203, D-14412 Potsdam, Germany*

2 *Research Centre for Genomics and Bioinformatics, Council for Agricultural Research and Economics, via S. Protaso, 302, I-29017 Fiorenzuola d'Arda PC, Italy*

3 *EXCO GmbH, Adam-Opel-Str- 9-11, D-67227 Frankenthal, Germany*

4 *Dept. of Forest Sciences, Swiss Fed. Inst. of Technology,
ETH-Zentrum HG G21.3, CH-8092 Zuerich, Switzerland*

5 *Friedrich-Schiller-Universität Jena, Institut für Informatik, Heinz Nixdorf Chair for Distributed Information Systems, Ernst-Abbe-Platz 1-4, D07743 Jena, Germany*

6 *German Federal Institute for Risk Assessment, Unit 43: Epidemiology, Zoonoses and Antimicrobial Resistance, Department Biological Safety, Max-Dohrn-Straße 8-10, D-10589 Berlin, Germany*

Potsdam, 2018

DOI: 10.2312/pik.2018.006



POTSDAM INSTITUTE FOR
CLIMATE IMPACT RESEARCH

CONTENTS

Contents	2
Figures	6
Tables	8
1 Overview	10
2 Stand structure	14
2.1 Canopy structure, foliage distribution	14
2.2 Tree architecture/ geometry	15
2.3 Root system	16
2.3.1 Root distribution.....	16
2.3.2 Root depth.....	17
2.4 Stand initialisation	17
2.4.1 Initialisation using averaged stand data.....	17
2.4.2 Initialisation using single tree data	25
2.4.3 Initialisation of saplings.....	26
3 Environment	28
3.1 Climate	28
3.2 Potential evapotranspiration	28
3.2.1 Penman-Monteith.....	28
3.2.2 Priestley-Taylor	29
3.2.3 Turc-Ivanov.....	29
3.2.4 Haude.....	30
3.3 CO₂ concentration	31
3.4 Nitrogen deposition	31
3.5 Light absorption	32
3.5.1 Light model 1 (LM1)	33
3.5.2 Light model 2 (LM2)	35
3.5.3 Light model 3 (LM3)	37
3.5.4 Light model 4 (LM4)	40
4 Dry matter production and growth	50
4.1 Phenology	50
4.1.1 Promotor-Inhibitor-Model.....	50
4.1.2 The Cannel and Smith model (CSM).....	54
4.1.3 The linear temperature sum model (TSM)	55
4.2 Photosynthesis	56
4.2.1 The assimilation model at the leaf and canopy level	56
4.2.2 Nitrogen demand.....	58
4.2.3 Water limitation.....	59
4.2.4 Nitrogen limitation.....	59
4.3 Autotrophic respiration	62

4.4	Allocation and growth	62
4.4.1	Determination of the partitioning coefficients	63
4.4.2	Height growth	67
4.4.3	Diameter growth.....	68
4.4.4	Root biomass	70
4.4.5	Sapling growth	70
5	Water processes.....	73
5.1	Actual evapotranspiration.....	73
5.2	Interception.....	73
5.3	Transpiration	74
6	Soil processes	75
6.1	Soil water balance	75
6.1.1	Percolation	75
6.1.2	Snow water.....	76
6.1.3	Water uptake by roots	76
6.2	Soil heat balance	78
6.2.1	Heat conduction equation.....	78
6.2.2	Thermal conductivity.....	78
6.2.3	Heat capacity	81
6.2.4	Soil surface temperature.....	82
6.3	Soil carbon and nitrogen budget	82
6.3.1	Carbon and nitrogen input	82
6.3.2	Carbon and nitrogen turnover.....	83
6.3.3	Reduction of mineralisation and nitrification	85
6.3.4	Transport of nitrogen.....	87
6.3.5	Nitrogen uptake.....	88
7	Mortality and senescence	89
7.1	Age related (intrinsic) mortality	89
7.2	Stress induced mortality.....	89
7.3	Senescence	91
8	Regeneration.....	92
8.1	Seed rates.....	92
8.2	Establishment of seedlings	92
8.3	Growth of seedlings.....	93
8.4	Mortality of seedlings.....	93
8.5	Ingrowth into the tree layer	93
9	Forest management.....	94
9.1	Thinning.....	94
9.2	Harvesting	94

9.3	Planting	95
9.4	Short rotation coppice.....	96
9.5	Timber assortment.....	98
9.6	WPM and SEA.....	101
9.6.1	Main processes of the WPM.....	102
9.6.2	Results of the WPM.....	103
9.6.3	WPM for Brandenburg.....	104
9.6.4	Spin up for WPM.....	105
9.6.5	Socio economic analysis (SEA)	105
10	Disturbances	108
10.1	Mistletoe	108
10.2	Pests	109
10.2.1	Defoliation	110
10.2.2	Fine root damage	111
10.2.3	Xylem damage.....	111
10.2.4	Phloem feeding	111
10.2.5	Stem rot.....	111
10.3	Carbon flows from the C-reserve within disturbance simulations	111
11	Climatic and risk indices.....	113
11.1	Forest Fire Index (Käse)	113
11.2	Bruschek-Index.....	115
11.3	Nesterov-Index.....	115
11.4	Nun moth risk index	116
11.5	Climatic and continentality indices.....	118
11.5.1	Index according to Coutange	118
11.5.2	Index according to Wissmann	119
11.5.3	Index according to De Martonne.....	119
11.5.4	Aridity Index.....	119
11.5.5	Climatic water balance	120
11.5.6	Index according to Emberger	120
11.5.7	Index according to Lang.....	121
11.5.8	Reichel Index.....	121
11.5.9	Weck Index.....	122
11.5.10	Budyko radiaton index.....	122
11.5.11	Seljaninov Index	122
11.5.12	Continentality Index according to Gorczynski.....	123
11.5.13	Continentality Index according to Currey	123
11.5.14	Continentality Index according to Conrad	124
11.6	Late frost danger indices	124
11.7	Climatic characteristics.....	125
12	References.....	126
Appendix	1

Appendix 1 List of variablesError! Bookmark not defined.
Appendix 2 List of model parametersError! Bookmark not defined.
Appendix 3 List of Species Parameters**24**
Appendix 4 Classification of the forest typeError! Bookmark not defined.
Appendix 5 Abbreviations.....Error! Bookmark not defined.

FIGURES

Figure 1-1 General structure of the model 4C.....	11
Figure 2-1 Tree geometry in 4C, $H_{dbh}=137$ cm.....	16
Figure 2-2 Relative share of root biomass in different depths for temperate deciduous and coniferous trees as cumulative and absolute fraction.....	17
Figure 3-1 Time series of CO_2 concentration of the historical reconstruction, the Mauna Loa series and four climate scenarios.....	31
Figure 3-2 Conceptual scheme of the stand structure in LM1.	33
Figure 3-3 Concept of leaf area distribution and light absorption in LM1. $i_x(j)=i_1(j)=i_2(j)=i_3(j)$, $j=1,2,3,4$	34
Figure 3-4 Conceptual scheme of the stand structure in LM2-LM4.	35
Figure 3-5 Concept of leaf area distribution and light absorption in LM3	37
Figure 3-6 Conceptual scheme of a tree layer cuboid with height z and side length $l_c(j)$. Light falls through the cuboid with inclination β . The areas where light absorption is calculated differently are indicated by different green colours and labelled $f_{c,i}(j)$. The region with yellow colour indicated light from and into the pool $I_p(j)$. Represented is the case $c_p(j) \geq \frac{1}{P_o} \sum_{c=1}^{n_c} l_c(j) \cdot y \cdot n_{o,c}$ and $y \leq l_c(j)$	41
Figure 3-7 Conceptual scheme of a tree layer cuboid. Represented is the case $c_p(j) \geq \frac{1}{P_o} \sum_{c=1}^{n_c} l_c(j) \cdot y \cdot n_o^c$ and $y > l_c(j)$	43
Figure 3-8 Conceptual scheme of a tree layer cuboid. Represented is the case $c_p(j) < \frac{1}{P_o} \sum_{c=1}^{n_c} l_c(j) \cdot y \cdot n_o^c$ and $y \leq l_c(j)$	44
Figure 3-9 Conceptual scheme of a tree layer cuboid. Represented is the case $c_p(j) < \frac{1}{P_o} \sum_{c=1}^{n_c} l_c(j) \cdot y \cdot n_o^c$ and $y > l_c(j)$ with two sub cases: $y - l \leq w$ and $y - l > w$	46
Figure 3-10 Conceptual scheme of a tree layer cuboid. Represented is the case $y - w > w + l$	47
Figure 4-1 Initialisation of species specific nitrogen reduction factor R_N^S of two species with $\kappa_N^{pine} = 0.0062$ for <i>Pinus sylvestris</i> and $\kappa_N^{beech} = 0.0068$ for <i>Fagus sylvatica</i> in dependence of the C/N ratio of active organic matter of soil γ_{aom}	60
Figure 4-2 Nitrogen reduction factor R_N^S in dependence of the ratio of nitrogen uptake to nitrogen demand for the approaches d) to g).....	61
Figure 6-1 Structure of the soil model	75

Figure 6-2 Water resistance functions (left) and the appropriate water uptake (right) of three soil types: ms – pure sand, Su3 - silty sand, and Tl – loamy clay for two types of calculation (bluish lines – type a), reddish lines – type b))77

Figure 6-3 Thermal conductivities, calculated with the approaches de Vries, Campbell and Neuspina81

Figure 6-4 Reaction model of carbon and nitrogen turnover with reaction coefficients of the following processes: k_1, k^*_1 - conversion of C and N pools of primary organic matter into active organic matter k_2, k^*_2 - mineralisation of C and N pools of primary organic matter k_{aom} - mineralisation of active organic matter k_{nit} - nitrification of active organic matter $\gamma_{pom}, \gamma_{aom}$ - C/N ratio of primary and active organic matter83

Figure 6-5 Influence of water content on mineralisation (left) and nitrification (right) in dependence on different saturation water content (SWC)86

Figure 6-6 Influence of temperature (left) and pH value (right) on mineralisation and nitrification....87

Figure 9-1 Scheme of stem geometry.....99

Figure 9-2 Flow chart of the WPM for Brandenburg (Fürstenau, 2008). Abbreviations see Chapter 9.6.1105

TABLES

Table 3-1 Monthly Haude factor for the calculation of potential evapotranspiration (DVWK, 1996) ..	30
Table 4-1 Promotor-Inhibitor Models (PIMs) derived from the general framework in Equation (4.1) and the imposed restrictions described in the paragraph above. ΔI_{phen} , ΔP_{phen} rates of change of the inhibitor I and promotor P_{phen} . f_i ($i = I, P$) are temperature dependent triangular functions according to Equation (4.1) for the inhibitor I_{phen} and promotor P_{phen} , respectively, each having three parameters T_{min} , T_{opt} , T_{max} . p_i ($i = 1, \dots, 4$) are scaling parameters. $I_{phen}(t_0) = 1$, $P_{phen}(t_0) = 0$. time step: one day. t_0 = day of leaf colouring the previous year. Bud burst: $P_{phen} > 1$	51
Table 4-2 Parameter values for the PIMs. For a description of the parameters see Equation (4.2) and Table 4-1 . min, max: allowed ranges for the parameters during model fits. min SSR: Parameters for the PIM that performed best in terms of SSR (sum of squared residuals) for model fitting. mean: Average parameters after ten optimisation runs. stderr: Standard error of the average parameters after ten optimisation runs.....	53
Table 4-3 Parameter values for the CSM. min, max: allowed ranges for the parameters during model fits. min SSR: Parameters for the fit that performed best in terms of SSR among ten different runs. mean: Average parameters after ten optimisation runs. stderr: Standard error of the average parameters after ten optimisation runs.....	54
Table 4-4 Parameter values for the TSM. min, max: allowed ranges for the parameters during model fits. min SSR: Parameters for the fit that performed best in terms of SSR among ten different runs. mean: Average parameters after ten optimisation runs. stderr: Standard error of the average parameters after ten optimisation runs.....	55
Table 6-1 Parameters of the thermal conductivity calculation of (de Vries, 1963).....	79
Table 6-2 Reduction coefficient of mineralisation R_p^{min} and nitrification R_p^{nit} in dependence of the pH value	87
Table 7-1 Parameter Y_s for stress mortality according to Keane et al. (1996)	90
Table 9-1 Number of sprouts n_{sprout} and table function f_{ac} (empirical assumptions) for Aspen and Black locust	97
Table 9-2 Parameter [cm] for sorting of harvested and remaining stems into the different groups (forest expert knowledge) according to Frommhold (2001)	101
Table 9-3 Timber grades in SEA (o.b. – over bark (diameter including bark), wo.b. – under bark). ...	106
Table 10-1: Implemented functional groups of insects and pathogens as proposed by Dietze and Matthes (2014). The indirect and direct effects on the allocation process of 4C are also listed. NSC = non-structural carbohydrates	110
Table 10-2: Relative (p_i^{NSC} , $i=\{tb,s,crt\}$) maximum size of the NSC-pool (starch and sugar) for the three implemented compartments. Maximum size is relative to dry matter mass of the specific compartment biomass ($M_{i,c}$, $i=\{tb,s,crt\}$).....	112

Table 11-1 Fire hazard level definition.....	114
Table 11-2 Parameters of calculation of dew point temperature (DVWK, 1996) in dependence on air temperature T_a	116
Table 11-3 Fire danger levels of Nesterov-Index.....	116
Table 11-4 Parameters of the nun moth life stages; T_m – related monthly mean temperature for the calculation of T_{sum} , T_4, \dots, T_9 - monthly mean temperature from April to September	117
Table 11-5 Index de Martonne	119
Table 11-6 Aridity Index	120
Table 11-7 Emberger Index	120
Table 11-8 Lang Index	121
Table 11-9 Reichel Index	121
Table 11-10 Budyko Index.....	122
Table 11-11 Classification of index I_{shc}	123
Table 11-12 Currey Index	124
Table 11-13 Conrad Index	124
Table 11-14 Classification scheme for the late frost danger index I_{lf}	125
Table 11-15 Annual late frost indices in 4C.....	125
Table 11-16 Characteristic climatic values.....	125

1 OVERVIEW

The 4C model provides descriptions of tree species composition, forest structure, and total ecosystem carbon content as well as leaf area index and of the whole carbon, water, and nitrogen fluxes of a forest stand. The model is designed to contain mechanistic ecological responses to gradients of climate, nitrogen, and CO₂, and allows to realistically simulating forest management. The main features of 4C are

- the assumption of horizontal homogeneity on the considered forest patch, which makes it possible to restrict spatial explicitness to the vertical dimension
- the modelling of light extinction in the canopy according to the Beer-Lambert law
- the explicit modelling of establishment, growth, and mortality of tree individuals/cohorts (Bugmann et al., 1997).

Furthermore, major features of the model are

- the explicit simulation of water and nutrient availability as perceived by individual trees, based on the assumption of scramble competition (Krebs, 1994)
- comparably detailed sub-models of heat flux, water, carbon and nitrogen dynamics in the soil
- a mechanistic formulation of the annual course of net photosynthesis as a function of environmental influences (temperature, water and nitrogen availability, global radiation, and CO₂) based on optimisation theory (Haxeltine and Prentice, 1996b)
- a mechanistic description of allocation patterns derived from the model of Mäkelä (1986), extended to respond dynamically to water and nutrient limitations
- calculation of total tree respiration following the concept of constant annual respiration fraction as proposed by Landsberg and Waring (1997)
- a phenology model developed by Schaber and Badeck (2003)
- fine root distribution is estimated by depth depending power function (Jackson et al., 1996).
- improved modelling of establishment and mortality rates in forest stands (Keane et al., 1996; Loehle and LeBlanc, 1996; Sykes and Prentice, 1996)
- the incorporation of forest management and natural (biotic) disturbances at the scale of the forest stand
- consideration of soil (ground) vegetation
- the additional possibility of applying a wood product model (WPM) and a socio-economic analysis (SEA)
- simulating short rotation coppices with different species

A number of points deserve to be emphasized here:

- (1) Growth is modelled describing of net primary production (NPP) and its allocation to tree compartments including foliage, sapwood, and fine roots. Since heartwood formation and height growth are treated explicitly, tree diameter is merely an output variable in 4C.
- (2) Competition in terms of light availability is expanded by the explicit competition for water and nutrients.
- (3) We introduce formulations for mortality that conform more to biological expectations (Keane et al., 1996).

Different integration steps are used for the various sub-models (see Figure 1-1) , ranging from a daily time step for soil water dynamics, over one week for soil carbon & nitrogen dynamics and the simulation of NPP, to an annual time step for tree demography and carbon allocation.

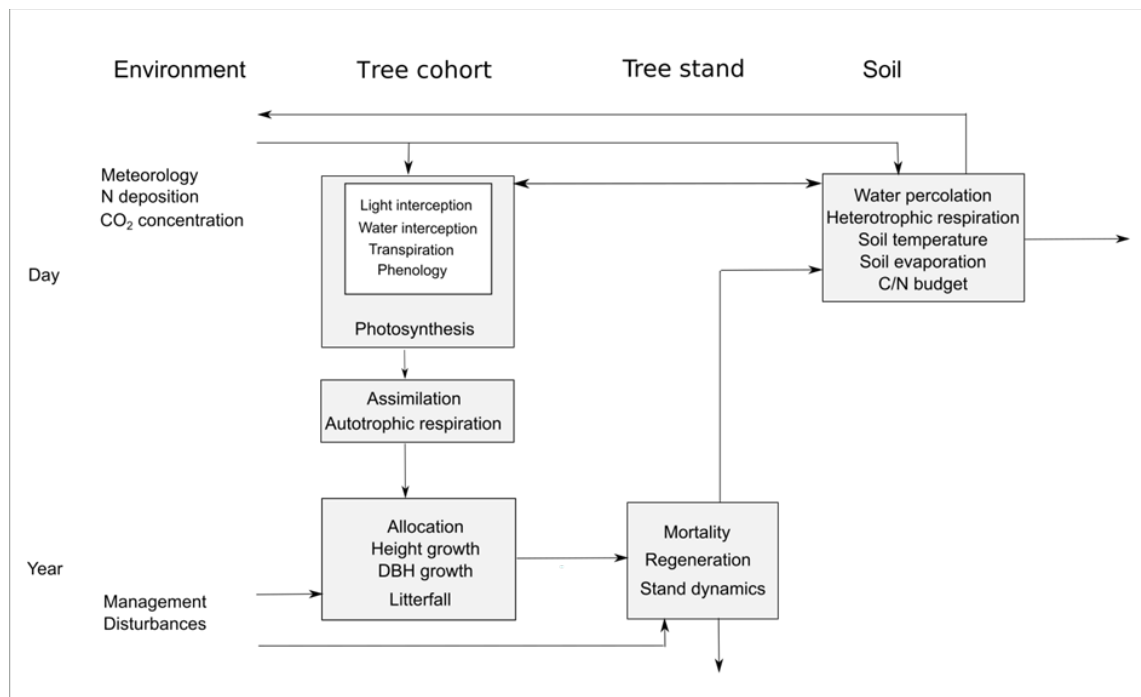


Figure 1-1 General structure of the model 4C

Currently the model is parameterised for the five most abundant tree species of Central Europe (beech (*Fagus sylvatica* L.), Norway spruce (*Picea abies* L. Karst.), Scots pine (*Pinus sylvestris* L.), oaks (*Quercus robur* L., and *Quercus petraea* Liebl.), and birch (*Betula pendula* Roth)) as well as other tree species, namely aspen (*Populus tremula* (L.), *P. tremuloides* (Michx.)), Douglas-fir (*Pseudotsuga menziesii* (Mirb.) Franco), black locust (*Robinia pseudoacacia* L.), Aleppo pine (*Pinus halepensis* Mill.), Ponderosa pine (*Pinus ponderosa*

Dougl.), Lodgepole pine (*Pinus contorta* Dougl.), and Eucalyptus (*Eucalyptus globulus*, *Eucalyptus grandis*).

The model has been used to simulate impacts of global change in the forest sector in Germany (Lasch et al., 2002) or regional water balances and carbon storage in Brandenburg, Germany (Gerstengarbe et al., 2003; Lasch et al., 2005; Suckow et al., 2002). Furthermore, 4C has been validated using measurements of soil temperature and soil water content at Level-II sites in Germany (Badeck et al., 2007; Meiwes et al., 2007). The performance of 4C in comparison with other models against long-term data from Scots pine stands in Finland was investigated using volume growth and survival graphs (Mäkelä et al., 2000; Sievänen et al., 2000). Moreover, 4C was evaluated together with other process-based forest models and applied on the scale of a management unit to develop adaptive management measures and to compare different forest functions (Fürstenau, 2008; Fürstenau et al., 2007; Kellomäki and Leinonen, 2005). Further applications concern the analysis of forest conversion management (Kint et al., 2009), competition in mixed-forests (Reyer et al., 2010), alternative forest management strategies (Gutsch et al., 2011) or the analysis of short-rotation coppices (Kollas et al., 2009; Lasch et al., 2010) under climate change. The impacts of climate change and management on carbon sequestration were analysed for a forest district in Thuringia (Germany) by (Borys, 2015; Borys et al., 2015; Borys et al., 2013; Borys et al., 2016). On a European scale regional changes in net primary productivity were projected under different climate change scenarios in the framework of the EC FP7 MOTIVE project (Reyer et al., 2014). 4C was applied on national scale to analyse possible impacts on Germany's forests, their risks and opportunities (Gerstengarbe and Welzer, 2013; Gutsch et al., 2015; Lasch-Born et al., 2015). In Central Siberia, benefits and risks of a pine stand under climate change were assessed with 4C (Suckow et al., 2016).

The model has been used to simulate impacts of global change in the forest sector in Germany (Lasch et al., 2002) or regional water balances and carbon storage in Brandenburg, Germany (Gerstengarbe et al., 2003; Lasch et al., 2005; Suckow et al., 2002). Furthermore, 4C has been validated using measurements of soil temperature and soil water content at Level-II sites in Germany (Badeck et al., 2007; Meiwes et al., 2007). The performance of 4C in comparison with other models against long-term data from Scots pine stands in Finland was investigated using volume growth and survival graphs (Mäkelä et al., 2000; Sievänen et al., 2000). Moreover, 4C was evaluated together with other process-based forest models and applied on the scale of a management unit to develop adaptive management measures and to compare different forest functions (Fürstenau, 2008; Fürstenau et al., 2007; Kellomäki and Leinonen, 2005). Further applications concern the analysis of forest conversion management (Kint et al., 2009), competition in mixed-forests (Reyer et al., 2010), alternative forest management strategies (Gutsch et al., 2011) or the analysis of short-rotation coppices (Kollas et al., 2009; Lasch et al., 2010) under climate change. The impacts of climate change and management on carbon sequestration were analysed for a forest district in Thuringia

(Germany) by (Borys, 2015; Borys et al., 2015; Borys et al., 2013; Borys et al., 2016). On a European scale regional changes in net primary productivity were projected under different climate change scenarios in the framework of the EC FP7 MOTIVE project (Reyer et al., 2014). 4C was applied on national scale to analyse possible impacts on Germany's forests, their risks and opportunities (Gerstengarbe and Welzer, 2013; Gutsch et al., 2015; Lasch-Born et al., 2015). In Central Siberia, benefits and risks of a pine stand under climate change were assessed with 4C (Suckow et al., 2016).

2 STAND STRUCTURE

The forest dynamics is simulated for patches (forest area) varying from 200 m² to 10000 m². The stand structure is represented by a number of tree cohorts, each of which is characterized by species, age, tree dimensions, and number of trees it comprises. Production and growth is simulated for each cohort separately. The tree cohorts compete for light, water, and nutrients. Their relative success in this competition determines their performance in terms of growth, regeneration, and mortality. Each cohort is represented in the model as horizontally homogeneous, i.e. the model is distance independent. The vertical structure of crown space and rooting zone is represented by a resolution into vertical layers.

The forest dynamics for natural forests in 4C proceed from recruitment (if it allows) of individual tree cohorts through to the death of the dominating tree individual(s). Several additional routines are included in order to allow for the simulation of growth and competition in managed forests, too. Species composition and cohort structure can be initialized according to different kind of data like mensuration data or single tree data. Then, cohorts are defined based on the frequency distribution of diameter at breast height d_{bh} and additional information as height H , or bole height H_b . Silvicultural treatments can be taken into account by prescribed reduction of tree number in the cohorts (see Chapter 9).

Each cohort is characterized by the number of trees it comprises, by the mass of foliage M_f , fine roots M_r , sapwood M_s , heartwood M_{hw} , and other coarse material, branches and coarse roots, M_{tbc} , as well as the tree dimensions height H , diameter at breast height d_{bh} , bole height H_b , average height of sapwood pipes H_s , diameter of the crown d_{cb} , and rooting depth. The variables M_{tbc} and d_{crb} are coupled to the other variables by allometric relationships. All the other variables are updated any year as a result of partitioning of assimilates to the growth of different organs.

2.1 Canopy structure, foliage distribution

The canopy structure of the forest stand is defined by the number of crown layers per cohort characterised by the thickness of layers z_{cr} and the crown height as difference of H and H_b .

The foliage mass as well as the leaf area is distributed equally inside the crown space assumed as a cylinder. The projected crown coverage area a_{cr}^c of the cohort c is calculated:

$$a_{cr}^c = \pi \cdot \min((a_c \cdot d_{bh} + b_c), c_c)^2 \quad (2.1)$$

For detailed description see Chapter 3.5.

2.2 Tree architecture/ geometry

Stems are approximated as truncated cones of diameter d_{bh} at height of 137 cm up to bole height H_b and as cones inside the crown space with a base diameter d_{bs} . The stem is composed of heartwood and sapwood, which coated the heartwood and has a constant cross sectional area A_s . The heartwood truncated cone is described by the cross sectional area at the tree base A_{hb} and the cross sectional area at the crown base A_{hc} . It yields for the diameter at the base of the stem:

$$d_{bs} = \sqrt{\frac{(A_{hb} + A_s) \cdot 4}{\pi}} \quad (2.2)$$

And therefore

$$A_{hb} = \pi \cdot \left(\frac{d_{bs}}{2}\right)^2 - A_s \quad (2.3)$$

The sapwood cross sectional area is calculated from the sapwood biomass M_s by:

$$A_s = \frac{M_s}{\rho_s \cdot H_s} \quad (2.4)$$

Where the sapwood height is calculated by:

$$H_s = H_b + \frac{H - H_b}{3} = \frac{2H_b + H}{3} \quad (2.5)$$

due to the length H_b of sapwood pipes in the truncated cone and in the cone (see Figure 2-1).

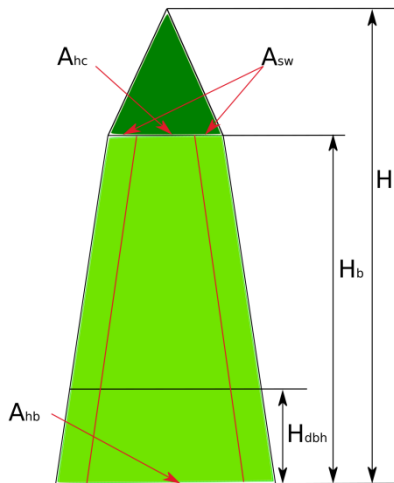


Figure 2-1 Tree geometry in 4C, $H_{dbh}=137$ cm

2.3 Root system

2.3.1 Root distribution

The biomass of coarse and fine roots is determined by the allocation rules (see Chapter 4.4). This biomass is distributed over all soil layers (see Chapter 6) by different schemes in the same way for both coarse and fine roots.

- The biomass is equally distributed over all layers with the root fractions $r_{fr}(z_i)$ depending on the depth of the soil layer i .
- The vertical root density profile is assumed to follow an asymptotic equation (Jackson et al., 1996)

$$r_{cum}(z) = 1 - \gamma^z \quad (2.6)$$

with r_{cum} is the cumulative root fraction from surface up to depth z and γ is a coefficient, which is fitted for temperate deciduous trees ($\gamma = 0.966$) and temperate coniferous trees ($\gamma = 0.976$) (see Figure 2-2).

The root fraction per layer of each tree is calculated by

$$r_{fr}(z_1) = r_{cum}(z_1)$$

and

$$r_{fr}(z_i) = r_{cum}(z_i) - \sum_{j=1}^{i-1} r_{fr}(z_j) \quad (2.7)$$

with $i=2,3,\dots,n_r$ and n_r is the number of rooting layers.

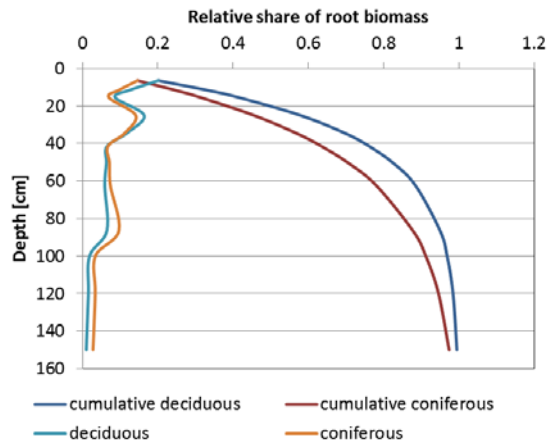


Figure 2-2 Relative share of root biomass in different depths for temperate deciduous and coniferous trees as cumulative and absolute fraction.

2.3.2 Root depth

The root depth and the number of the rooting layers n_r respectively can be estimated in following ways:

- a) The root depth depends on the tree height. If tree height is less than the soil profile the number of rooting layers is set to the tree height and the number of rooting layers to the corresponding number of the soil layer. Otherwise n_r is set to the number of the last soil layer.
- b) The number of rooting depth can be given as fixed input value. It applies to all cohorts and does not change.

2.4 Stand initialisation

When 4C shall be used for a simulation run starting with a given stand structure as e.g. determined by a forest inventory, 6 variables are needed for every cohort in the initialisation procedure: diameter at breast height (d_{bh}), total tree height (H), height to the base of the crown (H_b), number of trees in the cohort (n^c_o), sapwood/heartwood-area-ratio at breast height and stem volume. Since the last two variables are rarely determined in inventories, the sapwood/heartwood-ratio and stem volume are estimated from the tree dimensions as detailed in the following sections.

2.4.1 Initialisation using averaged stand data

Data requirement

The initialisation requires per stand

- species type

- averaged diameter at breast height d_g
- averaged height H_g
- age and
- basal area G of the stand.

Species specific parameters of various functions are necessary:

- $p_0 - p_4$ for Weibull distribution function, Equation (2.9)
- c_1, c_2 for bole height function, Equation (2.15)
- $a_0 - a_2$ for height function, Equation (2.11)
- $b_0 - b_2$ for height function, Equation (2.11)
- $k_{c0} - k_{c2}$ for height function, Equation (2.11)
- w_{k1}, w_{k2} for height function, Equation (2.13)

Method

2.4.1.1.1 Generating of single tree data

A capping limit $L_T = 7$ [cm] is defined. If $(d_g - L_T) < 3$ then $L_T = d_g - 4$. The maximum diameter d_{max} is estimated from d_g by a function of Gerold (1990):

$$d_{max} = 8.2 + 1.8 d_g - 0.1 (d_g)^2 \quad (2.8)$$

Two parameters b and c of a Weibull distribution are calculated:

$$\begin{aligned} b &= p_0 + p_1 d_g \\ c &= p_2 + p_3 d_g + p_4 d_{max} \end{aligned} \quad (2.9)$$

The generation of a single tree with the diameter d_{bh} is realized by a number x equally distributed between 0 and 1 and the following function (Weibull distribution):

$$d_{bh} = b \cdot \left(\left(\frac{L_T}{b} \right)^c - \log(1 - x) \right)^{\frac{1}{c}} \quad (2.10)$$

The height of the tree with diameter d_{bh} is estimated by different height functions. For pine and birch the height function from Kuleschis (see Gerold (1990)) is used with the parameters k_{ua}, k_{ub}, k_{uc} :

$$\begin{aligned} k_{ua} &= 1 - (a_0 + a_1 d_g + a_2 d_g^2) \\ k_{ub} &= 1 - (b_0 + b_1 d_g + b_2 d_g^2) \\ k_{uc} &= 1 - (k_{c0} + k_{c1} d_g + k_{c2} d_g^2) \end{aligned} \quad (2.11)$$

and the function:

$$H = H_g \left(k_{ua} + \left(\frac{k_{ub}}{\left(d_{bh} + \frac{d_g}{2} \right)} \right) d_g + \left(\frac{k_{uc}}{\left(d_{bh} + \frac{d_g}{2} \right)} \right)^2 d_g^2 \right) \quad (2.12)$$

For other species (beech, spruce, oak) the height function of Weimann (1980) is applied with the parameter w_f :

$$w_f = w_{k1} + w_{k2} H_g \quad (2.13)$$

For the case d_{bh} is greater or equal $D_g - H_g/2$ the following function is used:

$$H = \begin{cases} H_g + w_f (\log(H_g - d_g + d_{bh}) - \log(H_g)) & d_{bh} \geq D_g - 0.5 H_g \\ \left(H_g + w_f \left(\log\left(\frac{H_g}{2}\right) - \log(H_g) \right) - 1.3 \right) \sqrt{\frac{d_{bh}}{\left(d_g - \frac{H_g}{2} \right)}} + 1.3 & \text{otherwise} \end{cases} \quad (2.14)$$

For Douglas fir (Nagel, 2002) and Eucalyptus (Medhurst et al., 1999; Ranatunga et al., 2008) specific height functions are implemented.

The bole height H_b of the tree is estimated according to a function of Nagel (1995):

$$H_b = H(1 - e^x) \quad (2.15)$$

with

$$x = - \left(c_1 + c_2 \frac{H}{d_{bh}} \right)^2$$

For Eucalyptus the bole height is estimated by a function of Nutto et al. (2006):

$$H_b = -5.12 - 0.407 d_{bh} + 1.193 H \quad (2.16)$$

The generation of single tree data stops if the basal area G is reached.

2.4.1.1.2 Building cohorts

The generated trees are classified into tree cohorts. The maximum number of cohorts per species is 60. The class width is calculated from the maximum and minimum diameter at breast height.

The further initial data of the cohorts are estimated as follows.

a) *Initialisation of sapwood/heartwood ratio*

An approximation of the sapwood fraction can be derived based on the simplifying assumption of constant annual diameter increment d_{inc} , thus

$$d_{inc} = \frac{d_{bh}}{a_{ring}^{max}} \quad (2.17)$$

with a_{ring}^{max} is the cambial age of the innermost ring. The sapwood area $A_{SWring}(0)$ of a given ring in the year of growth of the ring is then given by:

$$A_{SWring}(0) = \frac{\pi}{4} \left(\left\{ d_{inc} [a_{ring}^{max} - a_{ring}] \right\}^2 - \left\{ d_{inc} [a_{ring}^{max} - a_{ring}] - d_{inc} \right\}^2 \right) \quad (2.18)$$

with a_{ring} is the current age of ring under consideration. The sapwood fraction of the ring at n years after formation of the ring is then given by:

$$A_{SWring}(n) = (1 - s_{sap})^n A_{SWring}(0) \quad (2.19)$$

Summation of the current sapwood fractions of all rings and division by the total cross sectional area A_{tot} gives the current sapwood fraction r_{sap}

$$\begin{aligned} r_{sap} &= \frac{A_s}{A_{tot}} \\ &= \frac{1}{(a_{ring}^{max})^2} \sum_{i=0}^{a_{ring}^{max}-1} e^{x_i} \end{aligned} \quad (2.20)$$

with

$$x_i = i \ln(1 - s_{sap}) \left(2 \cdot (a_{ring}^{max} - i) - 1 \right)$$

b) *The height of sapwood pipes*

The height of sapwood pipes H_s is calculated as

$$H_s = \frac{2H_b}{3} + \frac{H}{3} \quad (2.21)$$

c) *Initialisation of stem volume*

The stem volume V_D is calculated with different function per species.

For Douglas fir the following functions are used (Nagel, 2002):

$$V_D = \frac{F_D \pi d_{bh}^2}{4000} \quad (2.22)$$

with the form factor F_D

$$F_D = \frac{-200.31914}{H d_{bh}^2} + \frac{0.8734}{d_{bh}} - 0.0052 \log(d_{bh}^2) + \frac{7.3594}{H d_{bh}} + 0.46155 \quad (2.23)$$

For other species (model SILVA, Pretzsch et al. (2002)) the following form factor is used

$$F_D = e^{(k_1 + k_2 \log(H) + k_3 \log(H)^2)} \quad (2.24)$$

with

$$\begin{aligned} k_1 &= s_1 + s_2 \log(d_{bh}) + s_3 \log(d_{bh})^2 \\ k_2 &= s_4 + s_5 \log(d_{bh}) + s_6 \log(d_{bh})^2 \\ k_3 &= s_7 + s_8 \log(d_{bh}) + s_9 \log(d_{bh})^2 \end{aligned} \quad (2.25)$$

and the species specific parameters $s_1 - s_9$.

For pine stem volume is calculated as follows:

$$V_D = e^{(\rho_1 + \rho_2 \log(d_{bh}) + \rho_3 \log(H))} \quad (2.26)$$

For Eucalyptus a function of Binkley et al. (2002) is used:

$$V_D = 0.00005447 (d_{bh})^{1.921157} \left(\frac{H}{100} \right)^{0.950581} \quad (2.27)$$

or a function of Stape et al. (2010) depending on the site is used:

$$V_D = \frac{\rho_1 (d_{bh})^{\rho_2} \left(\frac{H}{100} \right)^{\rho_3}}{500} \quad (2.28)$$

ρ_1, ρ_2, ρ_3 – site depending parameters, which are implemented in the program code.

d) Sapwood area

The diameter at base of the crown d_{cb} is calculated with a breast height $H_{dbh}=137$ [cm] by

$$d_{cb} = \frac{d_{bh}}{H} (H_{dbh} - H_b) + d_{bh} \quad (2.29)$$

and the sapwood area A_s by

$$A_s = \begin{cases} \frac{\pi}{4} (d_{cb})^2 r_{sap} & H_b < H_{dbh} \\ \frac{\pi}{4} (d_{bh})^2 r_{sap} & H_b \geq H_{dbh} \end{cases} \quad (2.30)$$

with

$$r_{sap} = \frac{A_s}{\frac{\pi}{4} (d_{bh})^2} \quad (2.31)$$

e) Sapwood biomass

The sapwood biomass M_s is calculate by sapwood density ρ_s

$$M_s = \rho_s \cdot A_s \cdot H_s \quad (2.32)$$

f) Cross sectional areas of heartwood at crown base and at stem base

In case of $H_b \leq H_{dbh}$ the cross sectional area of heartwood at stem base A_{hb} is calculated by

$$A_{hb} = \frac{\pi}{4} \left(\frac{d_{cb} \cdot a}{a_{ring}^{max}} \right)^2 - A_s \quad (2.33)$$

with the estimated parameter a_{ring}^{max} (see a)) and the age a and analogous the cross sectional area of heartwood at crown base A_{hc} is calculated by

$$A_{hc} = \frac{\pi}{4} (d_{cb})^2 - A_s \quad (2.34)$$

If $H_b > H_{dbh}$ the cross sectional area of heartwood at crown base is estimated by a Newton algorithm with the initial value

$$A_{hc} = 0.04 \frac{\pi}{4} (d_{cb})^2 (1 - r_{sap}) \quad (2.35)$$

and the function F

$$F = M_{bio} - \rho_s \cdot V_D \quad (2.36)$$

with the stem volume V_D estimated by yield table functions.

Stem biomass M_{bio} is considered as a truncated cone with the base area A_{bs} , the diameter d_{cb} , and the height H_b as well as a cone with height $H-H_b$ and ground base A_s+A_{hc} (see Figure 2-1) and is calculated as sum of sapwood and heartwood biomass.

The ground base of heartwood A_{hb} is

$$A_{hb} = A_{bs} - A_s \quad (2.37)$$

The heartwood biomass is calculated from the truncated cone with the ground base area A_{hb} , the upper area A_{hc} and the height H_b as well as the cone with the height $H-H_b$ and the base area A_{hc} .

The sapwood biomass is calculated as

$$M_s = \frac{A_s}{3} (2H_b + H) \quad (2.38)$$

and the heartwood biomass as

$$M_{hw} = \frac{1}{3} \left(x(H - H_b) + H_b \left(x + \left(\frac{\pi}{4} d_{bs}^2 - A_s + \sqrt{x \left(\frac{\pi}{4} d_{bs}^2 - A_s \right)} \right) \right) \right) \quad (2.39)$$

Then the total stem biomass then results from

$$\begin{aligned} M_{bio} &= M_s + M_{hw} \\ &= \frac{A_s}{3} (2H_b + H) + \frac{1}{3} \left[x(H - H_b) + H_b \left(x + \left(\frac{\pi}{4} d_{bs}^2 - A_s + \sqrt{x \left(\frac{\pi}{4} (d_{bs})^2 - A_s \right)} \right) \right) \right] \\ &= \frac{1}{3} \left(H(A_s + x) + H_b \left(2A_s - x + x - A_s + \frac{\pi}{4} (d_{bs})^2 + \sqrt{x \left(\frac{\pi}{4} (d_{bs})^2 - A_s \right)} \right) \right) \\ &= \frac{1}{3} \left(H(A_s + x) + H_b \left(A_s + \frac{\pi}{4} (d_{bs})^2 + \sqrt{x \left(\frac{\pi}{4} (d_{bs})^2 - A_s \right)} \right) \right) \end{aligned} \quad (2.40)$$

The diameter d_{bs} of the area A_{bs} is calculated as follows.

The diameter d_{cb} of the upper base area of the truncated cone with height H_b of the total biomass is

$$d_{cb} = \sqrt{\frac{4}{\pi} (A_s + x)} \quad (2.41)$$

According to the intercept theorem the relations between d_{bs} and d_{bh} are

$$\begin{aligned} \frac{d_{bh} - d_{cb}}{d_{bs} - d_{cb}} &= \frac{H_b - H_{dbh}}{H_b} \\ &= \left(1 - \frac{H_{dbh}}{H_b}\right) \end{aligned} \quad (2.42)$$

and it follows

$$d_{bs} - d_{cb} = \frac{d_{bh} - d_{cb}}{\left(1 - \frac{H_{dbh}}{H_b}\right)} \quad (2.43)$$

Finally it holds

$$\begin{aligned} d_{bs} &= \frac{d_{bh} - d_{cb}}{\left(1 - \frac{H_{dbh}}{H_b}\right)} + d_{cb} \\ &= \frac{d_{bh} - d_{cb} + d_{cb} \left(1 - \frac{H_{dbh}}{H_b}\right)}{\left(1 - \frac{H_{dbh}}{H_b}\right)} \\ &= \frac{d_{bh} - d_{cb} \frac{H_{dbh}}{H_b}}{\left(1 - \frac{H_{dbh}}{H_b}\right)} \end{aligned} \quad (2.44)$$

Together with Equation (2.42) it yields:

$$d_{bs} = \frac{d_{bh} - \sqrt{\frac{4}{\pi} (A_s + x)} \frac{H_{dbh}}{H_b}}{\left(1 - \frac{H_{dbh}}{H_b}\right)} \quad (2.45)$$

and

$$\frac{d}{dx} d_{bs} = \frac{-H_{dbh}}{H_b \pi \left(1 - \frac{H_{dbh}}{H_b}\right) \sqrt{\frac{1}{\pi} (A_s + x)}} \quad (2.46)$$

A solution for x is found by assuming $F(x)=0$ (see (2.36)) with the Newton algorithm.

g) Heartwood biomass

The heartwood biomass M_{hw} is calculated as the difference between the total biomass and the sapwood biomass

$$M_{hw} = M_{bio} - M_s \quad (2.47)$$

h) Foliage biomass and foliage area

The foliage biomass M_f is proportional to the sapwood area

$$M_f = \eta_s \cdot A_s \quad (2.48)$$

with the species specific foliage to sapwood area relationship η_s .

The foliage area A_{fol} is estimated by

$$A_{fol} = M_f s_{min}^c + 0.5 s_a^c \quad (2.49)$$

with two species parameters: the minimum specific one-side leaf area s_{min}^c and the light depended specific one-side leaf area s_a^c

i) Fine root biomass

For the fine root biomass M_r a rough estimation is used

$$M_r = M_f \quad (2.50)$$

2.4.2 Initialisation using single tree data

Data requirements

The initialisation requires per tree the following data:

- Patch size P_a [m²]
- Species type
- Diameter at breast height d_{bh} [mm]
- Tree height H [m]
- Bole height H_b [m] (mandatory)
- Age a

Method

The given data are classified into diameter classes to build cohorts. The class width is 1 cm, but could be changed. If H_b is not available, the functions (2.15) and (2.16) are used to calculate H_b . For each diameter class an averaged d_{bh} , H and H_b and the number of trees are

calculated as values of the cohort. Further on, all cohort variables described in Chapter 2.4.1.1.2 are calculated.

2.4.3 Initialisation of saplings

Data requirements

If the height of planted trees is less than a specific limit (e.g. 200 cm) the diameter at breast height is not available. In this case a more simple way of initialisation of cohorts is realised. It requires:

- Species type
- Age
- Given number of saplings n_{tot}
- Number of trees n_{pl}
- Mean height H_p
- Minimum height H_{min}^p
- Standard deviation of height σ_H

Method

2.4.3.1.1 Height and number of trees per cohort

A number of saplings n_{pl} is generated, standard values of plants per hectare are given in the model, as well as the other required data (management file, planting). A number of cohorts n_c is calculated in different way, e.g. the integer of H is used or a number is fixed ($n_s = 20$). For each sapling class/cohort $c=1,2,\dots,n_c$ the height H_c is calculated:

$$H_c = H_{min} + (c - 1) \quad (2.51)$$

The number of trees per cohort n_a^{c*} is calculated:

$$n_a^{c*} = \frac{1}{\sqrt{2\pi}\sigma_H} e^{-\frac{1}{2}\left(\frac{H_c - H_{pl}}{\sigma_H}\right)^2} \quad (2.52)$$

The total number of trees n_{pl} of the stand is

$$n_{pl} = \sum_{c=1}^{n_c} n_a^{c*} \quad (2.53)$$

And following the number of trees per class/cohort n_a^c is recalculated:

$$n_a^c = n_a^{c*} \frac{n_{pl}}{n_{tot}} \quad (2.54)$$

2.4.3.1.2 Further initialisation of cohorts

For the calculation of sapwood biomass M_s^c per sapling cohort c the roots of the following equation has to solve for x

$$p_{h3} x^2 + p_{h2} x + p_{h1} - \log(H_c) = 0 \quad (2.55)$$

with the species specific parameters p_{h1} , p_{h2} , p_{h3} and then

$$M_s^c = 10^x \cdot 10^{-5} \quad (2.56)$$

The foliage biomass M_f^c is calculated as follows:

$$M_f^c = p_{sa} (M_s^c)^{p_{sb}} \quad (2.57)$$

with the species specific parameters p_{sa} , p_{sb}

And the fine root biomass M_r^c is estimated analogous to Equation (2.50) by

$$M_r^c = M_f^c \quad (2.58)$$

The parameterisation of saplings of the main tree species in 4C used here is based on data found in Barigah et al. (1994); Bond-Lamberty et al. (2002); (Dohrenbusch; Hauskeller-Bullerjahn; Mailly and Kimmins); Ter-Mikaelian and Korzukhin (1997); Van Hees (1997)

3 ENVIRONMENT

3.1 Climate

The model is driven by daily values of meteorological parameters:

- temperature (minimum, maximum, average),
- precipitation,
- global radiation,
- relative humidity,
- air pressure, and
- wind speed.

3.2 Potential evapotranspiration

Evapotranspiration includes evaporation of free water from soil and plant surfaces, transpiration from leaves of plants, and sublimation from snow surfaces. Potential evapotranspiration is the rate at which evapotranspiration would occur if vegetation has access to an unlimited supply of soil water. There are several options for estimating potential evapotranspiration.

3.2.1 Penman-Monteith

The Penman-Monteith equation (Monteith and Unsworth, 1990) is a so called combination model, which combines elements from both the energy budget and mass transfer models. It regards the energy required for evaporation as well as aerodynamic and surface resistance terms:

$$\lambda_v E_{pot} = \frac{\Delta(R_n - G) + \frac{1}{r_a} \rho c_{air} \delta}{\Delta + \gamma_p \left(1 + \frac{r_c}{r_a}\right)} \quad (3.1)$$

where E_{pot} is the potential evaporation rate, λ_v the latent heat of vaporisation, R_n the net radiation, G the ground heat flux (is neglected), r_a the surface aerodynamic resistance for water vapour, r_c the canopy surface resistance, Δ the slope of the saturation vapour pressure temperature relationship, δ the saturation vapour pressure deficit of air, ρ_a the mean air density at constant pressure, c_{air} the specific heat capacity of air, and γ_p the modified psychrometric constant.

The latent heat of vaporisation depends on air temperature T_a (DVWK, 1996)

$$\lambda_v = (2.498 - 0.00242 T_a) \cdot 10^3 \quad (3.2)$$

The psychrometric constant ψ is modified by the actual air pressure P_{act} (DVWK, 1996)

$$\gamma_p = \psi P_{act} \quad (3.3)$$

The saturation vapour pressure deficit δ is calculated from the saturated vapour pressure P_{sat} and the relative humidity h_r

$$\delta = P_{sat}(1 - h_r) \quad (3.4)$$

with the estimation of the saturated vapour pressure from air temperature following Murray (1967)

$$P_{sat} = 6.1078 * e^{\left(\frac{17.2694 T_a}{T_a + 273.3}\right)} \quad (3.5)$$

The density of air ρ_a is calculated by (Monteith and Unsworth, 1990)

$$\rho_a = (1.2917 - 0.00434 T_a) \cdot 10^{-3} \quad (3.6)$$

and the slope of the saturation vapour pressure temperature relationship as (DVWK, 1996)

$$\Delta = P_{sat} \frac{4158.6}{(T_a + 273.3)^2} \quad (3.7)$$

3.2.2 Priestley-Taylor

The Priestley/Taylor model is a shortened version of the original Penman combination equation from 1948 (Priestley and Taylor, 1972). The aerodynamic component of the original Penman equation is here reduced to a coefficient that modifies the original equation.

$$\lambda_v E_{pot} = \alpha_{pT} R_n \frac{\Delta}{\Delta + \gamma_p} \quad (3.8)$$

with the Priestley-Taylor coefficient α_{pT} (DVWK, 1996; Flint and Childs, 1991).

3.2.3 Turc-Ivanov

An empirical approach of Turc estimates the potential evapotranspiration from air temperature and global radiation R_g at $T_a \geq 5^\circ\text{C}$

$$E_{pot} = 0.0031 f_{korr} (R_g + 209) \frac{T_a}{T_a + 15} \quad (3.9)$$

with a modification factor f_{korr} which depends on the relative humidity h_r

$$f_{\text{korr}} = \begin{cases} 1 + \frac{50 - h_r}{70}, & h_r < 50 \\ 1, & h_r \geq 50 \end{cases} \quad (3.10)$$

At $T_a < 5^\circ\text{C}$ potential evapotranspiration E_{pot} is calculated by an approach of **Ivanov** from air temperature and relative humidity (DVWK, 1996; Dyck and Peschke, 1989)

$$E_{\text{pot}} = 3.6 \cdot 10^{-4} \cdot (100 - h_r) \cdot (T_a + 25) \quad (3.11)$$

3.2.4 Haude

In Germany, the simple empirical approach from Haude can be used. It based on the vapour pressure deficit at noonday δ_{13} (DVWK, 1996; Haude, 1955).

$$E_{\text{pot}} = f_H \cdot \delta_{13} \quad (3.12)$$

with a special factor for each month (Table 3-1)

Table 3-1 Monthly Haude factor for the calculation of potential evapotranspiration (DVWK, 1996)

Month	Factor f_H
October - March	0.22
April – May	0.29
June	0.28
July	0.26
August	0.25
September	0.23

The vapour pressure deficit at noon is calculated as difference between the estimated vapour pressure P_{vap}^{13} and saturated vapour pressure P_{sat}^{13} at noon (DVWK, 1996) from maximum air temperature and relative humidity

$$\begin{aligned}
 p_{sat}^{13} &= 6.1078 \cdot e^{\left(\frac{17.62 \cdot T_{max}}{243.12 + T_{max}}\right)} \\
 p_{vap}^{13} &= p_{sat}^{13} \cdot \frac{h_r}{100} \\
 \delta_{13} &= p_{sat}^{13} - p_{vap}^{13}
 \end{aligned}
 \tag{3.13}$$

3.3 CO₂ concentration

The simulations are driven by time series or given time depending functions of atmospheric CO₂ concentration per year. In the standard case the model use a constant CO₂ concentration (350 ppm). Other constant CO₂ concentrations can be set. Different time series are implemented (see Figure 3-1):

- Mauna Loa series 1959-2016
- Historical reconstruction 1765-1958
- Long-term series according to climate scenario data following the Representative Concentration Pathways (RCP) and their extensions beyond 2100, the Extended Concentration Pathways (ECP) (Meinshausen et al., 2011) from 2006 to 2500 for RCP 2.6, RCP 4.5, RCP 6.0, and RCP 8.5. The RCPs are developed for the Fifth Assessment Report of the United Nations Intergovernmental Panel on Climate Change (IPCC, 2013).

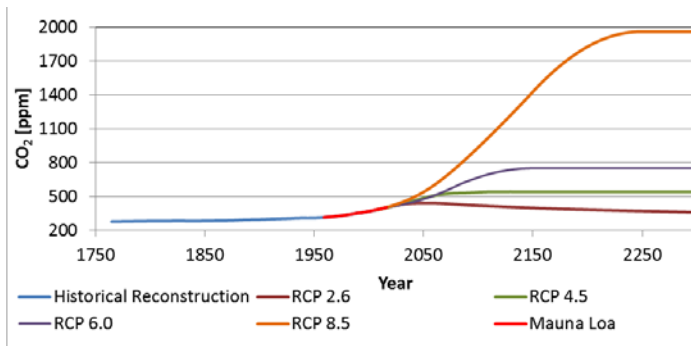


Figure 3-1 Time series of CO₂ concentration of the historical reconstruction, the Mauna Loa series and four climate scenarios.

3.4 Nitrogen deposition

Time series of ammonia and nitrate deposition can be processed by the model. The bulk deposition is added to the respective mineral nitrogen pools of the first layer and hence it is a part of the nitrogen dynamic of the soil. It is sufficient to specify the deposition at any time. Similarly, a constant value for the entire simulation period can be given. The corresponding amount is applied at the given date. Furthermore, nitrogen deposition can be

given as concentration. In this case, the deposition amount is computed with the actual precipitation and serves only as input into the soil with precipitation events.

3.5 Light absorption

The absorbed photosynthetically active radiation I_{PAR} is the fraction of global radiation R_g , which is not reflected by the albedo α_{refl}

$$I_{par} = \alpha_{refl} \eta_R R_g \quad (3.14)$$

where η_R is a factor which converts the incident radiation from $J\ cm^{-2}$ to $mol\ m^{-2}$ under the assumption that only 50 % of incident radiation are photosynthetically active.

The share of any cohort in the total stand's net photosynthetic assimilation of carbon is proportional to its share of the absorbed photosynthetically active radiation I_{PAR} .

The total fraction f_{tot}^c of I_{PAR} absorbed by each cohort c is calculated each time stand phenology changes, based on the Lambert-Beer law. There are four different models to calculate light transmission and absorption through the canopy, abbreviated by LM1, LM2, LM3 and LM4 in the following. Whereas LM1 is based on the classical gap model approach that each tree covers the whole patch with its canopy, this simplistic view is refined in LM2 by attributing each cohort/tree c a specific projected crown coverage area a_{cr}^c depending on its d_{bh} . LM2 and LM3 differ in the way the light is transmitted through the canopy and LM4 additionally introduces an average growing season sun inclination angle β .

Every time phenology changes within the stand, e.g., a species has its bud burst or leaves are colouring, the light transmission through the canopy and accordingly light absorption changes. First, the light routines of the 4C model calculate the leaf area for each cohort $c=1, \dots, n_c$ and each canopy layer $j=0, \dots, n_l$ ($l_{a,c}(j)$), respectively, based on the leaf biomass M_f available per year and cohort, total height and height of crown base. This is achieved using a leaf area – leaf dry mass relationship. Because this species specific leaf area (SLA) varies within the canopy from sun to shade leaves, an average SLA (s_{av}^c) is calculated per cohort c depending on the average relative light regime in the cohort's canopy of the previous year:

$$s_{av}^c = s_{min}^c + s_a^c \left(1 - \frac{i_c(n_l) + i_c(1)}{2} \right) \quad (3.15)$$

where s_{min}^c denotes the minimal SLA per cohort c , as it is usually found in sun leaves at the top of the canopy and s_a^c stands for the slope with which s_{av}^c rises according to the average light regime. The calculation of the relative light intensity $i_c(j)$ available in layer j for cohort c depends on the light model and is described below. The s_{av}^c rises with increasing depth of

the cohort's canopy. The s_a^c can be approximated when the SLA of shade leaves (s_{max}^c) and the SLA of sun leaves s_{min}^c are known by

$$s_{max}^c = s_{min}^c + 0.5 s_{av}^c \quad (3.16)$$

It has to be noted, however, that the average light regime as calculated in Equation (3.16) is higher than the relative light in the middle of the canopy because of the concave nature of the light extinction curve and is also usually not 0.5.

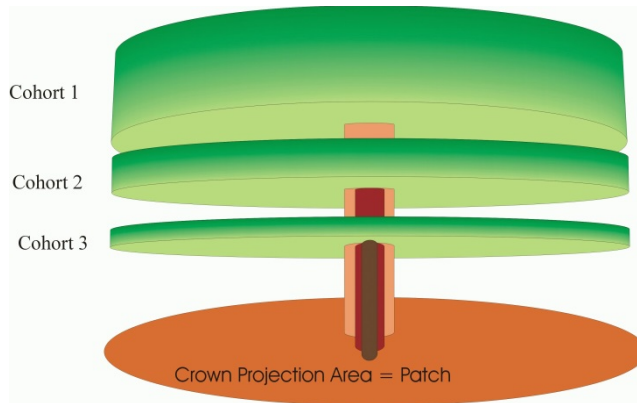


Figure 3-2 Conceptual scheme of the stand structure in LM1.

3.5.1 Light model 1 (LM1)

The first method describes the classical gap model approach that is used in most forest gap models. It assumes that the leaf area of each tree or cohort c is distributed evenly over the whole patch (Figure 3-2). All trees that have leaves in a certain layer j do mutually penetrate each other's crowns. Therefore the fraction of absorbed light $f_c(j)$ per cohort c and layer j is calculated as the total fraction of absorbed light $F_t(j)$ by all cohorts in layer j weighted by the share of leaf area of the respective cohort in this layer $l_{a,c}(j)/L_a(j)$, where $l_{a,c}(j)$ is the leaf area of cohort c in layer j and $L_a(j)$ is the total leaf area of all cohorts in layer j , i.e.

$$L_a(j) = \sum_{c=1}^{n_c} l_{a,c}(j) \quad (3.17)$$

With each cohort covering the whole patch with its canopy, each layer becomes a homogeneous structure concerning light absorption (Figure 3-3).

Therefore the relative light that is available in layer j is the same for each cohort, i.e. $i_1(j)=i_2(j)=\dots=i_{nc}(j)$, and calculated solely depending on the integrated leaf area index $L(j)$ from the top layer of the canopy n_l down to layer j (see Figure 3-3). Thus, the relative light intensity $i_c(j)$ available in layer j for cohort c is calculated as

$$i_c(j) = e^{-k L(j+1)} \quad (3.18)$$

for $j=0,1,\dots,n_l-1$ and $i_c(n_l)=1$.

k is the species specific extinction coefficient and $i_c(0)$ is the light intensity above the forest floor (Figure 3-3). The light intensity above the canopy is 100%, i.e. i_c is initialized with $i_c(n_l) = 1$ and calculated successively for the lower layers $n_l-1, n_l-2, \dots, 1$.

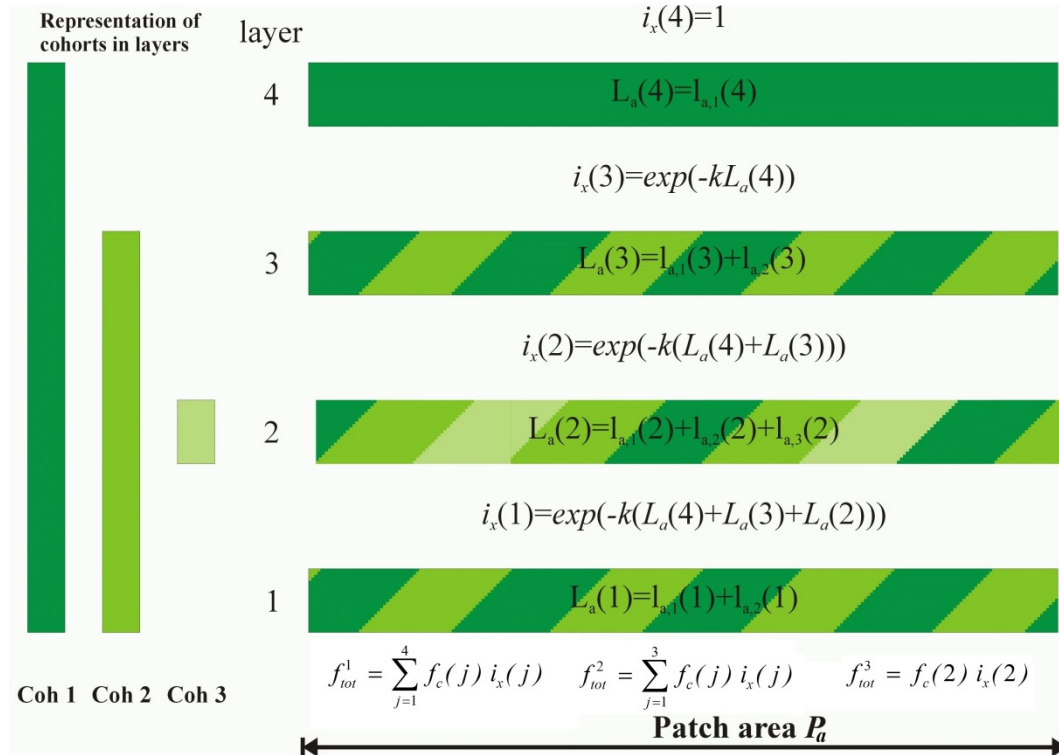


Figure 3-3 Concept of leaf area distribution and light absorption in LM1. $i_x(j)=i_1(j)=i_2(j)=i_3(j)$, $j=1,2,3,4$.

The fraction of absorbed light per cohort c and layer j becomes

$$f_c(j) = \frac{l_{a,c}(j)}{L_a(j)} (1 - e^{-k \frac{L_a(j)}{P_a}}) \quad (3.19)$$

where P_a denotes the patch size.

In order to obtain the total fraction of absorbed light f_{tot}^c of cohort c over all layers, the $f_c(j)$ have to be summed up over all layers where the respective cohort is present and modified by the available relative light in the respective layer

$$f_{tot}^c = \sum_{\substack{j=0 \\ l_{a,c}(j) \neq 0}}^{n_l} i_c(j) f_c(j) \quad (3.20)$$

$f_c(j)$ is dimensionless and can be considered as the fraction of absorbed radiation per square meter in layer j . In general this unit is arbitrary. Important is the entity this unit is related to.

In LM1 the related entity is the patch size P_a . Therefore f_{tot}^c becomes the fraction absorbed radiation (in % of total incident radiation) per square meter patch size per cohort c . In LM3, for instance, the related entity becomes the crown projection area. For reason of comparison, however, f_{tot}^c will in all light models always be related to the whole patch.

Because the extinction coefficient k is species specific and in LM1 the canopies of the different cohorts mix over the whole patch, one has to introduce some kind of average extinction coefficient in LM1, when multi-species stands are considered. Another shortcoming of LM1 is that the dominant cohort is always shading all other cohorts that are not of the same height. However, especially for young stands, cohorts of different size can well stand side by side not covering each other and receive full light. Thus LM1 seems unrealistic and leads to the concept of the crown coverage area or crown projection area (PA) (Figure 3-4).



Figure 3-4 Conceptual scheme of the stand structure in LM2-LM4.

3.5.2 Light model 2 (LM2)

The tree does in fact not cover the whole patch with its crown projection area, but the crown area is increasing with age or rather diameter. Here we use a simple species specific linear relationship between crown radius and stem diameter. Thus, the fraction of absorbed light per cohort and layer $f_c(j)$ is related to the leaf area index of the PA rather than the leaf area on the patch as in LM1. With

$$C(j) = \sum_{\substack{c=1 \\ l_{a,c}(j) \neq 0}}^{n_c} \alpha_{cr}^c \quad (3.21)$$

as the sum of all PAs of all cohorts in a certain layer, the fraction of the patch $c_c(j)$ covered by cohort c in layer j is calculated as

$$c_c(j) = \begin{cases} \frac{a_{cr}^c}{P} & \text{if } C(j) \leq P_a \\ \frac{a_{cr}^c}{C(j)} & \text{if } C(j) > P_a \end{cases} \quad (3.22)$$

The sum of all $c_c(j)$ cannot exceed 1. Therefore when the sum of the PAs of the cohorts present in layer j is larger than the size of the patch, the projection areas are related to their sum and thus ‘squeezed’ together to sum up to 1. To obtain a $f_c(j)$ that is still related to the whole patch, the light absorption in layer j has to be weighted by $c_c(j)$

$$f_c(j) = c_c(j) \left(1 - e^{-k \frac{l_{a,c}(j)}{P_a \cdot c_c(j)}} \right) \quad (3.23)$$

The total fraction of absorbed light f_{tot}^c of cohort c over all canopy layers is then obtained as in (3.20).

The introduction of a PA per cohort breaks with the assumption of the homogeneity of the canopy layer because each tree now absorbs light individually according to its leaf area index (LAI) per PA in the respective layer and extinction coefficient. To determine the relative light that is available for the next layer, the absorbed fractions of all cohorts are summed up. From this the relative light in the next layer can be calculated:

$$i_c(j-1) = i_c(j) \left(1 - \sum_{\substack{c=1 \\ l_{a,c}(j) \neq 0}}^{n_c} f_c(j) \right) \quad (3.24)$$

As in LM1 the relative light that is available in layer j is the same for each cohort, i.e. $i_1(j)=i_2(j)=\dots=i_{nc}(j)$.

The consequence of the above described approach is, in general, that the cohorts absorb less light per layer than with the algorithm of LM1. At first, however, the light absorption of the single cohort per layer is actually higher in M2 than in LM1 due to the higher LAI. The leaf area that was distributed over the whole patch is now being compressed on the crown projection area. This means that the terms in brackets in Equation (3.19) and (3.23) is higher in Equation (3.23) due to the higher exponent. The first factor, however, is in most cases higher in Equation (3.19) than in Equation (3.23). This is because even when $c_c(j)$ is small, $l_{a,c}(j)/L_a(j)$ can be larger when only few cohorts are present in layer j . The higher first factor has a larger influence than the exponent in the second expression as can be seen by differentiation and monotony considerations.

This leaves, in general, more light for the following layers and cohorts. Therefore the overall consequence of LM2 is that the dominant trees absorb less light leaving more light for the suppressed cohorts. This approach breaks the absolute dominance of the highest trees giving the smaller trees more competitive strength. Still, the lower trees cannot receive full light. In each layer the same relative light is available for all cohorts. There are no 'light gaps' in the canopy. Such light gaps are introduced in LM3.

3.5.3 Light model 3 (LM3)

Light model 3 describes the light transmission and absorption for the canopy of each tree individually. In LM3 each cohort layer receives light only from its own predecessor layers or out of light gaps within the stand's canopy. However, the model is still a point model, i.e. the single cohorts have no defined spatial location within the patch area.

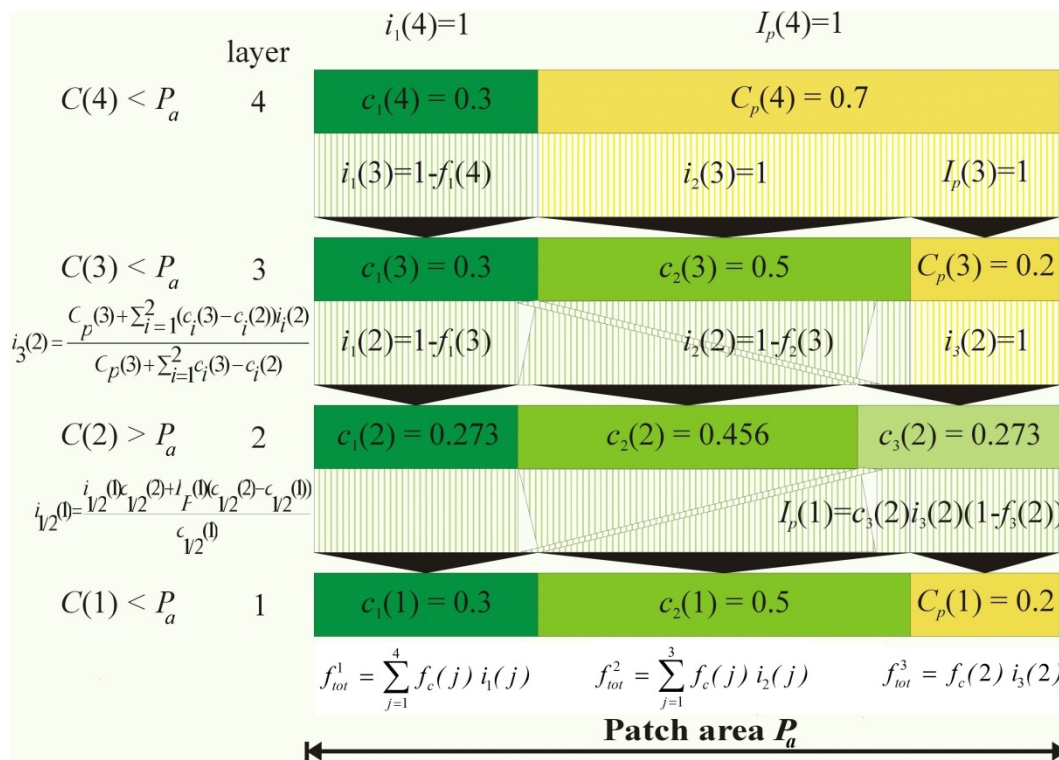


Figure 3-5 Concept of leaf area distribution and light absorption in LM3

The fraction of the patch that is not covered by trees, i.e. the difference between the sum of all PAs of all cohorts in a certain layer $C(j)$ (Equation (3.21)) and patch size P_a normed by P_a , is introduced as a pool with its own light regime. Thus

$$C_p(j) = \max\left(\frac{P_a - C(j)}{P_a}, 0\right) \quad (3.25)$$

is the fraction of the patch not covered by the PAs of the cohorts in layer j and $I_p(j)$ is defined as the relative light intensity that is available within this pool. The pool $C_p(j)$ is the area that is assigned to new cohorts that appear when the calculation of light transmission and absorption runs from the top layer to the bottom layer of the canopy. Now, a cohort can still receive 100% light intensity relative to the top of the canopy even when it is not present in the highest layers (e.g. $i_3(2)=1$ in Figure 3-5). This concept reflects the observation that trees in the lower canopy do normally not stand under the dominant trees but rather grow within gaps to reach the top canopy. Suppressed trees that grow right under a dominant tree receive not enough light to survive.

To maintain a closed light balance three special cases have to be considered. Firstly, the PAs of the cohorts do not change between two layers. Secondly, the PAs of the cohorts decrease when the sum of all PAs become larger than the patch size and therefore the PAs are squeezed together to fit the patch (see Equation (3.22)). Thirdly, the PAs of the cohorts increase again to their original size. In each of these cases light has to be distributed differently between cohorts and the pool. The three cases are also illustrated in Figure 3-5. For the highest canopy layer of a cohort (Figure 3-5 cohort 1 in layer 4, cohort 2 in layer 3, cohort 3 in layer 3)

$$i_c(j) = I_p(j) \quad (3.26)$$

The fraction of absorbed light per cohort is always calculated as

$$f_c(j) = \begin{cases} 1 - e^{-k \frac{I_{a,c}(j)}{P_a c_c(j)}} & \text{if } C(j) \leq P_a \\ \frac{P}{C(j)} \left(1 - e^{-k \frac{I_{a,c}(j)}{P_a c_c(j)}} \right) & \text{if } C(j) > P_a \end{cases} \quad (3.27)$$

Here the $f_c(j)$ denotes the fraction of absorbed light per PA in contrast to Equation (3.19) of LM1 and Equation (3.23) of LM2 that were related to P_a . However, if $C(j) > P_a$ there still is a modification factor needed because the PA is reduced because the PAs of all cohorts do not fit on the predefined patch size. In general, the patch size P_a can be enlarged such that all PAs can always fit on the patch. This, however, is not realistic because then no competition for light takes place.

First case:

$$c_c(j) = c_c(j-1) \quad \forall c \text{ and } \{c(j) | I_{a,c}(j) \neq 0\} = \{c(j-1) | I_{a,c}(j-1) \neq 0\}$$

∨

$$(C(j) < P_a \wedge C(j-1) < P_a)$$

The second sub case is illustrated in Figure 3-5. The number of cohorts changes from layer 4 to layer 3 but there still is enough space on the patch such that the PA of both cohorts fit on the patch. In this first case the light available for the next layer of each cohort that also has leaves in the next layer is

$$i_c(j-1) = i_c(j) \cdot (1 - f_c(j)) \quad (3.28)$$

In case a number $d_c(j)$ of trees of a cohort c has no leaves in layer $j-1$ (cohort No. 3 in layer 1 of Figure 3-5) then the light leaving the layer of those trees is fed into the pool weighted by their patch coverage area $c_c(j)$. Thus,

$$I_p(j-1) = \frac{1}{C_p(j) + \sum_{c=1}^{n_c} d_c(j) \cdot c_c(j)} \left(C_p(j) \cdot I_p(j) + \sum_{c=1}^{n_c} d_c(j) \cdot c_c(j) \cdot i_c(j-1) \right) \quad (3.29)$$

Second case:

$$C(j+1) \leq P_a \wedge C(j) > P_a \text{ (Figure 3-5 transition from layer 3 to layer 2)}$$

In this case $c_c(j+1) > c_c(j) \forall c$ with $I_{a,c}(j+1) = I_{a,c}(j)$ because of Equation (3.22). The fraction of the patch that will be covered by the new cohorts $C_n(j)$ consists of the pool in layer $j+1$ plus the fraction that is lost by the other cohorts due to new PAs.

$$C_n(j) = C_p(j+1) + \sum_{\substack{c=1 \\ I_{a,c}(j+1) \neq 0 \\ I_{a,c}(j) \neq 0}}^{n_c} n_a^c (c_c(j+1) - c_c(j)) \quad (3.30)$$

n_a^c is the number of trees in cohort c . The relative light that is available for the new cohorts in this layer is the average from $I_p(j+1)$ and from the other cohorts weighted by the area they contribute to the area covered by the new cohorts.

$$I_p(j) = \frac{1}{C_n(j)} \left(C_p(j+1) \cdot I_p(j+1) + \sum_{\substack{c=1 \\ I_{a,c}(j+1) \neq 0 \\ I_{a,c}(j) \neq 0}}^{n_c} n_a^c (c_c(j+1) - c_c(j)) \cdot i_c(j) \right) \quad (3.31)$$

Then $i_c(j)$ for the new cohorts can be calculated using Equation (3.26).

Third case:

$$C(j+1) > P_a \wedge C(j) \leq P_a$$

Here the full PA requirements for each cohort can be met again (Figure 3-5 transition from layer 2 to 1). For all new cohorts apply Equation (3.26) and (3.27) where $I_p(j)$ is calculated as in Equation (3.29) with $C_p(j)=0$. For all other cohorts

$$i_c(j) = \frac{1}{c_c(j)} (i_c(j) \cdot c_c(j+1) + I_p(j) \cdot (c_c(j) - c_c(j+1))) \quad (3.32)$$

This completes the description of all possible cases of how light is transferred and absorbed through the canopy in LM3.

As mentioned above $f_c(j)$ in LM3 is related to the PA rather than to P_a as in LM1 and LM2. To make all light models comparable in terms of light absorption f_{tot}^c is related to the PA

$$f_{tot}^c = \sum_{\substack{j=1 \\ I_{a,c}(j) \neq 0}}^{n_j} f_c(j) \cdot i_c(j) \cdot c_c(j) \quad (3.33)$$

In case the bottom layer of a cohort is higher than the top layer of another cohorts, the lower cohort can never receive full light even stand density would allow for that. This is because the light of the lowest layer of a cohort is always mixed into the pool (see Equation (3.29)). There are no separate pool for real stand gaps and the understory of a stand. They could be introduced, however.

3.5.4 Light model 4 (LM4)

Light model 4 (LM4) is the next extension to LM3. In LM4 a sun inclination angle β is introduced. In general, this increases the LAI that is passed through by the incident radiation and thus the absorbed radiation is also increased. To keep the calculations as efficient as possible some simplifying assumption are made.

- Because light absorption is only calculated when the phenology of the stand changes and not every day, an average sun inclination angle over the vegetation period is assumed. Because the length of the vegetation period is not (yet) calculated in advance a fixed average vegetation period starting DOY 120 and ending DOY 280 is assumed.
- The geometry of a tree crown layer is assumed to be a quadratic cuboid with a side length of l and height z that is directed perpendicularly to the sun. A simulation study was conducted to estimate the difference in absorbed radiation when the crown layer was assumed to be a circular disk or a cuboid (results not shown). The difference was found to be negligible and because of the easier mathematics of a cuboid in terms of light absorption this geometry was preferred.

In general, in LM4 the same three cases as in LM3 occur. The light balance between the layers is calculated as in LM3. However, for the light absorption within the layers some special cases have to be considered additionally. The simplest situation is illustrated in Figure 3-6.

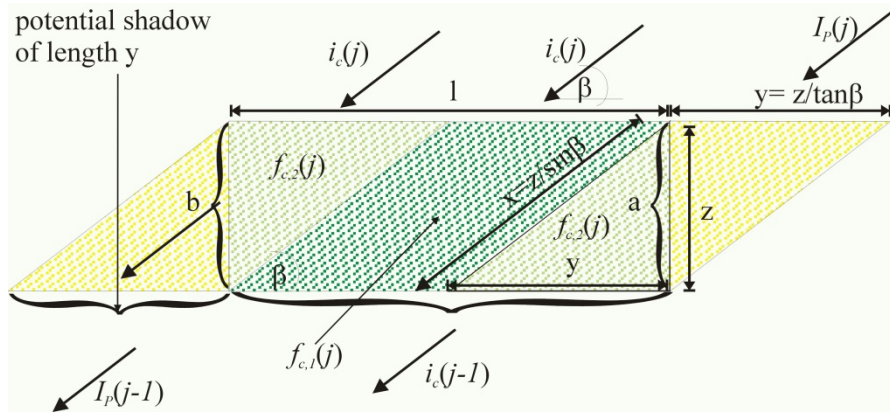


Figure 3-6 Conceptual scheme of a tree layer cuboid with height z and side length $l_c(j)$. Light falls through the cuboid with inclination β . The areas where light absorption is calculated differently are indicated by different green colours and labelled $f_{c,i}(j)$. The region with yellow colour indicated light from and into the pool $I_p(j)$. Represented is the case $c_p(j) \geq \frac{1}{P_a} \sum_{c=1}^{n_c} l_c(j) \cdot y \cdot n_{a,c}$ and $y \leq l_c(j)$.

Each crown layer j of cohort c is assumed to be a quadratic cuboid of height z and side length $l_c(j)$ that is derived from the crown PA in this layer $c_c(j)$. Further assuming an average sun inclination angle β and a perpendicular direction of the cuboid towards the sun, the light rays fall on the top and on exactly one side a of the cuboid and leaving the cuboid on the bottom and side b , opposite to side a , as indicated in Figure 3-6. Two distinct regions of the cuboid can be identified that are displayed in light and dark green in Figure 3-6. In the dark region, the light falling on the top of the tree layer crosses the cuboid on the longest possible way. In this region the fraction of absorbed radiation is calculated as

$$f_{c,1}(j) = 1 - e^{-k \frac{l_{a,c}(j)}{P_a \cdot c_c(j) \cdot \sin \beta}} \tag{3.34}$$

similar to Equation (3.27), only that here the crossed LAI ($l_{a,c}(j)/(P_a c_c(j))$) is increased by the sun inclination through $\sin \beta$. For a sun inclination angle of 90° Equation (3.34) equals Equation (3.27). For those regions of the cuboid where either light penetrates from the side (side a) and leaves at the bottom of the tree layer or penetrates the top and leaves on side b , the LAI that the light passes through changes with the location where a hypothetical light beam hits the cuboid. Thus, for the light that falls onto the side a of the cuboid the passed LAI increases with the height of side a where the light beams penetrates the cuboid. The average fraction of absorbed light for this region is averaged over all possible LAIs within this region or over y , thus

$$\begin{aligned}
 f_{c,2}(j) &= \frac{1}{y} \int_0^y 1 - e^{-k \frac{l_{a,c}(j)}{P_a \cdot c_c(j) \cdot \sin \beta} t} dt \\
 &= 1 + \frac{P_a \cdot c_c(j) \cdot \sin \beta}{k l_{a,c}(j)} \left(e^{-k \frac{l_{a,c}(j)}{P_a \cdot c_c(j) \cdot \sin \beta} y} - 1 \right) \\
 &= 1 - \frac{P_a \cdot c_c(j) \cdot \sin \beta}{k l_{a,c}(j)} f_{c,1}(j)
 \end{aligned} \tag{3.35}$$

The same average fraction of absorbed light leaves the cuboid at the side b . It does not matter whether $f_{c,2}(j)$ is averaged horizontally over y or vertically over z . In the following it will always be integrated horizontally in similar situations. For the total fraction of absorbed light per tree in layer j (related to patch size P_a) we obtain

$$f_c(j) = \frac{1}{P_a} \left((l - y) \cdot l_c(j) \cdot f_{c,1}(j) \cdot i_c(i) + y l_c(j) \cdot (f_{c,2}(j) \cdot i_c(j) + f_{c,2}(j) \cdot l_p(j)) \right) \tag{3.36}$$

Further we obtain for the available light for the next layer of this cohort

$$i_c(i-1) = \frac{1}{l_c(j)} \left((l_c(j) - y) \cdot i_c(j) \cdot (1 - f_{c,1}(j)) + y \cdot l_p(j) \cdot (1 - f_{c,2}(j)) \right) \tag{3.37}$$

and the pool of the next layer similar to Equation (3.29)

$$\begin{aligned}
 I_p(j-1) &= \frac{1}{C_p(j) + \sum_{c=1}^{n_c} d_c(j) \cdot c_c(j)} \cdot \\
 &\left(I_p(j) \cdot \left(C_p(j) - \frac{1}{P_a} \sum_{c=1}^{n_c} l_c \cdot (j) \cdot y \cdot n_a^c \right) + \right. \\
 &\left. \sum_{c=1}^{n_c} (d_c(j) \cdot c_c(j) \cdot i_c(j-1)) + \frac{1}{P_a} (l_c(j) \cdot y \cdot n_a^c (1 - f_{c,2}(j)) \cdot i_c(j)) \right)
 \end{aligned} \tag{3.38}$$

Equations (3.34) and (3.35) describe the light absorption in a cuboid as displayed in Figure 3-6. Here $y \leq l_c(j)$. In case that $y > l_c(j)$ (Figure 3-7) no light that falls on the top of a tree layer leaves the bottom but only in region b of the cuboid.

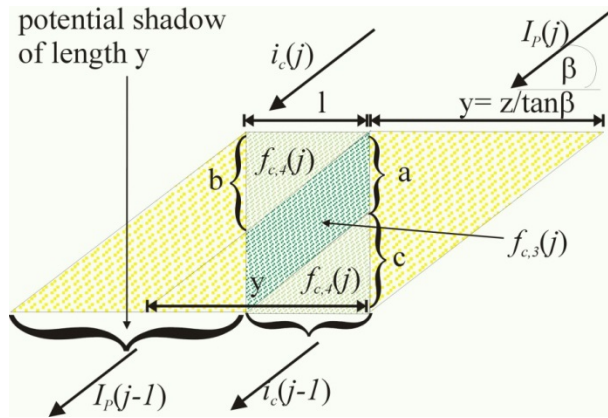


Figure 3-7 Conceptual scheme of a tree layer cuboid. Represented is the case $c_p(j) \geq \frac{1}{P_a} \sum_{c=1}^n l_c(j) y n_c^c$ and $y > l_c(j)$

This case occurs when either z or $l_c(j)$ is small. The light that falls onto one side and leaves the other side (region a coloured in dark green in Figure 3-7) passes a constant LAI. Light absorption in this region is calculated similar to Equation (3.34) as

$$f_{c,3}(j) = 1 - e^{-k \frac{l_{a,c}(j) \cdot l_c(j)}{P_a \cdot c_c(j) \cdot y \cdot \sin \beta}} \quad (3.39)$$

Absorption of the light that falls onto one side and leaves the cuboid at the bottom (region c coloured in light green in Figure 3-7) or light the falls on the top of the cuboid and leaves in region b is calculated as

$$\begin{aligned} f_{c,4}(j) &= \frac{1}{l_c(j)} \int_0^{l_c(j)} 1 - e^{-k \frac{l_{a,c}(j) \cdot t}{P_a \cdot c_c(j) \cdot y \cdot \sin \beta}} dt \\ &= 1 + \frac{P_a \cdot c_c(j) \cdot y \cdot \sin \beta}{k \cdot l_{a,c}(j) \cdot l_c(j)} \left(e^{-k \frac{l_{a,c}(j) \cdot l_c(j)}{P_a \cdot c_c(j) \cdot y \cdot \sin \beta}} - 1 \right) \\ &= 1 - \frac{P_a \cdot c_c(j) \cdot y \cdot \sin \beta}{k \cdot l_{a,c}(j) \cdot l_c(j)} f_{c,3}(j) \end{aligned} \quad (3.40)$$

For the total fraction of absorbed light per tree in layer j (related to patch size P_a) we obtain

$$f_c(j) = \frac{1}{P_a} \left((y - l) \cdot l \cdot f_{c,3}(j) \cdot I_p(i) + l^2 \left(f_{c,4}(j) \cdot i_c(j) + f_{c,4}(j) \cdot I_p(j) \right) \right) \quad (3.41)$$

Here the light available for the next layer of cohort c is

$$i_c(i - 1) = I_p(j) \cdot (1 - f_{c,4}(j)) \quad (3.42)$$

And the average light intensity for the pool available for the next layer is calculated as

$$I_p(j-1) = \frac{1}{C_p(j) + \sum_c d_c(j) \cdot c_c(j)} \left(\left(C_p(j) - \frac{1}{P_a} \sum_c l_c(j) \cdot y \cdot n_a^c \right) I_p(j) + \sum_c d_c(j) \cdot c_c(j) \cdot i_c(j-1) + \frac{1}{P_a} \left(\sum_c l_c(j) \cdot (y - l_c(j)) \cdot n_a^c (1 - f_{c,3}(j)) \cdot I_p(j) + \sum_c (l_c(j))^2 \cdot n_a^c (1 - f_{c,4}(j)) \cdot i_c(j) \right) \right) \quad (3.43)$$

All the above equations apply for the situation $C_p(j) \geq \frac{1}{P_a} \sum_c l_c(j) \cdot y \cdot n_a^c$, i.e. when the area of all shadow casts of all trees is not larger than the area not covered by trees in this layer, i.e. the pool $C_p(j)$. In dense stands, however, it can be the case that $C_p(j) < \frac{1}{P_a} \sum_c l_c(j) \cdot y \cdot n_a^c$. It can even occur that $C_p(j)=0$ as also described for LM3. This situation is illustrated in Figure 3-8.

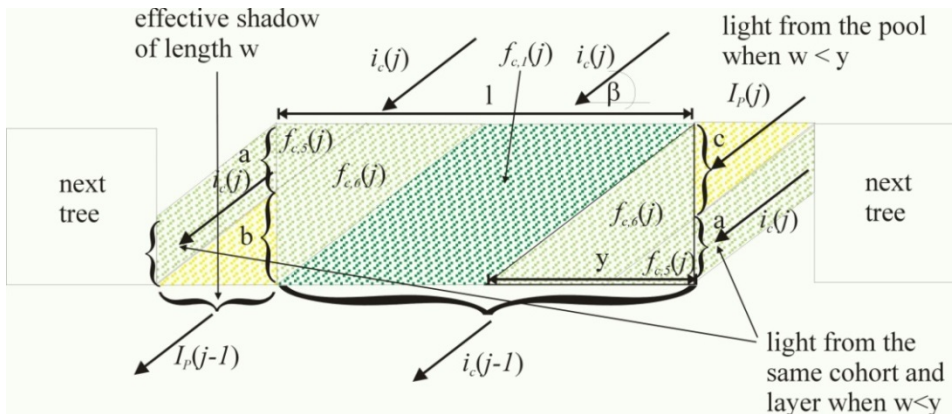


Figure 3-8 Conceptual scheme of a tree layer cuboid. Represented is the case $C_p(j) < \frac{1}{P_a} \sum_{c=1}^{n_c} l_c(j) \cdot y \cdot n_a^c$ and $y \leq l_c(j)$

Only part of the light that leaves the cuboid on the side (region *b* in Figure 3-8) is available for the pool of the next layer (yellow area in Figure 3-8). The length of this region is called the effective shadow cast $w(j)$ in layer j and is calculated as

$$w(j) = y \frac{C_p(j)}{\frac{1}{P_a} \sum_c l_c(j) \cdot y \cdot n_a^c} \quad (3.44)$$

Light leaving the side of the cuboid in region *a* in Figure 3-8 is not available for the pool but hits the cuboid of the next tree in Figure 3-8. According to the structural concept of the stand that does not associate an exact position of each tree on the patch but rather a mere

PA the neighbouring tree is not determined. Thus, the light leaving the side of the cuboid in region a is fed into the same cohort again on the opposite side of the cuboid, also indicated as region a in Figure 3-8. Light penetrating one side of the cuboid at region c is assumed to come from the pool (Figure 3-8). If $C_p(j)=0$ this region is also zero and all light leaving the cuboid on the one side is used as input for the other side. This way the light absorption of each tree can be calculated separately without knowing the tree's neighbours and the light balance remains closed.

Again, the two cases $y \leq l_c(j)$ and $y > l_c(j)$ have to be considered.

The case $y \leq l_c(j)$:

To calculate the total fraction of absorbed light for this layer, at first, the absorbed light in region a in Figure 3-8 has to be determined.

$$\begin{aligned}
 f_{c,5}(j) &= \frac{1}{y-w(j)} \int_0^{y-w(j)} 1 - e^{-k \frac{l_{a,c}(j) \cdot t}{P_a \cdot c_c(j) \cdot y \cdot \sin \beta}} dt \\
 &= 1 + \frac{P_a \cdot c_c(j) \cdot y \cdot \sin \beta}{k \cdot l_{a,c}(j) \cdot (y-w(j))} \left(e^{-k \frac{l_{a,c}(j) \cdot (y-w(j))}{P_a \cdot c_c(j) \cdot y \cdot \sin \beta}} - 1 \right)
 \end{aligned} \tag{3.45}$$

The average light intensity that leaves the cuboid in region b in Figure 3-8 is

$$\begin{aligned}
 f_{c,6}(j) &= \frac{1}{w(j)} \int_{y-w(j)}^y 1 - e^{-k \frac{l_{a,c}(j) \cdot t}{P_a \cdot c_c(j) \cdot y \cdot \sin \beta}} dt \\
 &= 1 + \frac{P_a \cdot c_c(j) \cdot y \cdot \sin \beta}{k l_{a,c}(j) \cdot w(j)} \left(e^{-k \frac{l_{a,c}(j)}{P_a \cdot c_c(j) \cdot \sin \beta}} - e^{-k \frac{l_{a,c}(j) \cdot (y-w(j))}{P_a \cdot c_c(j) \cdot y \cdot \sin \beta}} \right) \\
 &= 1 + \frac{P_a \cdot c_c(j) \cdot y \cdot \sin \beta}{k l_{a,c}(j) \cdot w(j)} \left(1 - f_{c,1}(j) - e^{-k \frac{l_{a,c}(j) \cdot (y-w(j))}{P_a \cdot c_c(j) \cdot y \cdot \sin \beta}} \right)
 \end{aligned} \tag{3.46}$$

Thus,

$$f_c(j) = \frac{1}{P_a} \left((l-y) \cdot l \cdot f_{c,1}(j) \cdot i_c(j) + (y-w) \cdot l \cdot f_{c,5}(j) \cdot \left(i_c(j) + (1-f_{c,5}(j)) \cdot i_c(j) \right) + w \cdot l \cdot f_{c,6}(j) \cdot (i_c(j) + l_p(j)) \right) \tag{3.47}$$

and

$$i_c(i-1) = \frac{1}{l} \left((l-y) \cdot i_c(j) \cdot (1-f_{c,1}(j)) + w \cdot I_p(j) \cdot (1-f_{c,6}(j)) + (y-w) \cdot (1-f_{c,5}(j))^2 \cdot i_c(j) \right) \quad (3.48)$$

and

$$I_p(j-1) = \frac{1}{C_p(j) + \sum_c d_c(j) \cdot c_c(j)} \left(\sum_c d_c(j) \cdot c_c(j) \cdot i_c(j-1) + \frac{1}{P} \left(\sum_c w(j) \cdot l_c \cdot (j) \cdot n_a (1-f_{c,6}(j)) \cdot i_c(j) \right) \right) \quad (3.49)$$

The case $y > l_c(j)$:

This case has two sub cases that are illustrated in Figure 3-9.

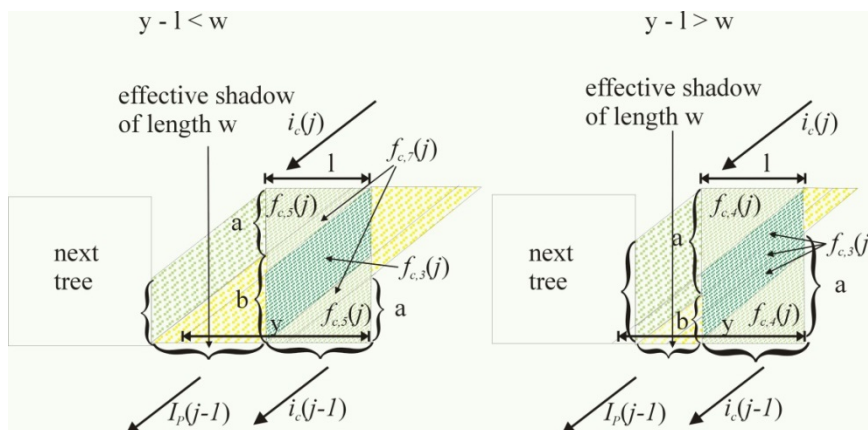


Figure 3-9 Conceptual scheme of a tree layer cuboid. Represented is the case

$$C_p(j) < \frac{1}{P_a} \sum_{c=1}^n l_c(j) \cdot y \cdot n_a^c \text{ and } y > l_c(j) \text{ with two sub cases: } y-l \leq w \text{ and } y-l > w.$$

The first case can be characterized by the condition $y - l \leq w$. As a consequence some light that hits the top of the tree layer is again fed into the pool. Additional light that leaves the tree layer in region a is used as input from the side comes exclusively from the top of the cuboid. In the second case $y - l > w$ (see Figure 3-9) the gap between the cohorts w is so small that light that leaves the tree layer in region a and is used as input from the side comes partly from the pool, i.e. from the side.

It is clear that the concept of using light that leaves the one side as input for the other side has its limits. This concept does not work in the case when first $y > l_c(j)$ and second, light that leaves the tree layer in region a partly uses light from region a of the opposite side, i.e. the

light intensity in region a is determined by itself. This case occurs when $y - w > w + l$ (see Figure 3-10).

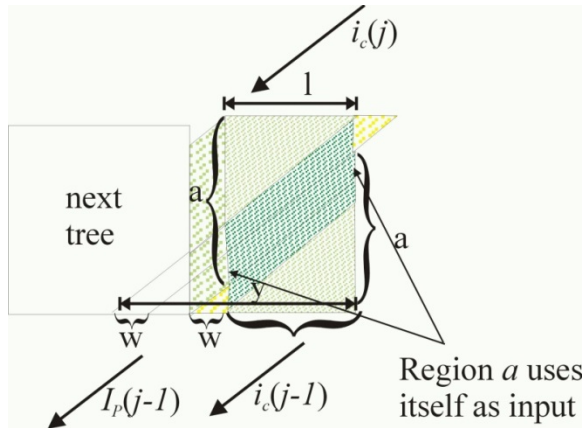


Figure 3-10 Conceptual scheme of a tree layer cuboid. Represented is the case $y - w > w + l$.

First sub case $y - l \leq w$:

The absorbed light in region a is the same as in Equation (3.45), i.e. $f_{c,5}(j)$. The absorbed light in region b that is further used for the light pool comes from two sources. The first part comes from the top of the cuboid

$$f_{c,7}(j) = \frac{1}{l_c(j) - y + w} \int_{y-w}^{l_c(j)} 1 - e^{-k \frac{l_{a,c}(j) \cdot t}{P_a \cdot c_c(j) \cdot y \cdot \sin \beta}} dt \quad (3.50)$$

$$= 1 + \frac{P_a \cdot c_c(j) \cdot y \cdot \sin \beta}{k l_{a,c}(j) \cdot (l_c(j) - y + w(j))} \left(e^{-k \frac{l_{a,c}(j) \cdot l_c(j)}{P_a \cdot c_c(j) \cdot y \cdot \sin \beta}} - e^{-k \frac{l_{a,c}(j) \cdot (y-w(j))}{P_a \cdot c_c(j) \cdot y \cdot \sin \beta}} \right)$$

and the second part has the light from the pool as its source. The absorption in this part is calculated according to Equation (3.39), i.e. $f_{c,3}(j)$.

Thus,

$$f_c(j) = \frac{1}{P_a} \left(\begin{aligned} & (l_c(j) - y + w) \cdot l_c(j) \cdot f_{c,7}(j) \cdot (i_c(j) - I_p(j)) + \\ & (y - l_c(j)) \cdot l_c(j) \cdot f_{c,3}(j) \cdot I_p(j) + \\ & (y - w) \cdot l_c(j) \cdot f_{c,5}(j) \cdot (i_c(j) + (1 - f_{c,5}(j)) \cdot i_c(j)) \end{aligned} \right) \quad (3.51)$$

and

$$i_c(i-1) = \frac{1}{l_c(j)} \left((l_c(j) - y + w) \cdot (1 - f_{c,7}(j)) \cdot I_p(j) + (y - w) \cdot (1 - f_{c,5}(j))^2 \cdot i_c(j) \right) \quad (3.52)$$

and

$$I_p(j-1) = \frac{1}{C_p(j) + \sum_{c=1}^{n_c} d_c(j) \cdot c_c(j)} \left(\sum_{c=1}^{n_c} \left(\frac{1}{P_a} \left(d_c(j) \cdot c_c(j) \cdot i_c(j-1) + \left((y - l_c(j)) \cdot l_c(j) \cdot n_a^c (1 - f_{c,3}(j)) \cdot I_p(j) + (l_c(j) - y + w) \cdot l_c(j) \cdot (1 - f_{c,7}(j)) \cdot i_c(j) \right) \right) \right) \right) \quad (3.53)$$

Second sub case $y - l > w$:

The absorbed light in region a comes from the top of the cube as well as from the pool. The absorbed light that comes from the top of the cube is calculated as in Equation (3.40) and the part, which comes from the pool, is calculated according to Equation (3.39).

The light average light absorption in region a is

$$f_{c,8}(j) = \frac{1}{y - w} (l_c(j) \cdot f_{c,4}(j) + (y - w - l_c(j)) \cdot f_{c,3}(j)) \quad (3.54)$$

It follows

$$f_c(j) = \frac{1}{P_a} \left(\begin{aligned} & l_c^2(j) \cdot f_{c,4}(j) \cdot i_c(j) + w \cdot l_c(j) \cdot f_{c,3}(j) \cdot I_p(j) + \\ & l_c^2(j) \cdot f_{c,4}(j) \cdot (1 - f_{c,8}(j)) \cdot (l_c(j) \cdot i_c(j) + (y - w - l) \cdot I_p(j)) + \\ & (y - l_c(j) - w(j)) \cdot f_{c,3}(j) \cdot (1 - f_{c,8}(j)) \cdot (l_c(j) \cdot i_c(j) + (y - w - l) \cdot I_p(j)) \end{aligned} \right) \quad (3.55)$$

and

$$i_c(j-1) = (1 - f_{c,4}(j)) \cdot (1 - f_{c,8}(j)) \cdot (l_c(j) \cdot i_c(j) + (y - w - l) \cdot I_p(j)) \quad (3.56)$$

and

$$I_p(j-1) = \frac{1}{C_p(j) + \sum_{c=1}^{n_c} d_c(j) \cdot c_c(j)} \cdot \left(\left(d_c(j) \cdot c_c(j) \cdot i_c(j-1) + \sum_{c=1}^{n_c} \frac{1}{P_a} \left(\begin{aligned} &(2w - y + l_c(j)) \cdot l_c(j) \cdot n_a^c(j) \cdot (1 - f_{c,3}(j)) \cdot I_p(j) + \\ &(y - w - l_c(j)) \cdot l_c(j) \cdot (1 - f_{c,3}(j)) \cdot (1 - f_{c,8}(j)) \cdot \left(\frac{l_c(j) \cdot i_c(j) + (y - w - l) \cdot I_p(j)}{2} \right) + \\ &l_2^2(j) \cdot (1 - f_{c,4}(j)) \cdot (1 - f_{c,8}(j)) \cdot (l_c(j) \cdot i_c(j) + (y - w - l) \cdot I_p(j)) \end{aligned} \right) \right) \right) \quad (3.57)$$

The total fraction of absorbed light per cohort per unit patch area is for all cases calculated as for LM3 (Equation (3.33))

4 DRY MATTER PRODUCTION AND GROWTH

4.1 Phenology

4.1.1 Promotor-Inhibitor-Model

The phenology model is based on simple interactions between inhibitory and promotory agents that are assumed to control the developmental status of a plant. The abundance or concentration of certain enzymes in cells is determined by the rates of synthesis and breakdown. Control of these processes is subject to a lot of research, however, it is known that temperature and photoperiod play a prominent role. Temperature, for instance, can act through pure physical mechanisms like its influence on viscosity and diffusion. Moreover, synthesis of proteins usually has an activation energy or temperature and an optimal temperature beyond that synthesis rates decrease again (Johnson and Thornley, 1985; Vegis, 1973). Photoperiod has been observed to be the driving force of a biochemical trigger acting through the photochromic system (Heide, 1993a; Heide, 1993b; Nitsch, 1957; Perry, 1971; Wareing, 1956). From these simple but basic principles a model for the abundance or concentration of an inhibitory compound I_{phen} and a promotory compound P_{phen} can be formulated as a system of two simple coupled difference equations:

$$\begin{aligned}\Delta I_{phen} &= p_1 f_1(T) g_1(d_l) - p_2 f_2(T) g_2(d_l) I_{phen} \\ \Delta P_{phen} &= p_3 f_3(T) g_3(d_l) (1 - I_{phen}) - p_4 f_4(T) g_4(d_l) P_{phen}\end{aligned}\quad (4.1)$$

where p_i are scaling parameters and the f_i and g_i , $i = 1, \dots, 4$, are functions of air temperature T_a and photoperiod (day length) d_l , respectively. Temperature T_a and photoperiod d_l are themselves functions of time, in our case of the day of the year. Breakdown of the compounds P_{phen} and I_{phen} , indicated by the negative terms in Equation (4.1), is assumed to be a first order reaction, whereas the synthesis terms, indicated by the positive terms in Equation (4.1), are formulated as simple forcing terms. The synthesis term of the promotor P_{phen} is coupled to or rather damped by the presence of the inhibitor I_{phen} . P_{phen} and I_{phen} are normalized arbitrarily to vary between one and zero.

To obtain an applicable model, assumptions about the parameters, functions, boundary and initial conditions have to be made: we let the model start at t_0 , the observed date of leaf colouring of the previous year. For reason of simplicity, on this date rest is assumed to be deepest. That means we assume the maximal concentration of inhibitory substances and minimal abundance of promotory compounds, setting $I_{phen}(t_0) = 1$ and $P_{phen}(t_0) = 0$. Bud burst takes place when P_{phen} reaches the threshold $P_{phen} = 1$.

Following the observation that almost all physiological processes have a minimum, optimal and maximum temperature, the temperature dependence of the functions f_i are modelled as a triangular function (Hänninen, 1995) where

$$f_i(T) = \begin{cases} \frac{T_a - T_{i,min}}{T_{i,opt} - T_{i,min}} & \text{for } T_{i,min} \leq T_a \leq T_{i,opt} \\ \frac{T_{i,max} - T_a}{T_{i,max} - T_{i,opt}} & \text{for } T_{i,opt} \leq T_a \leq T_{i,max} \\ 0 & \text{else} \end{cases} \quad (4.2)$$

for $i = I, P$ with T being daily mean temperature and $T_{i,min}$, $T_{i,opt}$, $T_{i,max}$ fixed temperature thresholds that are different for each f_i .

Since photoperiod is another important factor influencing tree phenology, the functions g_i are assumed as a day length d_i dependent function, i.e. they are set as either $d_i/24$ or $(24-d_i)/24$, depending on whether the process is assumed to be promoted by long days or long nights. Breakdown of inhibitor is assumed to be accelerated by long days, whereas build-up of inhibitor is assumed to be supported by long nights. The contrary is assumed for the promotor P_{phen} . Synthesis of the promotor is favoured by long days and breakdown of P_{phen} is accelerated by long nights (Nitsch, 1957; Perry, 1971; Wareing, 1956).

Table 4-1 Promotor-Inhibitor Models (PIMs) derived from the general framework in Equation (4.1) and the imposed restrictions described in the paragraph above. ΔI_{phen} , ΔP_{phen} rates of change of the inhibitor I and promotor P_{phen} . f_i ($i = I, P$) are temperature dependent triangular functions according to Equation (4.1) for the inhibitor I_{phen} and promotor P_{phen} , respectively, each having three parameters T_{min} , T_{opt} , T_{max} . p_i ($i = 1, \dots, 4$) are scaling parameters. $I_{phen}(t_0) = 1$, $P_{phen}(t_0) = 0$. time step: one day. $t_0 =$ day of leaf colouring the previous year. Bud burst: $P_{phen} > 1$

PI M No.	Inhibitor Model	Promotor Model
1	$\Delta I_{phen} = -p_2 f_i(T_a) I_{phen}$	$\Delta P_{phen} = \frac{p_3 f_p(T_a) (1 - I_{phen}) - p_4 P_{phen} (24 - d_i)}{24}$
2	$\Delta I_{phen} = \frac{-p_2 f_i(T_a) I_{phen} d_i}{24}$	$\Delta P_{phen} = \frac{p_3 f_p(T_a) (1 - I_{phen}) d_i}{24} - \frac{p_4 P_{phen} (24 - d_i)}{24}$
3	$\Delta I_{phen} = \frac{p_1 (24 - d_i)}{24} - \frac{p_2 f_i(T_a) I_{phen} d_i}{24}$	$\Delta P_{phen} = \frac{p_3 f_p(T_a) (1 - I_{phen}) d_i}{24}$

To keep the number of parameters as low as possible some restrictions were introduced in the general framework of Equation (4.1). It was imposed that $f_1(T_a) = f_4(T_a) = 1$, i.e. the forcing term of the inhibitor I_{phen} and the breakdown term of the promotor P_{phen} only depend on photoperiod. Hereinafter it holds $f_2 = f_i$ and $f_3 = f_p$. Further it was imposed that either p_1 or p_4 is zero. This resulted in 12 possible models each one having nine parameters (Schaber, 2002b). The three models used in 4C are listed in Table 4-1 and are called Promotor-Inhibitor model (PIM) in the following.

For each species it was determined which of these model formulations best suited the observed dates of bud burst (BB) and corresponding course of temperature and day length.

The different favoured model structures for each species indicated that for the late spring phases (BB of *F. sylvatica* and *Q. robur*) the photoperiod played a more dominant role than for early spring phases (BB of *B. pendula*). Chilling only plays a subordinate role for spring BB compared to temperatures preceding BB. The modelling approach allowed for a species specific weighting of the dominating processes.

Table 4-2 Parameter values for the PIMs. For a description of the parameters see Equation (4.2) and Table 4-1 . min, max: allowed ranges for the parameters during model fits. min SSR: Parameters for the PIM that performed best in terms of SSR (sum of squared residuals) for model fitting. mean: Average parameters after ten optimisation runs. stderr: Standard error of the average parameters after ten optimisation runs.

		f_I					f_P				
		$T_{I,min}$	$T_{I,opt}$	$T_{I,max}$	ρ_1	ρ_2	$T_{P,min}$	$T_{P,opt}$	$T_{P,max}$	ρ_3	ρ_4
Allowed range	min	-25	-15	0	0	0	-20	0	5	0	0
	max	10	20	35	1	1	15	40	45	1	1
Betula pendula PIM 1	min SSR	-24.96	-10.0	15.05		0.0306	-7.03	21.8	25.35	0.064803	0.045432
	mean	-22.32	-9.29	12.75		0.0402	-7.27	28.25	33.82	0.079167	0.048417
	stderr	0.79	0.16	0.29		0.002	0.48	1.72	2.06	0.004	0.001
Fagus sylvatica PIM 2	min SSR	-10.34	-0.89	18.11		0.0583	-10.03	28.61	44.49	0.109494	0.039178
	mean	-9.15	-2.39	21.2		0.0554	-9.47	28.89	33.81	0.11551	0.039986
	stderr	0.38	0.32	0.97		0.002	0.25	1.24	1.77	0.004	0.000
Quercus robur PIM 3	min SSR	-23.05	-0.3	16.91	0.010379	0.0551	3.46	34.55	34.55	0.331253	
	mean	-24.29	-0.4	17.3	0.01165	0.0594	3.42	27.47	35.7	0.25418	
	stderr	0.22	0.22	0.28	0.001	0.003	0.06	1.87	1.49	0.02	

4.1.2 The Cannel and Smith model (CSM)

The Cannel and Smith model (CSM) empirically describes the observation that increased chilling in winter decreases the required temperature sum for bud burst in spring. It was developed by Cannell and Smith (1983) and modified by Menzel (1997).

Table 4-3 Parameter values for the CSM. min, max: allowed ranges for the parameters during model fits. min SSR: Parameters for the fit that performed best in terms of SSR among ten different runs. mean: Average parameters after ten optimisation runs. stderr: Standard error of the average parameters after ten optimisation runs.

		T_c	T_b	a_{cs}	b_{cs}
Allowed range	min	-5	-5	-1000	0
	max	20	20	0	3000
B. pendula	min SSR	18.42	4.19	3075.99	-573.67
	mean	15.8	3.83	2694.38	-498.02
	stderr	1.67	0.42	247.02	48.16
F. sylvatica	min SSR	11.03	6.5	3039.75	-574.49
	mean	10.26	5.39	2810.75	-519.51
	stderr	0.75	1.16	127-14	31.2
Q. robur	min SSR	18.31	5.58	3451.18	-631.5
	mean	17.65	5.55	3008.55	-546.96
	stderr	0.85	0.04	137.41	26.06

Chilling C_{chill} is modelled as a simple counter of 'chill days', i.e. days whose mean temperature falls below a certain threshold T_c , starting on $t_1 = 1$. Nov.

$$C_{chill} = \sum_{t_1}^t 1 \quad \text{for } T_a \leq T_c \quad (4.3)$$

Chilling reduces the required temperature sum for bud burst T_{crit} in a logarithmic manner with parameters a_{cs} , b_{cs} .

$$T_{crit} = a_{cs} + b_{cs} \ln(C_{chill}) \quad (4.4)$$

Temperature sum T_{sum}^* is formed by integrating daily mean air temperatures T above a certain threshold T_b starting on $t_2 = 1. \text{ Feb.}$

$$T_{sum}^* = \sum_{t_2}^t (T_a - T_b) \quad \text{for } T_a > T_b \quad (4.5)$$

Bud burst occurs on the day when $T_{sum}^* > T_{crit}$.

Including T_c , a_{cs} , b_{cs} and T_b the model has four parameters (see Table 4-3).

4.1.3 The linear temperature sum model (TSM)

The temperature sum model (TSM) (Kramer, 1994; Menzel, 1997; Wang, 1960) simply integrates daily mean temperatures T_a above a certain threshold T_b starting from a defined date t_1 up to a fixed critical value T_{crit} .

Table 4-4 Parameter values for the TSM. min, max: allowed ranges for the parameters during model fits. min SSR: Parameters for the fit that performed best in terms of SSR among ten different runs. mean: Average parameters after ten optimisation runs. stderr: Standard error of the average parameters after ten optimisation runs

		T_b	T_{crit}	t_1
Allowed range	min	-10	0	1
	max	10	4000	131
B. pendula	min SSR	-6.07	672.9	108
	mean	-4.77	586.02	111.3
	stderr	0.77	52.82	2.29
F. sylvatica	min SSR	-6.98	664.88	131
	mean	-6.97	664.07	131
	stderr	0.16	7.87	0.0
Q. robur	min SSR	0.49	372.06	131
	mean	0.5	372.06	131
	stderr	0.03	2.0	0.0

The starting date t_1 was assumed to vary between the 1st November and the 31 of March , i.e.between 1 and 131.

$$T_{sum}^* = \sum_{t_1}^t (T_a - T_b) \quad \text{for } T_a > T_b \quad (4.6)$$

Bud burst occurs on the day when $T_{sum}^* > T_{crit}$.

Including T_b , T_{crit} and t_1 the model has three parameters (see Table 4-4).

4.2 Photosynthesis

The photosynthesis sub-model is based on the photosynthesis model of Haxeltine and Prentice (1996b). The model is described under the assumption of abundant water and nutrient supply. Reductions of photosynthesis by these factors are described in chapter 4.2.3. and 4.2.4..

Main features of this model are as follows:

- it is based on the mechanistic photosynthesis model of Farquhar et al. (1980) as simplified by Collatz et al. (1991); hence it represents a major step forward compared to the empirical schemes used to calculate tree growth in earlier gap models (see Shugart et al. (2018)),
- it does not prescribe identical photosynthetic characteristics for all the leaves across the canopy; instead, it is based on the assumption that enzyme concentrations in the leaves are regulated so as to optimize net assimilation rates,
- this optimisation is performed explicitly while developing the model (see Haxeltine and Prentice (1996b)),
- the resulting model is still fairly simple and can easily be extended to the whole canopy.

The photosynthesis is calculated for the single tree which is representative of the cohort.

4.2.1 *The assimilation model at the leaf and canopy level*

Here, the approach of Haxeltine and Prentice (1996a) is used to calculate the daily net photosynthesis A_{dt} and the leaf maintenance respiration R_d of a tree. The model applied has the important feature that the resulting net photosynthesis is a linear function of the photosynthetically active radiation I_{PAR} (see Chapter 3.5). Given this linearity, it is not necessary to integrate photosynthesis explicitly across the canopy, but it is sufficient to calculate the total radiation absorbed by the canopy and then to calculate the total daily net

photosynthesis A_{nd} as a function of the absorbed radiation $f(I_{PAR})$ that results for the whole canopy at once.

The total amount of optimum gross (nitrogen limited) assimilation per tree or cohort A_c is then obtained by

$$A_c = A_{sp} \cdot \frac{P_a}{1000} \cdot \frac{1}{c_{part}} \quad (4.7)$$

where P_a is patch size [m^2]; A_{sp} is the specific gross photosynthesis rate and c_{part} is the part of carbon in biomass and is used to convert A_{sp} from carbon to dry weight. The factor 1000 converts A_{sp} [$g\ C\ m^{-2}\ d^{-1}$] from g to kg. A_c thus is in [$kg\ DW\ m^{-2}\ d^{-1}$].

The rate A_{sp} is calculated from the (nitrogen limited) light use efficiency L_{UE} [$g\ C\ \mu mol^{-1}$], the daily incident photosynthetic radiation I_{PAR} [$mol\ m^{-2}$] and the fraction of the absorbed photosynthetically active radiation f_{tot}^c [-] per cohort (see Chapter 3.5)

$$A_{sp} = L_{UE} \cdot f_{tot}^c \cdot I_{PAR} \quad (4.8)$$

L_{UE} is derived from the optimal light use efficiency $L_{UE,opt}$ (Haxeltine and Prentice, 1996b) reduced by a reduction factor R_N^c which describes the influence of nitrogen availability (see Chapter 4.2.2)

$$L_{UE} = R_N^c \cdot L_{UE,opt} \quad (4.9)$$

Using the specific daily leaf respiration R_{ds} [$g\ m^{-2}\ d^{-1}$], calculated according to Haxeltine and Prentice (1996a), the nitrogen limited daytime photosynthesis A_{dt} [$g\ C\ m^{-2}$] is calculated by

$$A_{dt} = A_{sp} - \frac{d_l}{24} \cdot R_{ds} \quad (4.10)$$

with the daily length of photoperiod d_l .

This photosynthesis rate is related to the unstressed stomatal conductance of the tree through the CO_2 diffusion gradient between the atmosphere and intercellular air space and g^c is calculated according to Haxeltine and Prentice (1996a):

$$g^c = \max \left(g_{min}, \frac{1.56 \cdot A_{dt}}{(1 - \lambda) \cdot c_a \cdot c_{mass}} \right) \quad (4.11)$$

where the factor 1.56 [-] accounts for the difference in the diffusion coefficients of CO_2 and water vapour, $\lambda = c_i/c_a = 0.7$ is the optimum ratio of ambient to intercellular CO_2 concentration [-], and g_{min} [$mol\ m^{-2}\ d^{-1}$] is the minimum conductance (e.g. due to cuticular

transpiration). The division of A_{dt} by c_{mass} is required for the conversion of its unit into $\text{mol CO}_2 \text{ m}^{-2} \text{ d}^{-1}$.

Summation over all cohorts yields the stomatal conductance of the canopy of the stand g_{tot} .

The realized net daily (water and nitrogen limited) assimilation rate A_{net} is then calculated by

$$A_{net} = I_{drps}^c \cdot (A_c - R_{dc}) \quad (4.12)$$

where I_{drps}^c is the water limitation of the photosynthesis (see Chapter 4.2.3), A_c is the gross assimilation per patch (see equation (4.7)) and the daily leaf respiration rate R_{dc} per patch is defined by

$$R_{dc} = R_{ds} \cdot \frac{P_a}{1000} \cdot \frac{1}{c_{part}} \quad (4.13)$$

with the parameter c_{part} which gives the part of C in biomass.

Finally, the daily net primary production f_{NPP} is

$$f_{NPP} = A_{net} \cdot (1 - r_{co}) \quad (4.14)$$

where r_{co} is the (growth) respiration coefficient following the concept of constant annual respiration fraction as proposed by Landsberg and Waring (1997). The total daily NPP of the stand f_{NPP} is summarized over all trees of the cohort, over all cohorts of the forest stand and over all days/weeks of the year to an annual net primary production of the stand.

4.2.2 Nitrogen demand

The daily nitrogen demand of each tree $N_{dem}^{c,d}$ is calculated from its daily net primary production f_{NPP}

$$N_{dem}^{c,d} = f_{NPP} \cdot p_{NC} \quad (4.15)$$

It depends on the species specific nitrogen/carbon ratio of the total biomass p_{NC} (see Chapter 4.4.1).

The cumulative nitrogen demand of a tree N_{dem}^c at the current day t is

$$N_{dem}^c(t) = \sum_{i=1}^t N_{dem}^{c,d}(i) \quad (4.16)$$

In particular, the annual total nitrogen demand of a tree is equal to $N_{dem}^c(365)$. The demand of a cohort is the sum of the demand of all trees of the cohort. The cumulative nitrogen

demand of a species N_{dem}^s N_{dem}^s is the sum over the cumulative demand of all cohorts of the same species.

4.2.3 Water limitation

The water limitation of the photosynthesis I_{drps}^c (see Equation (4.12)), varying from zero to one, is calculated for each cohort by the ratio of its supply of water W_{upt}^c (see Chapter 6.1.3) and its transpiration demand E_{trd}^c (see Chapter 5.3)

$$I_{drps}^c(t) = \frac{W_{upt}^c(t)}{E_{trd}^c(t)} \quad (4.17)$$

4.2.4 Nitrogen limitation

The nitrogen limitation of photosynthesis is realised for each cohort by a reduction factor R_N^c varying from zero to one. It modifies the light use efficiency (see Equation (4.9)) calculated according to Haxeltine and Prentice (1996a) and as a consequence the gross assimilation A_c . The reduction factor of each cohort is initialized by a species specific reduction factor R_N^s which is calculated for each species by a function of the C/N ratio of active organic matter of the soil γ_{aom} and the species specific photosynthesis response to Nitrogen κ_N^s (Lindner, 1998).

$$R_N^s = \begin{cases} 1 - (N_{lim} - N_{min}) \kappa_N^s & \gamma_{aom} \geq 13.2 \\ 1 & \gamma_{aom} < 13.2 \end{cases} \quad (4.18)$$

with

$$N_{lim} = 120 \text{ and } N_{min} = \frac{480}{\gamma_{aom} - 9.2}$$

It is assumed, that there is no reduction of growth above a nitrogen availability of 120 kg ha^{-1} (Kopp and Schwanecke, 1994). Therefore the limitation factor N_{lim} in Equation (4.18) is set to 120. Below that value, a growth reduction and following a reduction of photosynthesis is calculated from a nitrogen mineralisation rate $N_{min} [\text{kg ha}^{-1}]$, which is estimated from data by (Kopp and Schwanecke, 1994). The dependence of R_N^s on the C/N ratio is shown in Figure 4-1.

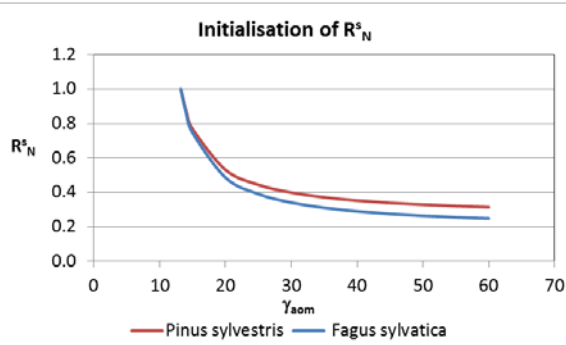


Figure 4-1 Initialisation of species specific nitrogen reduction factor R_N^s of two species with $\kappa_N^{pine} = 0.0062$ for *Pinus sylvestris* and $\kappa_N^{beech} = 0.0068$ for *Fagus sylvatica* in dependence of the C/N ratio of active organic matter of soil γ_{aom}

The nitrogen reduction factor R_N^c is calculated in the course of the simulation using one of the following methods:

- a) R_N^c is kept **constant** over the simulation time.
- b) The nitrogen limitation is calculated **daily** by the actual ratio of the cumulative nitrogen uptake N_{upt}^c and the cumulative nitrogen demand N_{dem}^c of the cohort

$$R_N^c(t) = \frac{N_{upt}^c(t)}{N_{dem}^c(t)} \quad (4.19)$$

Because of the daily calculation the value of R_N^c fluctuates very strongly and therefore the use of this approach is not recommended.

- c) For each species, a nitrogen reduction factor R_N^s is calculated **year by year** in dependence on the nitrogen uptake N_{upt}^s and nitrogen demand N_{dem}^s of the species, i. e. of all cohorts of the same species (Bugmann, 1994; Lindner, 1998).

$$R_N^s(t_y) = 1 - \exp(-a(t_y) \cdot 10 \cdot N_{upt}^s(t_y - 1) - 0.3) \quad (4.20)$$

with

$$a(t_y) = \frac{\ln(0.01)}{10 \cdot N_{dem}^s(t_y - 1)}$$

The coefficient a is calculated for the actual year t_y from the nitrogen demand of the species of the last year (t_y-1).

- d) In analogy to b) the nitrogen reduction factor R_N^s of the species is calculated **daily** by the actual ratio of the cumulative nitrogen uptake N_{upt}^s and the cumulative nitrogen demand N_{dem}^s of the species

$$R_N^s(t) = \frac{N_{upt}^s(t)}{N_{dem}^s(t)} \quad (4.21)$$

e) A modification of approach d) is the following equation

$$R_N^s(t) = 2 \frac{\left(\frac{N_{upt}^s(t)}{N_{dem}^s(t)} + 0.01 \right)}{\left(\frac{N_{upt}^s(t)}{N_{dem}^s(t)} + 1 \right)} \quad (4.22)$$

f) Another approach of **daily** calculating the species specific R_N^s follows an exponential function that depends on the ratio of the cumulative nitrogen uptake N_{upt}^s and the cumulative nitrogen demand N_{dem}^s of the species

$$R_N^s(t) = \exp\left(\frac{N_{upt}^s(t)}{N_{dem}^s(t)} - 1\right) \quad (4.23)$$

g) A modification of approach f) is described as

$$R_N^s(t) = \begin{cases} \exp\left(\frac{N_{upt}^s(t)}{N_{dem}^s(t)} - 0.7\right) - 0.5 & \frac{N_{upt}^s(t)}{N_{dem}^s(t)} \leq 10 \\ 1 & \text{otherwise} \end{cases} \quad (4.24)$$

The shape of the approaches d) to g) is shown in Figure 4-2. The application of approach e) is recommended for two reasons: If there is no N uptake, photosynthesis is not completely reduced and with increasing satisfaction the reduction factor approximates faster to 1 than the other approaches. An exception is the species *Pinus sylvestris*. In this case approach g) is recommended.

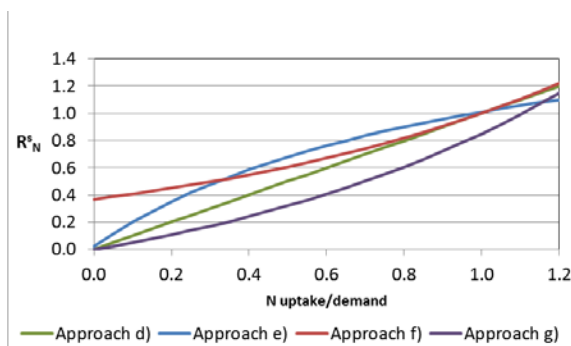


Figure 4-2 Nitrogen reduction factor R_N^s in dependence of the ratio of nitrogen uptake to nitrogen demand for the approaches d) to g)

4.3 Autotrophic respiration

Respiration can be calculated with two alternative approaches. Either total tree respiration is a constant fraction of gross photosynthetic carbon assimilation or growth and maintenance respiration are calculated separately for all tree components.

Daily maintenance respiration of sapwood, foliage and fine roots is calculated as

$$f_{mres,i} = r_{m,i} \cdot M_i \quad (4.25)$$

where the r_{mi} [d^{-1}] are specific maintenance respiration rates and M_i [kg DW] are the biomasses of the sapwood, foliage or fine roots. Note that maintenance respiration of foliage is calculated in the photosynthesis submodel.

4.4 Allocation and growth

The trees in the cohorts grow when net assimilation is distributed onto their components. The rules for the partitioning of assimilates are derived from four general relationships:

- an allometric relationship between sapwood cross sectional area and foliage biomass,
- the assumption of a functional balance between fine root and foliage specific activities,
- rise in bole height, when the photosynthetic production of the lowermost branches, drops below compensation of the sum of their respiratory losses and senescence fluxes,
- height growth is a function of growth in foliage mass and the relative irradiance in the crowns of the cohort under consideration.

At the end of every simulation year growth of the trees in the individual cohorts is calculated by allocating the yearly net primary production f_{NPP} to the biomass compartments foliage, stem, fine roots and coarse roots, twigs and branches according to the four general relationships outlined above. The allocation scheme is derived from the principle of functional balance (Davidson, 1969) and mass conservation, the pipe model theory (Shinozaki et al., 1964) and the relationships describing tree architecture as outlined in Chapter 2. Based on the law of mass conservation the change in dry mass of foliage, stem and fine roots can be described by:

$$\frac{dM_i}{dt} = \lambda_i f_{NPP} - f_{s,i} \quad (4.26)$$

with $\lambda_f + \lambda_s + \lambda_r + \lambda_c = 1$, where f_{NPP} is annual net primary productivity, the λ_i are the partitioning coefficients for foliage (f), sapwood (s), fine roots (r) and coarse roots (c), $f_{s,i}$ are the senescence rates and the compartments under consideration are $i=s, f, r$.

The heartwood mass increases by addition of senescing sapwood:

$$\frac{dM_{hw}}{dt} = f_{s,s} \quad (4.27)$$

Senescence is determined on the basis of specific senescence rates, s_i , $i=s, f, r$ [$\text{kg kg}^{-1} \text{a}^{-1}$]:

$$f_{s,i} = s_i M_i \quad (4.28)$$

4.4.1 Determination of the partitioning coefficients

A first constraint on the partitioning of biomass is set by the functional balance of fine roots and leaves. The principle of functional balance (Davidson, 1969) states that the assimilation of carbon and the uptake of nutrients (most notably nitrogen) should be balanced such that growth at a given elemental composition of plant materials can be realized. The biomass of the plant functional compartments that assimilate carbon and take up nutrients, i. e. leaves and fine roots, should be optimised in order to meet this aim under the boundary condition that they operate at specific activity σ_r [$\text{kg N kg}^{-1} \text{DM a}^{-1}$] for fine roots with respect to N uptake N_{upt}^c (see Equation (6.38)) [g m^{-2}] and σ_f [$\text{kg kg}^{-1} \text{a}^{-1}$] for leaves with respect to net carbon assimilation:

$$N_{upt}^c = \rho_{NC} f_{npp} \Rightarrow \sigma_r M_r = \rho_{NC} \sigma_f M_f \quad (4.29)$$

where ρ_{NC} is the overall N:C ratio of new biomass.

The specific leaf activity rate is defined as

$$\sigma_f = \frac{f_{NPP}}{M_f} \quad (4.30)$$

and the specific root activity rate as

$$\sigma_r = \frac{N_{upt}^c}{M_r} \quad (4.31)$$

Actually, a species specific parameterisation of σ_r is used, which is modified by an annual drought stress index I_{dral} . This index is calculated from the average of the daily ratio of water demand to water availability/uptake (see Chapter 6.1)

We define a composite parameter α_r by

$$\alpha_r = \rho_{nc} \frac{\sigma_f}{\sigma_r} \quad (4.32)$$

A second constraint for allocation is set by the relationship between foliage mass and conducting vessel needed for the supply of water and nutrients. The pipe model theory (Shinozaki et al., 1964) states that there is a proportionality between the sapwood cross-sectional area at crown base A_s , and the leaf biomass:

$$\begin{aligned} M_f &= \eta_s A_s \\ A_s &= \frac{M_f}{\eta_s} \end{aligned} \quad (4.33)$$

where η_s is a species specific parameter. To derive a relationship between sapwood biomass and foliage biomass, we need to express the former in terms of sapwood area. This is possible by taking into account the average length of the sapwood pipes H_s

$$M_s = \rho_s H_s A_s \quad (4.34)$$

where ρ_s [kg cm⁻³] is the sapwood density. It follows that

$$\begin{aligned} M_s &= \frac{\rho_s}{\eta_s} M_f H_s \\ &= \alpha_s M_f H_s \end{aligned} \quad (4.35)$$

where

$$\alpha_s = \frac{\rho_s}{\eta_s} \quad (4.36)$$

α_s is a composite parameter analogous to α_r (see Equation (4.32)).

From Equation (4.33) and Equation (4.34) it holds:

$$\frac{M_s}{M_f} = \alpha_s H_s \quad (4.37)$$

For the sapwood pipe length yields:

$$\begin{aligned}
 H_s &= H_b + \frac{H - H_b}{3} \\
 &= \frac{2H_b + H}{3}
 \end{aligned} \tag{4.38}$$

And therefore, based on this equation and Equation (4.35) it is derived:

$$\begin{aligned}
 \frac{M_s + \Delta M_s}{M_f + \Delta M_f} &= \alpha_s (H_s + \Delta H_s) \\
 \frac{M_s + \lambda_s f_{NPP} - f_{s,s}}{M_f + \lambda_f f_{NPP} - f_{s,f}} &= \alpha_s \left(\frac{2}{3} (H_b + \Delta H_b) + \frac{1}{3} (H + \Delta H) \right)
 \end{aligned} \tag{4.39}$$

We assume

$$\Delta H = \alpha_h \cdot \Delta M_f = \alpha_h (\lambda_f \cdot f_{NPP} - f_{s,f}) \tag{4.40}$$

And following we write Equation (4.39) as:

$$M_s + \lambda_s f_{NPP} - f_{s,s} = \alpha_s \left(\frac{2}{3} (H_b + \Delta H_b) + \frac{1}{3} (H + \Delta H) \right) (M_f + \lambda_f f_{NPP} - f_{s,f}) \tag{4.41}$$

This equation is solved for λ_s :

$$\lambda_s = \left(\alpha_s \frac{2}{3} f_{NPP} \right) \lambda_f^2 + \alpha_s \left(\frac{2}{3} (H_b + \Delta H_b) + \frac{H}{3} + \frac{\alpha_h}{3} (M_f - 2f_{s,f}) \right) \lambda_f + \beta_s \tag{4.42}$$

with

$$\beta_s = \frac{\alpha_s \left(\frac{2}{3} (H_b + \Delta H_b) + H - \frac{\alpha_s}{3} f_{s,f} \right) (M_f - f_{s,f}) + f_{s,s} - M_s}{f_{NPP}}$$

From Equation (4.29) and (4.32) (the metabolic activities of the roots and the photosynthetic organs are in balance) and the assumption, that the tree will allocate its carbon in a way such that its compartment relation would be optimally adapted to the environmental conditions of the present time step in the following time step it follows:

$$M_r + \lambda_r f_{NPP} - f_{s,r} = \alpha_r (M_f + \lambda_f f_{NPP} - f_{s,f}) \tag{4.43}$$

$$\lambda_r = \alpha_r \lambda_f + \beta_r$$

with

$$\beta_r = \frac{f_{s,r} - M_r + \alpha_r (M_f - f_{s,f})}{f_{NPP}} \tag{4.44}$$

Together with the mass conservation it follows:

$$\begin{aligned}
 1 &= \lambda_f + \lambda_s + \lambda_r \\
 &= \lambda_f + \left(\alpha_s \frac{2}{3} f_{NPP} \right) \lambda_f^2 + \alpha_s \left(\frac{2}{3} (H_b + \Delta H_b) + \frac{H}{3} + \frac{\alpha_h}{3} (M_f - 2f_{s,f}) \right) \lambda_f + \\
 &\quad \beta_s + \alpha_r \lambda_f + \beta_r
 \end{aligned} \quad (4.45)$$

Twigs and branches are introduced by the parameter α_c with:

$$\lambda_f + (1 + \alpha_c) \lambda_s + \lambda_r = 1 \quad (4.46)$$

α_c – parameter describing share of coarse roots, twigs and branches relative to sapwood

Calculation of λ_f by solving the quadratic equation and introducing a term $(1+\alpha_c)$ for coarse roots and twigs:

$$\begin{aligned}
 a_1 \lambda_f^2 + a_2 \lambda_f + a_3 &= 0 \\
 \text{with} \\
 a_1 &= (1 + \alpha_c) \frac{\alpha_s}{3} \alpha_h f_{NPP} \\
 a_2 &= 1 + \alpha_r + (1 + \alpha_c) \frac{\alpha_s}{3} (2(H_b + \Delta H_b) + H + \alpha_h (M_f - 2f_{s,f})) \\
 a_3 &= (1 + \alpha_c) \beta_s + \beta_r - 1 \\
 \lambda_{f1,2} &= \frac{1}{2a_1} \left(-a_2 \pm \sqrt{a_2^2 - 4a_1 a_3} \right)
 \end{aligned} \quad (4.47)$$

The third allocation parameter λ_s is then calculated from Equation (4.42).

$$\lambda_s = \frac{\alpha_s}{3} \left(2(H_b + \Delta H_b) + H + \alpha_h (M_f + \lambda_f f_{NPP} - 2f_{s,f}) \right) \lambda_f + \beta_s \quad (4.48)$$

The solution λ_{f1} is not always less than 1 and greater than zero. In this case a more simple allocation scheme is used.

Following λ_r is calculated by Equation and λ_s by Equation (4.48). If λ_s is less than zero or greater than 1 then according to Equation it follows:

$$\begin{aligned}
 \lambda_s &= 0 \\
 \lambda_f &= (1 - \beta_r) (1 + \alpha_r) \\
 \lambda_r &= 1 - \lambda_f
 \end{aligned} \quad (4.49)$$

If λ_f is not less than 1 and greater than zero:

$$\begin{aligned}\lambda_f &= 0.5 \\ \lambda_r &= 0.5\end{aligned}\quad (4.50)$$

Or if λ_r is less than zero:

$$\begin{aligned}\lambda_r &= 0 \\ \lambda_f &= 1\end{aligned}\quad (4.51)$$

If it is necessary, e.g. for litter calculations, the share of twigs and branches biomass is calculated from the coarse material (twigs, branches and coarse roots) using the parameter C_{frac} .

4.4.2 Height growth

The third constraint is set by the allometric and shading sensitivity of height growth.

Assuming for the relation between foliage mass and height the following function

$$H = \frac{p_{hv1}}{p_{hv3} + (M_f)^{p_{hv2}}}\quad (4.52)$$

with the three parameters p_{hv1} , p_{hv2} , p_{hv3} , it yields for the growth rate of height

$$\frac{dH}{dM_f} = \frac{-p_{hv1} \cdot p_{hv2} \cdot (M_f)^{(p_{hv2}-1)}}{\left((M_f)^{p_{hv2}} + p_{hv3}\right)^2} = p_h\quad (4.53)$$

where $b < 0$, dH/dM_f is determined at the end of every year before allocation is performed and used instead of the constant value as used in the first model.

Tree height growth is coupled to the growth of foliage mass

$$\frac{dH}{dt} = \alpha_h \frac{dM_f}{dt}\quad (4.54)$$

where α_h is a function of crown architecture of free growing trees and enhancement of acceleration of crown height growth by intra canopy shading.

$$\alpha_h = p_h + p_h \left(\frac{1}{\max(I_{relcan}, 0.25)} - 1 \right)\quad (4.55)$$

The new height in the year t is calculated by

$$H(t + 1) = H(t) + \alpha_h \frac{dM_f}{dt} \quad (4.56)$$

4.4.3 Diameter growth

The diameter is calculated annually after allocation of NPP and height growth. From the value of sapwood pipe length H_s (Equation (4.38)) and the calculation of A_s

$$A_s = \frac{M_s}{\rho_s H_s} \quad (4.57)$$

the diameter at the forest floor (tree base) is calculated as follows

$$d_{bs} = \sqrt{\frac{4(A_{hb} + A_s)}{\pi}} \quad (4.58)$$

with an actual A_{hb} calculated from A_s and the senescence rate of sapwood s_s :

$$A_{hb}(t + 1) = A_{hb}(t) + s_s A_s \quad (4.59)$$

Following the new A_{hc} is calculated as follows. For heartwood biomass (truncated cone with height H_b and cone with height $H - H_b$) the following holds:

$$M_{hw} = \rho_s \left[\frac{1}{3} A_{hc} (H - H_b) + \frac{1}{3} (A_{hb} + A_{hc} + \sqrt{A_{hb} A_{hc}}) H_b \right] \quad (4.60)$$

$$M_{hw} = \rho_s \frac{1}{3} \left[A_{hc} H + (A_{hb} + \sqrt{A_{hb} A_{hc}}) H_b \right]$$

$$\frac{3M_{hw}}{\rho_s} - A_{hc} H - A_{hb} H_b = \sqrt{A_{hb} A_{hc}} H_b$$

$$\left(\frac{3M_{hw}}{\rho_s} - A_{hc} H - A_{hb} H_b \right)^2 = A_{hb} A_{hc} H_b^2 \quad (4.61)$$

$$\left(\frac{3M_{hw}}{\rho_s} - A_{hc} H - A_{hb} H_b \right)^2 - A_{hb} A_{hc} H_b^2 = 0$$

$$A_{hc}^2 + \frac{-2 \left(3 \frac{M_{hw}}{\rho_s} - H_b A_{hb} \right) H - H_b^2 A_{hb}}{H^2} A_{hc} + \frac{\left(3 \frac{M_{hw}}{\rho_s} - H_b A_{hb} \right)^2}{H^2} = 0 \quad (4.62)$$

This equation was solved for A_{hc} . If H_b is greater than zero then

$$\begin{aligned}
 p &= -2 \frac{H_b}{H} \left(\frac{3M_{hw}}{\rho_s H} - A_{hb} \right) - A_{hb} \left(\frac{H_b}{H} \right)^2 \\
 q &= \left(\frac{\frac{3M_{hw}}{\rho_s H} - A_{hb} H_b}{H} \right)^2 \\
 d &= \frac{p^2}{4} - q
 \end{aligned} \tag{4.63}$$

If d is greater than zero, two solutions of Equation (4.62) are determined:

$$w_{1,2} = -\frac{p}{2} \pm \sqrt{d} \tag{4.64}$$

To find the suitable solution for A_{hc} we use Equation (4.60) and calculate for $A_{hc} = w_1$:

$$f = \frac{\rho_s}{3} \left(w_1 H + (A_{hb} + \sqrt{w_1 A_{hb}}) H_b \right) - M_{hw} \tag{4.65}$$

If f is less than or equal zero:

$$A_{hc} = w_1 \tag{4.66}$$

But if f is greater than zero a new value for f is calculated for $A_{hc}=w_2$:

$$f = \frac{\rho_s}{3} \left(w_2 H + (A_{hb} + \sqrt{w_2 A_{hb}}) H_b \right) - M_{hw} \tag{4.67}$$

If f is less than or equal 0:

$$A_{hc} = w_2 \tag{4.68}$$

It is possible that no valid solution for A_{hc} is found, because both test for w_1 and w_2 are not successful. In this case the tree cohort is removed!

Then the following diameters at crown base (d_{cb}) and at breast height (d_{bh}) are calculated:

$$d_{cb} = \begin{cases} d_{bs} & H_b = 0 \\ \sqrt{\frac{4(A_{hc} + A_s)}{\pi}} & H_b > 0 \end{cases} \tag{4.69}$$

$$d_{bh} = \begin{cases} 0 & H_t < H_b \\ \frac{d_{cb} (H - H_{dbh})}{H - H_b} & H > H_{dbh} \wedge H_b < H_{dbh} \\ d_{cb} - \frac{(d_{bs} - d_{cb}) H_{dbh}}{H_b} & H > H_{dbh} \wedge H_b > H_{dbh} \end{cases} \quad (4.70)$$

4.4.4 Root biomass

The root biomass of a single tree per soil layer is defined by its root fraction $r_{fr}^c(z_i)$ (see Chapter 2.3) from the total root biomass M_r^c of the tree

$$M_r^{c*}(z_i) = r_{fr}^c(z_i) \cdot M_r^c \quad (4.71)$$

For each layer, the root fraction of a cohort r_{MR}^c as part of the total root biomass is calculated by

$$r_{MR}^c(z_i) = \frac{n_a^c r_{fr}^c(z_i) M_r^c}{\sum_{j=1}^{n_c} n_a^j r_{fr}^j(z_i) M_r^j} \quad (4.72)$$

4.4.5 Sapling growth

Growth of saplings based on the same principles as growth of trees. We assume that saplings have no heartwood. The following relations yield.

a) Functional balance

Using Equation (4.29) and (4.32) it yields:

$$M_r + \lambda_r f_{NPP} - f_{s,r} = \alpha_r (M_f + \lambda_f f_{NPP} - f_{s,f}) \quad (4.73)$$

Solving for λ_r results in

$$\begin{aligned} \lambda_r &= \frac{\alpha_r (M_f + \lambda_f f_{NPP} - f_{s,f}) + f_{s,r} - M_r}{f_{NPP}} \\ &= \alpha_r \lambda_f + \beta_r \end{aligned} \quad (4.74)$$

with

$$\beta_r = \frac{f_{s,r} - M_r + \alpha_r (M_f - f_{s,f})}{f_{NPP}}$$

b) Relation between foliage biomass and sapwood biomass (shoot biomass)

A relationship (and parameterisation) exists

$$M_f = p_{sa} (M_s)^{p_{sb}}$$

$$\frac{dM_f}{dt} = p_{sa} p_{sb} (M_s)^{p_{sb}-1} \frac{dM_s}{dt} \quad (4.75)$$

We assume $f_{s,s}=0$ and

$$p_{ab} = p_{sa} p_{sb} (M_s)^{p_{sb}-1} \quad (4.76)$$

$$\lambda_f f_{NPP} - f_{s,f} = p_{ab} (\lambda_s f_{NPP} - f_{s,s})$$

$$\lambda_f = \frac{p_{ab} \lambda_s f_{NPP} + f_{s,f}}{f_{NPP}} \quad (4.77)$$

$$= p_{ab} \lambda_s + \frac{f_{s,f}}{f_{NPP}}$$

with the parameters p_{sa} and p_{sb} .

Furthermore, we assume a linear relationship between foliage mass and shoot mass, that means

$$M_f = c M_s$$

and

$$\frac{dM_f}{dt} = c + \frac{dM_s}{dt} \quad (4.78)$$

with

$$p_{ab} = c$$

where p_{ab} is a fixed species specific parameter in the model (not given in the species parameter file).

c) Mass conservation

The calculation of λ_f is derived from the mass conservation. It yields

$$\begin{aligned}
 \lambda_f + \lambda_s + \lambda_r &= 1 \\
 \lambda_s &= 1 - \lambda_f - \lambda_r \\
 \lambda_f &= \rho_{ab} \cdot (1 - \lambda_f - \lambda_r) + \frac{f_{s,f}}{f_{NPP}} \\
 &= \rho_{ab} \cdot (1 - \lambda_f - \alpha_r \lambda_f - \beta_r) + \frac{f_{s,f}}{f_{NPP}} \\
 &= -\lambda_f \cdot (\rho_{ab} + \rho_{ab} \cdot \alpha_r) + \rho_{ab} - \rho_{ab} \cdot \beta_r + \frac{f_{s,f}}{f_{NPP}} \\
 \lambda_f \cdot (1 + \rho_{ab} + \rho_{ab} \cdot \alpha_r) &= \rho_{ab} - \rho_{ab} \cdot \beta_r + \frac{f_{s,f}}{f_{NPP}}
 \end{aligned} \tag{4.79}$$

and for λ_f follows

$$\begin{aligned}
 \lambda_f &= \frac{\rho_{ab} - \rho_{ab} \cdot \beta_r + \frac{f_{s,f}}{f_{NPP}}}{1 + \rho_{ab} \cdot (1 + \alpha_r)} \\
 &= \frac{\rho_{ab} \cdot (1 - \beta_r) + \frac{f_{s,f}}{f_{NPP}}}{1 + \rho_{ab} \cdot (1 + \alpha_r)}
 \end{aligned} \tag{4.80}$$

The variable λ_s is calculated by Equation (4.74) and (4.80):

$$\lambda_s = 1 - \lambda_r - \lambda_f \tag{4.81}$$

The height of saplings is calculated with a parameterised function:

$$H = \rho_{h1} (M_s)^{\rho_{h2}} \tag{4.82}$$

5 WATER PROCESSES

5.1 Actual evapotranspiration

The actual evapotranspiration is the result of several processes which will be calculated separately and is limited by the potential evapotranspiration E_{pot} (Chapter 3.2). Although all processes run simultaneously, they are calculated one after the other up to the threshold of the potential evapotranspiration in the following order. First, rainfall or snow intercepted by the canopy evaporates or sublimates respectively (Chapter 5.2). The same calculation is done for the ground vegetation in case it is considered. After that the evaporated soil water is balanced. Soil evaporation includes the evaporation of free water from the soil surface and water which is transported from deeper soil layers to the surface. This removal of soil water is possible up to a certain depth. The depth depends on the soil and is set as a parameter. The last step calculates the remaining transpiration demand of the trees as well as the ground vegetation. Transpiration demand is satisfied by the plant available soil water (Chapter 5.3).

5.2 Interception

The total interception storage of the canopy is given by a special weighted mean of the species specific interception capacities depending on the leaf area index. The actual interception rate W_{int} of the current day t is given by the actual precipitation P_d and the remaining interception capacity as the difference between the maximal interception capacity W_{int}^{max} and the interception storage W_{int}^{st} of the previous day

$$W_{int}(t) = \min(P_d(t), W_{int}^{max} - W_{int}^{st}(t-1)) \quad (5.1)$$

The maximal interception capacity of the canopy is a function of the leaf area index L_{AI}

$$W_{int}^{max} = c_{int} \cdot L_{AI} \quad (5.2)$$

with c_{int} as the sum of the interception parameters of each cohort c_{int}^c (Jansson, 1991) weighted by its relative share of foliage mass .

The interception storage of the current day is the balance of the intercepted precipitation W_{int} and evaporated water E_{int} which is limited by the potential evapotranspiration E_{pot}

$$W_{int}^{st}(t) = W_{int}(t) - E_{int}(t) \quad (5.3)$$

and

$$E_{int}(t) = \min(W_{int}(t), E_{pot}(t)) \quad (5.4)$$

For mixed stands the maximal interception capacity of the canopy is calculated from the interception capacity from the respective species weighted by the share of each species

If air temperature is less than a threshold T_{snow} below this precipitation falls as snow interception will be accumulated as snow with a maximal capacity of double W_{int}^{max} .

5.3 Transpiration

Using the boundary layer parameterisation of Monteith (1995), the potential canopy transpiration demand E_{trd} is calculated from the potential evapotranspiration E_{pot} reduced by the evaporation of intercepted water E_{int} and the unstressed stomatal conductance g_{tot} of the forest canopy (Haxeltine and Prentice, 1996a)

$$E_{trd}(t) = (E_{pot}(t) - E_{int}(t)) \cdot \alpha_m \cdot \left(1 - e^{-\frac{g_{tot}(t)}{g_{max}}} \right) \quad (5.5)$$

with the Priestley-Taylor coefficient α_m and the maximum stomatal conductance g_{max} . The unstressed stomatal conductance of the canopy g_{tot} [$\text{mol m}^{-2} \text{d}^{-1}$] is calculated as the sum of the stomatal conductances of all trees of all n_c cohorts

$$g_{tot}(t) = \sum_{i=1}^{n_c} n_a(i, t) \cdot g^c(i, t) \quad (5.6)$$

where n_a is the number of all trees of the cohort and g^c is the stomatal conductance of a single tree a in the cohort (see Equation (4.11)), calculated according to Haxeltine and Prentice (1996a) from the net daytime photosynthesis A_{dt} .

The transpiration demand of each cohort E_{trd}^c is derived from the potential canopy transpiration demand E_{trd} by considering its relative stomatal conductance

$$E_{trd}^c(t) = \frac{g^c(t)}{g_{tot}(t)} E_{trd}(t) \quad (5.7)$$

The drought index of a cohort is defined as the average of the ratios of uptake and demand over the time period of interest (number of days) (see Chapter 4.2.3).

6 SOIL PROCESSES

Physical and chemical soil processes are described as one dimensional, spatial, and temporal discrete processes. For that purpose, the soil column with depth z_N is divided into N_z different layers with optional thickness following the horizons of the soil profile. Each layer, the humus layer and the deeper mineral layers, is regarded as homogeneous concerning its physical and chemical parameters. Water content and soil temperature of each soil layer are estimated as functions of the soil parameters, air temperature, and stand precipitation and control the decomposition and mineralisation of the organic matter (see Figure 6-1).

The time step of the soil model is one day due to the great dynamics of the water processes.

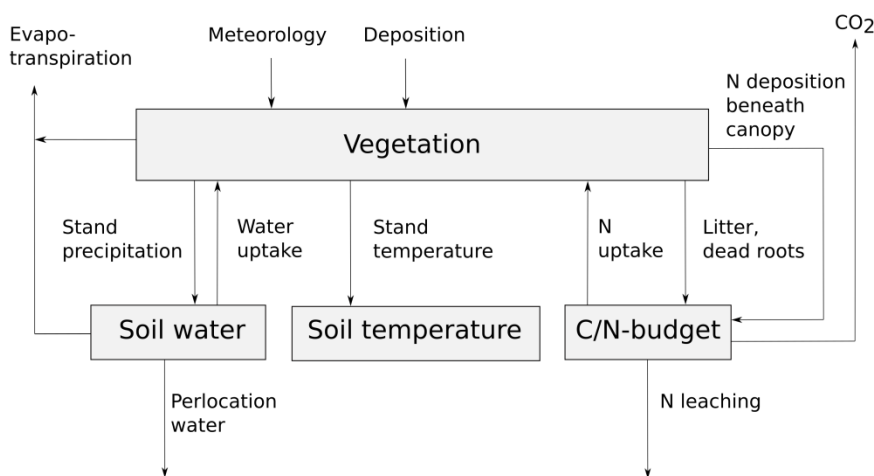


Figure 6-1 Structure of the soil model

6.1 Soil water balance

6.1.1 Percolation

A percolation model balances the soil water content. According (Glugla, 1969) the water content of each layer with depth z is calculated by

$$\frac{d}{dt} (W_s(z, t) - W_s^{FC}(z)) = W_p(z, t) - W_{upt}(z, t) - W_{ev}(z, t) - \lambda_w(z) \cdot (W_s(z, t) - W_s^{FC}(z))^2 \quad (6.1)$$

As input into the soil layer serves the percolating water W_p from the above layer respectively the net precipitation after canopy interception for the first layer. The output is estimated from the soil evaporation W_{ev} (up to a certain depth), the water uptake by roots W_{upt} and the outflow of gravitational water into the next layer, which is controlled by a soil texture depending percolation parameter λ_w (Glugla, 1969; Koitzsch, 1977).

6.1.2 Snow water

If air temperature T_a is less than 0°C , the precipitation is stored as a water equivalent in a snow pool W_{sn} , which is emptied as a function of positive average daily air temperature. The maximum snow water release W_{sn}^{pot} is determined for $T_a > 0^\circ\text{C}$ by

$$W_{sn}^{pot} = T_a (0.45 + 0.1T_a) \quad (6.2)$$

(Koitzsch and Günther, 1990). The melt-water is limited by the minimum of W_{sn} and W_{sn}^{pot} and will then be added to the uppermost soil layer. In the case of frozen soil no percolation occurs.

6.1.3 Water uptake by roots

The total water uptake W_{upt} from the soil layer used to balance the actual water content in Equation (6.1) is the sum of the water uptake $W_{upt,c}$ of all cohorts from this layer

$$W_{upt}(t) = \sum_{c=1}^{n_c} W_{upt,c}(t) \quad (6.3)$$

The water uptake of each cohort is controlled by its potential transpiration demand E_{trdem}^c (see Equation (5.7)) and the plant available soil water W_{av} (all soil water above the wilting point). The actual water uptake by the cohorts W_{upt}^c is then

$$W_{upt}^c(t) = \min \left(E_{trd,c}(t), \sum_{i=1}^{n_z} W_{av}(z_i, t) \right) \quad (6.4)$$

It is realised layer by layer. Furthermore, it is assumed that optimal conditions for water uptake exist only at a water content near the field capacity. Beyond that optimal range the water ability decreases with decreasing or increasing soil moisture (Chen, 1993).

$$W_{av}(z, t) = w_{ru}(z, t) (W_s(z, t) - W_s^{WP}(z)) \quad (6.5)$$

The appropriate water resistance function w_{ru} can be defined in two ways concerning the range between wilting point and field capacity (see Figure 6-2). In both cases, the optimal range varies 10 % around the field capacity and decreases linearly when the soil moisture level approaches the saturation W_s^{sat} .

- a) Linear increase with increasing soil moisture between wilting point W_s^{WP} and the optimal range

$$w_{ru}(z, t) = \begin{cases} 0 & W_s(z, t) \leq W_s^{WP}(z) \\ 1 - \frac{0.9 W_s^{FC}(z) - W_s(z, t)}{0.9 W_s^{FC}(z) - W_s^{WP}(z)} & W_s^{WP}(z) < W_s(z, t) < 0.9 W_s^{FC}(z) \\ 0.3 + 0.7 \frac{W_s^{sat}(z) - W_s(z, t)}{W_s^{sat}(z) - 1.1 W_s^{FC}(z)} & W_s(z, t) > 1.1 W_s^{FC}(z) \\ 1 & otherwise \end{cases} \quad (6.6)$$

b) Exponential increase with increasing soil moisture between wilting point W_s^{WP} and the optimal range

$$w_{ru}(z, t) = \begin{cases} 0 & W_s(z, t) < W_s^{WP}(z) \\ e^{(-5k_{expW}(z, t))} & W_s^{WP}(z) \leq W_s(z, t) < 0.9 W_s^{FC}(z) \\ 0.3 + 0.7 \frac{W_s^{sat}(z) - W_s(z, t)}{W_s^{sat}(z) - 1.1 W_s^{FC}(z)} & W_s(z, t) > 1.1 W_s^{FC}(z) \\ 1 & otherwise \end{cases} \quad (6.7)$$

with

$$k_{expW}(z, t) = \frac{0.9 W_s^{FC}(z) - W_s(z, t)}{0.9 W_s^{FC}(z) - W_s^{WP}(z)}$$

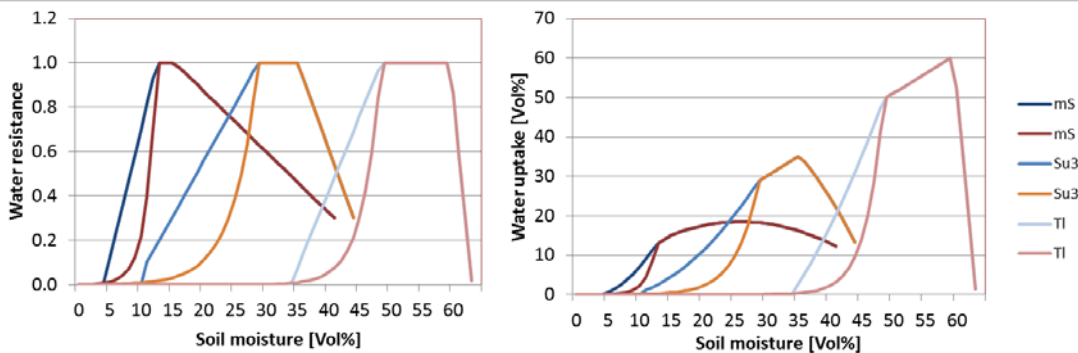


Figure 6-2 Water resistance functions (left) and the appropriate water uptake (right) of three soil types: ms – pure sand, Su3 - silty sand, and TI – loamy clay for two types of calculation (bluish lines – type a), reddish lines – type b))

In each soil layer, the available water is distributed according to the root fraction of the respective cohort (see Chapter 2.3).

6.2 Soil heat balance

6.2.1 Heat conduction equation

The dynamics of soil temperature T_s are described by a one-dimensional heat conduction equation with spatial and time depending heat capacity C_T and thermal conductivity λ_T (Suckow, 1989)

$$C_T(z, t) \frac{\partial}{\partial t} T_s(z, t) = \frac{\partial}{\partial z} \left(\lambda_T(z, t) \frac{\partial}{\partial z} T_s(z, t) \right) \quad (6.8)$$

where z is the soil depth in cm and t the time in days.

The appropriate initial condition

$$T_s(z, t_0) = T_{s,0}(z) \quad (6.9)$$

sets the initial temperature distribution in the soil profile.

The upper boundary condition

$$T_s(0, t) = T_{s,s}(t) \quad (6.10)$$

determines the temperature at the soil surface and the lower boundary condition

$$T_s(\infty, t) = T_\infty < \infty \quad (6.11)$$

means that the temperature is always finite.

The solution of the heat conduction equation with the aid of a non-negative-containing, conservative finite-difference method provides the daily soil temperature of all soil layers (Suckow, 1986). The heat capacity C_T and the thermal conductivity λ_T are calculated in each time step for each layer.

6.2.2 Thermal conductivity

The thermal conductivity λ_T depends on bulk density, water content, mineral composition, and organic matter content of the soil layer. There are several approaches to calculate the thermal conductivity.

- a) Neusyypina (1979) used a non-linear function of bulk density and water content of the respective soil layer

$$\lambda_T(z, t) = \frac{0.001(3\rho_s(z) - 1.7)}{1 + (11.5 - 5\rho_s(z))e^{k_{\text{exp}N}}}$$

with

$$k_{\text{exp}N}(z, t) = -50 \left(\frac{f_W(z, t)}{\rho_s(z)} \right)^{1.5}$$

and f_W volume fraction of soil water.

This assumption does not need any parameterisation of soil texture.

- b) de Vries (1963) describes the thermal conductivity in analogy to the electric conductivity of a granular material in a continuous medium.

$$\lambda_T(z, t) = \frac{f_0(z) \lambda_0 + \sum_{i=1}^N k_i f_i(z) \lambda_i}{f_0(z) + \sum_{i=1}^N k_i f_i(z)}$$

Table 6-1 Parameters of the thermal conductivity calculation of (de Vries, 1963)

Soil component	Shape factor g_a^i	Thermal conductivity λ_i [J cm ⁻¹ s ⁻¹ K ⁻¹]	Heat capacity C_i [J cm ⁻³ K ⁻¹]
Air	0.333	0.00026	0.0012
Water	-	0.005945	4.1868
Ice	0.125	0.021771	1.884
Quartz	0.144	0.0879228	2.01
Silt	0.144	0.02931	2.01
Clay	0.144	0.00251	2.01
Stone	0.144	0.041868	1.8
Organic matter	0.333	0.00251	2.512

The granular material is a mixture of soil particles of N different types with an elliptical shape. f_0 is the volume fraction of the continuum, f_i is the volume fraction of the N particle types, the weighting factor k_i is the ratio between the temperature gradients of the granulate and the medium ($i=1 \dots N$). For ellipsoidal granulates, k_i can be calculated as

$$k_i = \frac{1}{3} \left[2 \left(1 + \left(\frac{\lambda_i}{\lambda_0} - 1 \right) g_a^i \right)^{-1} + \left(1 + \left(\frac{\lambda_i}{\lambda_0} - 1 \right) (1 - 2g_a^i) \right)^{-1} \right] \quad i = 1, N \quad (6.14)$$

from the thermal conductivities of the granulates λ_i and the continuum λ_0 as well as the shape factors g_a^i (see Table 6-1).

For dry soil it is assumed that the continuous medium is air and for wet soil it is water. The last assumption holds for the frozen soil too, because the unfrozen water overlaps the particles of ice and soil.

- c) Campbell (1985) differentiates between dry and wet soil. In both cases, thermal conductivity is calculated in dependence of the water content by the following equation

$$\lambda(z, t) = k_a(z) + k_b(z) \cdot f_w(z, t) - (k_a(z) - k_d(z)) \cdot e^{k_{\text{exp } c}(z, t)} \quad (6.15)$$

with

$$k_{\text{exp } c}(z, t) = (-k_c(z) \cdot f_w(z, t))^4$$

and f_w volume fraction of soil water.

The coefficients k_a , k_b , k_c , and k_d depend on soil and were obtained by curve fitting.

$$k_a(z, t) = \frac{0.57 + 1.73f_q(z) + 0.93f_m(z)}{1. - 0.74f_q(z) - 0.49f_m(z)} - 2.8f_s(z)(1 - f_s(z)) \quad (6.16)$$

$$k_b(z, t) = 2.8 f_s(z) f_w(z, t) \quad (6.17)$$

For wet soil it is set $k_a = k_d$ and for dry soil it holds

$$k_c(z) = 1 + 2.6\sqrt{f_c(z)} \quad (6.18)$$

with the volume fraction of clay f_c and

$$k_d(z) = 0.03 + 0.7 f_s(z)^2 \quad (6.19)$$

The different values of thermal conductivity calculated by the three approaches above are shown in Figure 6-3.

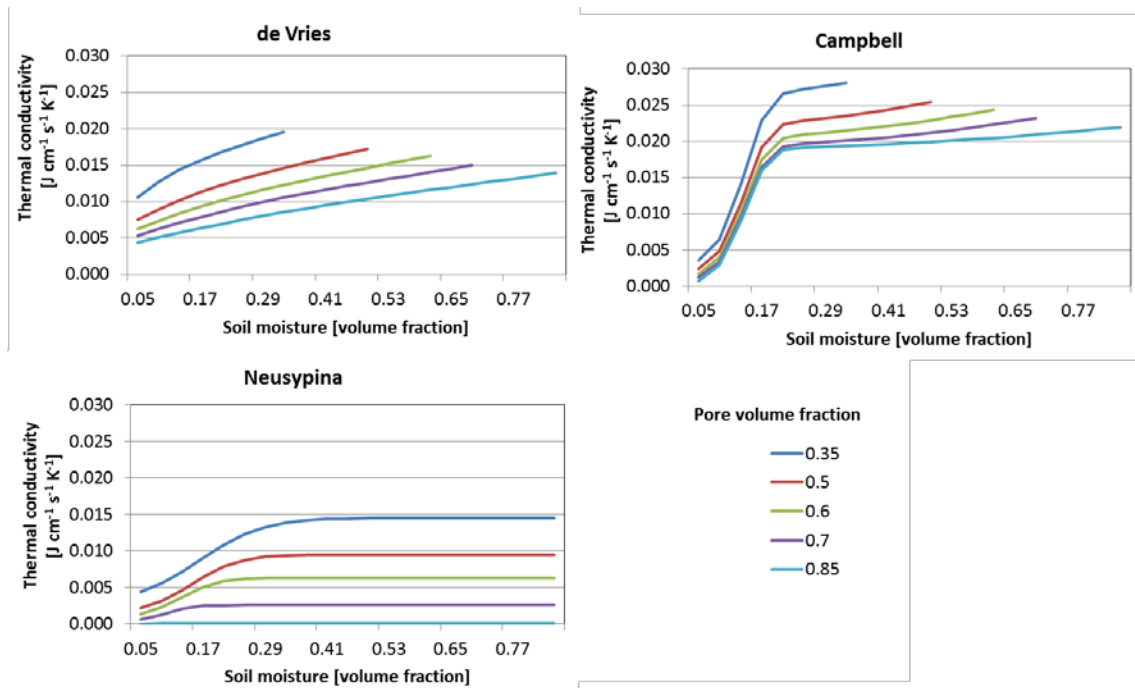


Figure 6-3 Thermal conductivities, calculated with the approaches de Vries, Campbell and Neusy pina

6.2.3 Heat capacity

The heat capacity $C_T(z,t)$ of the soil substrate is equal to the sum of the heat capacities of the different soil components multiplied with the respective volume proportion (van Wijk, 1963)

$$C_T(z,t) = \sum_{i=1}^{n_s} f_i(z) \cdot C_i + f_w(z,t) \cdot C_w \quad (6.20)$$

f_i ($i=1,\dots,n_s$) are the volume fraction of the n_s soil components as volume of soil component per volume of soil and C_i the heat capacity of the respective soil components (see Table 6-1). The volume fraction of soil water f_w changes with time and results in a changing heat capacity of the soil. The fraction of soil air can be neglected, because the heat capacity of air is much smaller than that of water or the solid soil components. This approach is used together with the calculation of thermal conductivity following (de Vries, 1963) or (Campbell, 1985) (chapter 6.2.2 b) and c)).

Otherwise, heat capacity is the product of density and specific heat capacity. Moreover, the heat capacity of water is approximately one and the heat capacity of the air can be neglected because it is very small, so that the heat capacity of the soil layer is calculated from the specific heat capacity of the total solid soil components c_s , the bulk density ρ_s , and the water content W_s

$$C_T(z,t) = \rho_s(z)c_s(z) + W_s(z,t)c_w \quad (6.21)$$

Because no further parameterisation of soil texture is necessary, Equation (6.21) is used together with Equation (6.12).

6.2.4 Soil surface temperature

The soil surface temperature $T_{s,s}$ as upper boundary condition (6.10) is estimated from the air temperature T_a of the last three days

$$T_{s,s}(t) = k_s(t) \sum_{i=0}^2 K_s^i \cdot T_a(t - i) \quad (6.22)$$

The coefficients K_s^i are used to estimate the influence of the air temperature on the soil surface temperature for an uncovered soil, whereas the set of daily correction coefficients $k_s(t)$ cause a seasonal variation of that relationship and simulates the damping effect of the stand on the temperature curve.

6.3 Soil carbon and nitrogen budget

The carbon and nitrogen cycle is based on a close relationship between soil and vegetation (see Figure 6-1). On the one hand, an input exists into the soil by addition of organic material through accumulating litter and dead fine roots, and on the other hand, there is a withdrawal from the soil of nitrogen by the vegetation (King, 1995). To describe the carbon and nitrogen budget a distinction is made between the carbon and nitrogen content of the dead organic matter (primary organic matter - pom) and the humus (active organic matter - aom). The primary organic matter of each species is separated in to five fractions (needle and foliage litter, twigs, branches, dead fine roots, dead coarse roots, and dead stems).

The mineralised nitrogen is balanced as ammonium and nitrate. Please note that mineralisation, nitrification, input, uptake, and transport of dissolved nitrogen are simulated for each soil layer.

6.3.1 Carbon and nitrogen input

The amount of nitrogen and carbon from litter (needle and foliage litter, twigs, and branches) entering the soil is added to the N_{pom} and C_{pom} pools of the first layer. In the same way, the nitrogen and carbon content of dead fine and coarse roots of trees as well as ground vegetation is added to the pom-pools of the respective layer.

It is assumed that the deposition is bound to the precipitation. Therefore, there is an immediately input to the pools N_{NH4} and N_{NO3} by the amount of the N deposition.

6.3.2 Carbon and nitrogen turnover

The carbon turnover of the organic matter is the dominant process influenced by water content, soil temperature, and pH value (Franko, 1990) (Kartschall et al., 1990). It provides the energy for the whole turnover of the organic matter and determines the nitrogen turnover. The primary organic matter of all fractions and all species types decomposes to a single humus pool. The mineralisation of these organic fractions results in mineral bounded nitrogen and CO₂ which returns to the atmosphere (Goto et al., 1994). These processes are described as first order reactions for each layer (Chertov and Komarov, 1997; Grote and Erhard, 1999; Parton et al., 1987). Depending on the carbon and nitrogen content of the organic matter pools and the matter specific reaction coefficients, the carbon and nitrogen pools in the soil can be estimated (Running and Gower, 1991). Figure 6-4 gives an overview of the turnover process whereas k_j resp. k_i^* ($i=1,2$) are reaction coefficients of C resp. N turnover and linked by the C/N ratios γ_{pom} and γ_{aom} of the primary and active organic matter.

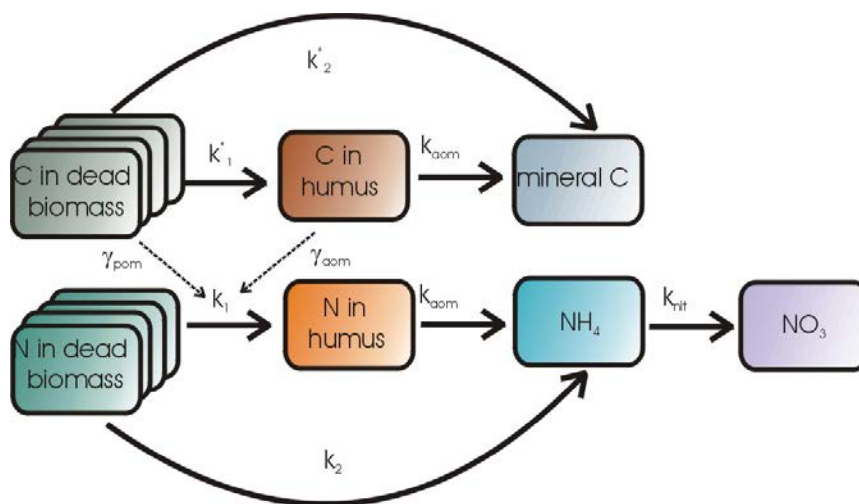


Figure 6-4 Reaction model of carbon and nitrogen turnover with reaction coefficients of the following processes:

- k_1, k_1^* - conversion of C and N pools of primary organic matter into active organic matter
- k_2, k_2^* - mineralisation of C and N pools of primary organic matter
- k_{aom} - mineralisation of active organic matter
- k_{nit} - nitrification of active organic matter
- $\gamma_{pom}, \gamma_{aom}$ - C/N ratio of primary and active organic matter

Following the concept of first order reaction kinetics, the description of the carbon and nitrogen turnover results in a system of linked differential equations. The carbon change in the primary organic matter $C_{pom}^{i,j}(z,t)$ is controlled by the total turnover coefficient $k_{pom}^{i,j}$ with $i \in \{\text{all matter fractions}\}$ and $j \in \{\text{all species types}\}$ and can be described by a set of $i \cdot j$ differential equations

$$\frac{\partial}{\partial t} C_{pom}^{i,j}(z,t) = -k_{pom}^{i,j} C_{pom}^{i,j}(z,t) \quad (6.23)$$

k_{pom} is the sum of the reaction coefficients of the conversion of primary organic matter into active organic matter ($k_{1,pom}^{i,j}$) and the mineralisation of primary organic matter (k_2)

$$k_{pom}^{i,j} = k_{1,pom}^{i,j} + k_2 \quad (6.24)$$

The transformation of primary organic matter $C_{pom}^{i,j}(z,t)$ to active organic matter $C_{aom}(z,t)$ is controlled by the synthesis coefficient $k_{syn}^{i,j}$, which is specific to the litter type (plant type and plant fraction) whereas

$$k_{1,pom}^{i,j} = k_{pom}^{i,j} k_{syn}^{i,j} \quad (6.25)$$

The turnover of carbon in active organic matter is made up from the synthesised portion minus the carbon used in the process of mineralisation:

$$\frac{\partial}{\partial t} C_{aom}(z,t) = \sum_{i,j} k_{syn}^{i,j} k_{pom}^{i,j} C_{pom}^{i,j}(z,t) - k_{aom} C_{aom}(z,t) \quad (6.26)$$

The heterotrophic respiration is calculated as the result of the turnover process.

How much nitrogen is absorbed into the active organic matter and what proportion is mineralised depends on the C/N ratios of all primary organic matter fractions and on the carbon used in the synthesis of the active organic matter. The net mineralisation of nitrogen in the primary organic matter is, analogously to Equation (6.23), again described as a reaction of the first order (Johnsson et al., 1987). The change in nitrogen in the active organic matter takes place in a similar way to the turnover of carbon, whereas the C/N ratios of all organic fractions $\gamma_{pom}^{i,j}$ and γ_{aom} modify the synthesis coefficient $k_{syn}^{i,j}$ to $k_{syn}^{*,i,j}$ (Kartschall et al., 1990).

$$k_{syn}^{*,i,j} = k_{syn}^{i,j} \frac{\gamma_{pom}^{i,j}}{\gamma_{aom}} \quad (6.27)$$

In addition, changes of nitrogen in the reserves of ammonia N_{NH4} and nitrate N_{NO3} are considered. Thus, the net turnover of nitrogen is described by the following system of differential equations (Klöcking, 1991) for each layer

$$\frac{\partial}{\partial t} N_{pom}^{i,j}(z,t) = -k_{pom}^{i,j} N_{pom}^{i,j}(z,t) \quad (6.28)$$

$$\frac{\partial}{\partial t} N_{aom}(z, t) = \sum_{i,j} k_{syn}^{*,i,j} k_{pom}^{i,j} N_{pom}^{i,j}(z, t) - k_{aom} N_{aom}(z, t) \quad (6.29)$$

$$\frac{\partial}{\partial t} N_{NH_4}(z, t) = \sum_{i,j} (1 - k_{syn}^{*,i,j}) k_{pom}^{i,j} N_{pom}^{i,j}(z, t) + k_{aom} N_{aom}(z, t) - k_{nit} N_{NH_4}(z, t) \quad (6.30)$$

$$\frac{\partial}{\partial t} N_{NO_3}(z, t) = k_{nit} N_{NH_4}(z, t) \quad (6.31)$$

The set of differential Equations (6.28) to (6.31), with the appropriate initial values, may be solved by means of the Laplace transformation.

6.3.3 Reduction of mineralisation and nitrification

The processes of carbon and nitrogen mineralisation as well as of nitrification strongly depend on soil temperature, soil water content and the pH-value. Under the assumption, that $k_{pom}^{i,j}$, k_{aom} , and k_{nit} are the reaction coefficients at optimal temperature and moisture and at pH=7 the explicit effect of these environmental conditions can be expressed by suitable reduction functions (Franko, 1990; Kartschall et al., 1990). The product of the three reduction functions depending on water R_w^i , soil temperature R_T^i , and pH value R_p^i forms the following overall reduction function

$$R^i(z, t) = R_w^i(z, t) \cdot R_T^i(z, t) \cdot R_p^i(z) \quad (6.32)$$

with $i=min$ for mineralisation and $i=nit$ for nitrification.

The mineralisation has its optimum at water content $W_s(z, t)$ of half of the saturated water content $W_s^{sat}(z)$ (Freytag and Lüttich, 1985)

$$R_w^{min}(z, t) = 4 \frac{W_s(z, t)}{W_s^{sat}(z)} \left(1 - \frac{W_s(z, t)}{W_s^{sat}(z)} \right) \quad (6.33)$$

Also the nitrification increases with increasing water content up to the maximum at water content $W_s(z, t) = 0.5 W_s^{sat}(z)$. In difference to the mineralisation the nitrification doesn't decrease after reaching the maximum because the dissolved oxygen is used for nitrification (Hotopp, 2014)

$$R_w^{nit}(z, t) = \begin{cases} 4 \frac{W_s(z, t)}{W_s^{sat}(z)} \left(1 - \frac{W_s(z, t)}{W_s^{sat}(z)} \right) & W_s(z, t) \leq 0.5 W_s^{sat}(z) \\ 1 & \text{otherwise} \end{cases} \quad (6.34)$$

The reduction of mineralisation and nitrification by water depends on the saturated water content of the soil. Figure 6-5 shows the reduction functions of two soils with different water saturations.

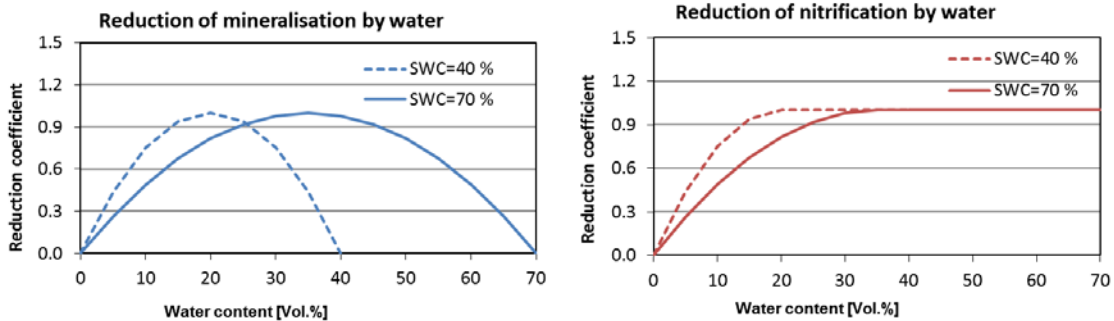


Figure 6-5 Influence of water content on mineralisation (left) and nitrification (right) in dependence on different saturation water content (SWC)

The influence of soil temperature $T_s(z,t)$ on mineralisation and nitrification is described by van't Hoff's rule (van't Hoff, 1884) (see Figure 6-6)

$$R_T^i = \left(Q_{10}^i\right)^{0.1 \cdot (T_s - T_{opt}^i)} \tag{6.35}$$

with $i=min, nit$ and $Q_{10}^{min} = 2.9$ and the optimal temperature $T_{opt}^{min} = 35^\circ\text{C}$ in case of mineralisation as well as $Q_{10}^{nit} = 2.8$ and $T_{opt}^{nit} = 30^\circ\text{C}$ in case of nitrification.

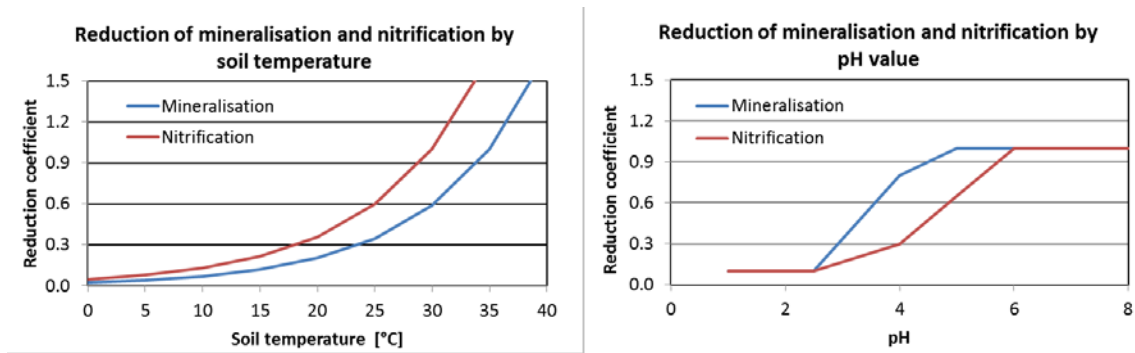


Figure 6-6 Influence of temperature (left) and pH value (right) on mineralisation and nitrification

Table 6-2 Reduction coefficient of mineralisation R_p^{min} and nitrification R_p^{nit} in dependence of the pH value

pH value	R_p^{min}	R_p^{nit}
2.5	0.1	0.1
4.0	0.8	0.3
5.0	1.0	0.65
6.0	1.0	1.0
8.0	1.0	1.0

Acid soils cause a reduction of mineralisation. Thus, it is assumed that at pH values above 5, the mineralisation is in an optimum (Painter, 1970). At lower values a reduction coefficient is determined by linear interpolation between the values of Table 6-2 (see Figure 6-6).

6.3.4 Transport of nitrogen

The easily soluble nitrate and the dissolved ammonium are transported together with the water movement between the layers. A transport of organic matter is not considered here, because this flux is only small in comparison to the absolute quantities available in the soil. Ammonium and nitrate are connected partly to the soil matrix and hence only a part of the total ammonium and nitrate is dissolved in the soil water. The amount of displaced dissolved ammonium and nitrate is proportional to the fraction of percolation water W_{upt} , relative to the total water content W_s .

$$N_{mov}^i(z, t) = f^i(z) \cdot N^i(z, t) \frac{W_p(z, t)}{W_s(z, t) + W_p(z, t) + W_{upt}(z, t)} \tag{6.36}$$

with $i=NH4$ in case of ammonium and $i=NO3$ in case of nitrate, f^i denotes the fraction of soluble ammonium and nitrate, respectively.

Based on the plant uptake of mineral nitrogen and its transport by water the ammonium and nitrate pools are balanced. This delivers the outflow of nitrogen from the rooted zone.

6.3.5 Nitrogen uptake

Similar to the concept of nitrogen transport, only dissolved nitrogen is plant available and can be taken up with the water. The uptake is calculated for each tree and is limited by its nitrogen demand. It is assumed that the plants do not prefer any nitrogen compound and thus the nitrogen uptake of a tree is estimated by

$$N_{upt}^{i,c}(z,t) = N^i(z,t) \frac{W_{upt}^c(z,t)}{W_s(z,t)} \quad (6.37)$$

with $i=NH_4$ in case of ammonium and $i=NO_3$ in case of nitrate.

The total daily nitrogen uptake of a tree $N_{upt}^{c,d}$ is the sum over the uptake of both fractions in all layers. The cumulative nitrogen uptake of a tree N_{upt}^c at the current day t is

$$N_{upt}^c(t) = \sum_{i=1}^t N_{upt}^{c,d}(i) \quad (6.38)$$

Particularly, the annual total nitrogen uptake of a tree is equal to $N_{upt}^c(t)$, $t=365$ or 366 respectively. The uptake of a cohort is the sum of the uptake of all trees of the cohort.

The cumulative nitrogen uptake of a species N_{upt}^s is the sum over the cumulative uptake of all cohorts of the same species and the total nitrogen uptake N_{upt} is the sum of the uptake of all cohorts

$$N_{upt} = \sum_{c=1}^{n_c} n_a^c N_{upt}^c(365) \quad (6.39)$$

In case of a pure stand it holds $N_{upt} = N_{upt}^s$.

7 MORTALITY AND SENESCENCE

Tree death may occur for different reasons like aging, growth suppression, disturbances (fire, diseases, storms) and harvesting. The mortality model of 4C considers two kinds of mortality. The so called ‘age related’ mortality basing on life span corresponds to the intrinsic mortality developed by Botkin et al. (1972). The response of trees to growth suppression is described by a carbon based stress mortality.

7.1 Age related (intrinsic) mortality

Based on a Weibull distribution depending on a_{max} (maximum age of species) and age $a(t)$ at time step t the annual mortality rate $p_{wint}(t)$ of each species is defined:

$$p_{wint}(t) = \alpha_{wint} \cdot \lambda_{wint} \cdot a(t)^{\alpha_{wint}-1} \quad (7.1)$$

where α_{wint} and λ_{wint} are parameters of the Weibull distribution. The parameter λ_{wint} is calculated using the survival function $S(t)$ of the Weibull distribution under the assumption that the survival probability at time $t = a_{max}$ is equal 0.01.

$$S(a_{max}) = e^{-\lambda_{wint} (a_{max})^{\alpha_{wint}}} = 0.01$$

$$\lambda_{wint} = \frac{-\ln(0.01)}{(a_{max})^{\alpha_{wint}}} \quad (7.2)$$

The parameter α_{wint} determines the increase or decrease of mortality rate with age.

7.2 Stress induced mortality

The model assumes that mortality depends on carbon balance. A measure of the carbon balance of a tree cohort is the annual foliage increment dM_f/dt . If the foliage increment is less zero the tree is not able to reproduce its foliage and the tree has stress. To take into account not only the carbon balance of the actual year t a concept developed by Keane et al. (1996) is used. The model counts the successive years of stress of each tree cohort by the stress counter c_{stress} and years without stress by the counter c_{health} in the following way:

$$c_{stress}(t) = \begin{cases} c_{stress}(t-1) + 1 & \frac{dM_f}{dt} < 0 \\ c_{stress}(t-1) - 1 & c_{health}(t) > 0 \square c_{stress}(t-1) \neq 0 \\ 0 & otherwise \end{cases} \quad (7.3)$$

and

$$c_{health}(t) = \begin{cases} c_{health}(t-1) + 1 & \frac{dM_f}{dt} \geq 0 \\ 0 & \frac{dM_f}{dt} < 0 \end{cases} \quad (7.4)$$

The stress counter is used as a predictor to calculate an annual probability of mortality of each tree cohort due to stress using the hazard function of the Weibull distribution:

$$p_{stress}(c_{stress}(t)) = \alpha_{wstress} \cdot \lambda_{wstress} \cdot c_{stress}(t)^{\alpha_{wstress}-1} \quad (7.5)$$

where $\alpha_{wstress}$ and $\lambda_{wstress}$ are scale and shape parameter of the Weibull distribution. The parameterisation of the function is species specific due to different tolerance of species with regard to stress. We define five tolerance classes j concerning stress and for each class a variable Y_s , which reflects the number of stress years leading to mortality with nearly 100%. The tolerance class is defined by the species specific parameter shade tolerance p_{st} , according to Keane et al. (1996). The variable Y_s is defined by a table function (see Table 7-1) for each species. The parameter $\lambda_{wstress}$ is calculated using the survival function $S(t)$ of the Weibull distribution assuming that after Y_s years the survival probability of a tree cohort is 0.01:

$$S(Y_s) = e^{-\lambda_{wstress} \cdot (Y_s)^{\alpha_{wstress}}} = 0.01$$

$$\lambda_{wstress} = \frac{-\ln(0.01)}{(Y_s)^{\alpha_{wstress}}} \quad (7.6)$$

Table 7-1 Parameter Y_s for stress mortality according to Keane et al. (1996)

Shade tolerance class p_{st}	Number of stress years Y_s
1	20
2	40
3	60
4	80
5	100

The total annual mortality probability p_{mort} of a tree cohort for year t is calculated as

$$p_{mort}(t) = p_{wint}(t) + (1 - p_{wint}(t)) \cdot p_{wstress}(t) \quad (7.7)$$

This mortality probability is used to update the number of living trees per cohort for year t

$$n_a^c(t) = \text{int}(n_a^c(t-1) \cdot p_{mort}(t)) \quad (7.8)$$

and the number of dead trees per cohort is than

$$n_d^c(t) = n_a^c(t-1) - n_a^c(t) \quad (7.9)$$

The described approach is applicable for mortality of trees but not seedlings. The mortality of seedlings growing from bare patches has some special characteristics which have to be taken into account. Mortality due to grazing, competition with ground vegetation is not modelled yet.

7.3 Senescence

The annual senescence of the compartments foliage, fine roots and sapwood per tree cohort $f_{s,i}$ are calculated by

$$f_{s,i} = s_i M_i \quad (7.10)$$

with $i \in \{f \text{ (foliage)}, s \text{ (sapwood)}, r \text{ (fine roots)}\}$, compartment specific annual senescence rates s_i and biomass M_i of the compartment i of the tree cohort.

8 REGENERATION

The regeneration model describes the processes of seed germination, growth and mortality of seedlings, and the recruitment of seedlings into cohorts.

8.1 Seed rates

A species specific number of available seeds is first estimated using an approach initially developed in the model SIMSEED (Rogers and Johnson, 1998). An annual potential seed rate n_{seed} of each species is calculated:

$$n_{seed} = -n_{seed}^{max} \ln(r_{ne}) \quad (8.1)$$

where r_{ne} is an equal distributed random number from [0,1] and n_{seed}^{max} is the species specific maximum number of seeds per m².

Germination success of these seeds depends on light availability, temperature and moisture conditions in the litter layer. In the current version, however, only the light regime is actually used as a driver. Germination of seeds fails if the leaf area index of all currently established seedlings in the seedling layer (0-50 cm height) is greater than 1.0, which indicates total coverage of the patch. In this case n_{seed} is equal zero. Otherwise, the number of germinated seeds is derived from the fraction of the patch not shaded by leaves in the seedling layer. Depending on the light module n_{seed} is modified by a factor between 0 and 1, which is calculated from the fraction of 'free crown space' or the relative light intensity of the not covered patch .

8.2 Establishment of seedlings

Species and annual numbers of seedlings are grouped into annual seedling cohorts. If for species which are allowed to regenerate a non-zero value of n_{seed} is calculated a new seedling cohort is established. Initial values of the main characteristics (variables) of a seedling cohort are calculated. To allocate the masses of shoot, root and foliage of a seedling the following relations are used:

$$\begin{aligned} M_f &= p_{sa} M_s^{p_{sb}} \\ M_f &= M_r \\ 2 p_{sa} M_s^{p_{sb}} + M_s - 0.7 M_{seed} &= 0 \end{aligned} \quad (8.2)$$

where M_f is foliage mass, M_r is fine root mass and M_s is shoot mass, assuming that shoot mass of a seedling is equal sapwood mass, and loss of 30% of seed mass M_{seed} during germination. From these equations solutions for M_s , M_f and M_r are calculated. The empirical

relationship between shoot mass and foliage is derived from experiments by Dohrenbusch (1997); Hauskeller-Bullerjahn (1997); Schall (1998). The height of seedlings is calculated by an allometric relation derived by Dohrenbusch (1997); Schall (1998); Van Hees (1997):

$$H = p_{h1} \cdot (M_s)^{p_{h2}} \quad (8.3)$$

where p_{h1} and p_{h2} are species specific parameters.

8.3 Growth of seedlings

Growth of each seedling cohort is updated annually. Net primary production and phenology are simulated similarly to those of older tree cohorts, using radiation, temperature, CO₂ concentration, water and nutrient availability as inputs. When the simulated height of the seedlings exceeds an arbitrary threshold value, the entire cohort is then transformed into a regular tree cohort.

More details of the allocation calculation and growth for seedlings see in Chapter 4.4 .

8.4 Mortality of seedlings

The mortality of seedlings is similar to tree mortality modelled. An intrinsic mortality is calculated depending on age (see Chapter 7.1) and a stress-related mortality is calculated with the same approach as for trees (see Chapter 7.2).

8.5 Ingrowth into the tree layer

A seedling cohort is considered as tree cohort if a defined tree height H_{thr} is reached. If this happens the cohort is growing and dying as described in Chapter 4.4.

9 FOREST MANAGEMENT

The model 4C allows the management of mono- and mixed species forests. For this purpose, a variety of thinning, harvesting and regeneration strategies are implemented.

9.1 Thinning

Thinning is defined mainly by the intensity and the method. The thinning intensity is given by a fixed portion of the stem number or stem biomass which has to remove. The stand differs in an upper storey and over storey layer if planting is realized during the simulation.

The thinning methods thinning from above and thinning from below are realised by means of a stochastic approach based on a Weibull distribution (Gerold, 1990; Wenk and Gerold, 1996). The diameter of a thinned tree d_t is calculated by means of Weibull-distributed random numbers:

$$d_t = b \sqrt[c]{-\ln((1-u))} + d_{\min} \quad (9.1)$$

where b and c are parameters of the Weibull distribution describing the part of the stand to be cut (removal), d_{\min} is the minimum diameter at breast height of the stand, u is a uniformly distributed number within the interval [0,1). The parameter b is determined by:

$$b = \frac{b_{st}}{k_b}, \quad (9.2)$$

where b_{st} is the scale parameter of the Weibull-distribution function of the stand before thinning, and the parameter k_b controls the thinning strategy affecting the distribution of the removal. Values of k_b greater than 1.8 realise a thinning from below, if k_b is nearly 1 or less than 1 thinning from above is described. The parameter b_{st} is estimated using the p-quantile ($p = 0.63$) of the diameter distribution d_{63} :

$$b_{st} = d_{63} - d_{\min} \quad (9.3)$$

It is assumed that the distribution function parameter c of the stand before thinning and of the thinning trees is identical and c is fixed equal to 2. In 4C $k_b=2.5$ is used for moderate thinning from below, $k_b=1.5$ for strong thinning from below, and $k_b=1.2$ (Lindner, 2000) for thinning from above.

9.2 Harvesting

The stand harvesting is determined by the rotation period, which is a parameter. Two harvesting methods are available. Clear cut is combined with or without planting of saplings

of one or more species. The mixture and number of saplings is arbitrary. Shelterwood management includes removing of a portion of trees from the over storey in a defined way combined with planting of saplings.

9.3 Planting

Planting of saplings includes the generation of a well-defined height class distribution using a specific mean height H_p , minimum value of height H_p^{min} , standard deviation of height σ_H , and a species specific number of planted saplings n_s . These values are given with default values. Additionally, the number of planted saplings can be modified by the management control file. A number of height classes n_{cl} representing sapling cohorts is calculated:

$$n_{cl} = (H_p + 3 \sigma_H) - H_p^{min} \quad (9.4)$$

For each sapling cohort i the height H_i is calculated by H_p^{min} and an increase by 1 cm from one height class to the next:

$$H_i = H_p^{min} + (i - 1) \quad (9.5)$$

The number of saplings per cohort $n_h^c(i)$ is calculated using the total number of planted saplings n_{pl} in the following way. Using a normal distribution the value $n_h(i)$ is calculated:

$$n_h(i) = \frac{1}{\sqrt{2\pi} \sigma_H} e^{-\frac{1}{2} \left(\frac{H_i - H_p}{\sigma_H} \right)^2} \quad (9.6)$$

with

$$n_{stot} = \sum_{i=1}^{n_{pl}} n_h(i) \quad (9.7)$$

and then

$$n_s^c(i) = n_h(i) \cdot \frac{n_s}{n_{stot}}. \quad (9.8)$$

The initial values for sapwood biomass $M_{s,i}$ and foliage biomass $M_{f,i}$ are calculated by the allometric functions using for seedling growth:

$$H = \rho_{h1} (M_s)^{\rho_{h2}} \quad (9.9)$$

$$M_{s,i} = e^{\frac{\ln H_i - \ln \rho_{h1}}{\rho_{h2}}} \quad (9.10)$$

$$M_{f,i} = p_{sa} \left(M_{s,i} \right)^{p_{sb}} \quad (9.11)$$

The growth of planted sapling cohorts is described like the growth of seedlings until the height exceeds a threshold value and the sapling cohort is transformed into a tree cohort (see Chapter 8).

Planting is possible in the case of clear cut, shelter wood management, and as generation of under storey without specific management.

9.4 Short rotation coppice

For the species Aspen (*Populus tremulus* (L.)) and Black locust (*Robinia pseudoacacia* L.) a short rotation coppice was implemented which realized pruning of the trees depending on the rotation year and following resprouting of trees from the remaining stock (with coarse roots).

Following the allocation scheme for the sprouts is described in more detail. These variables are used:

M_{crt} – coarse root of the stock after harvesting

M_{firt} – fine root biomass of the stock

$M_{firt}(i)$ – fine root biomass of sprout i

a) Root biomass of sprouts

The total coarse root and stump biomass is divided into the shares of a number n_{sprout} of sprouts. Depending on the species different number are used. The shoot mass $M_{sroot}(i)$ of sprout i is calculated as follows from the available coarse root M_{crt} of the stock after harvesting and the biomass M_{stump} of stump after harvesting using a table function f_{ac} (see Table 9-1)

$$M_{sroot}(i) = f_{ac}(i) \cdot (0.3 M_{crt} + 0.5 M_{stump}) \quad (9.12)$$

For the remainig stump after harvesting a height of 10 cm is assumed.

Table 9-1 Number of sprouts n_{sprout} and table function f_{ac} (empirical assumptions) for Aspen and Black locust

	Aspen	Black locust
n_{sprout}	3	5
f_{ac}		
1	0.25	0.0666
2	0.333	0.1332
3	0.41666	0.1998
4	-	0.2664
5	-	0.334

b) Sapwood of the sprouts

The foliage biomass M_f of the sprout i is estimated from the sapwood M_s of sprout i with a species specific parameter p_{sa} for shoot-foliage relationship (similar to saplings):

$$M_f(i) = p_{sa} M_s(i) \quad (9.13)$$

and then the following balance equation is solved:

$$M_s(i) + p_{sa} M_s(i) - M_{sroot}(i) = 0 \quad (9.14)$$

The solution is found with a regula falsi approach.

c) Foliage biomass

By application of equation (9.13) foliage biomass is calculated and following leaf area of the sprout.

d) Fine root biomass

$$M_r(i) = f_{ac}(i) * M_r \quad (9.15)$$

e) Height of the sprout

$$H(i) = p_{h1} \cdot M_s(i)^{p_{h2}} \quad (9.16)$$

f) *Bole height*

Bole height is defined by the height of the stump (10 cm) (see Chapter 8).

9.5 Timber assortment

For provision of information about timber assortment of standing and harvested biomass an algorithm was developed. The algorithm delivers a list of all timber products which are available from harvested trees but also standing volume. For this purpose a variety of diameter, height and volume calculations were carried out.

The stem of a tree is characterized by following terms:

- diameter at breast height d_{bh}
- height H
- diameter at crown base d_{cb}
- bole height H_b
- $H_{sto}=10$ cm (storey height)

Further on it is necessary to calculate:

- diameter d_{borg} at height H_{sto} of the original stem
- diameter d_b at base of the stem segment
- length S_l of the stem segment
- Diameter d_x at height H_x

A stem is assorted into different types of wood:

- Stem wood
- Stem segments of various length
- Industrial wood of various length
- Fuel wood

Corresponding to the stem geometry (see chapter 2.2) in 4C the relations between diameter at different heights and length of different stem segments (see Figure 9-1) are used to calculate the necessary terms. The calculation of the characteristic variables of stem form using geometric relationships is described as follows.

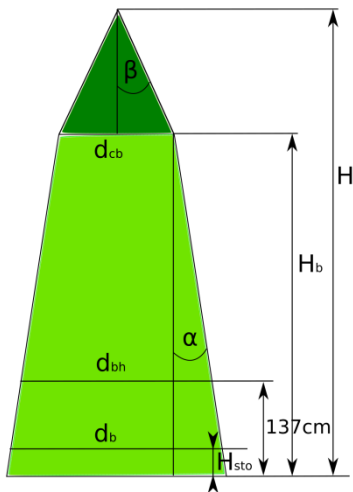


Figure 9-1 Scheme of stem geometry

a) Diameter d_b at height H_{sto}

$$d_b = d_{cb} + \frac{(d_{bh} - d_{cb})(H_b - 10)}{H_b - 137} \quad (9.17)$$

if $H_b = 0$ then yields

$$d_b = d_{bh} \frac{10}{H - 137} \quad (9.18)$$

For $H_b < 137$ cm the same function (Equation (9.18)) is used as a first approximation.

b) Diameter d_x at height H_x , if $H_x \leq H_b$

Using the tangent function for the angle α (see Figure 9-1) it yields

$$\frac{d_{borg} - d_{crb}}{H_b} = \frac{d_x - d_{crb}}{H_b - S_l - H_x} \quad (9.19)$$

$$d_x = d_{crb} + \frac{(d_{borg} - d_{crb})(H_b - S_l - H_x)}{H_b}$$

with the length S_l of stem always removed (measured).

c) Diameter d_x at height H_x , if $H_x > H_b$

Using the tangent function for the angle β (see Figure 9-1) it yields

$$\frac{d_{crb}}{2(H - H_b)} = \frac{d_x}{2(H - S_l - H_x)} \quad (9.20)$$

$$d_x = \frac{d_{crb}(H - S_l - H_x)}{H - H_b}$$

d) Height H_x at diameter d_x if $d_{crb} < d_x$

$$\frac{H_b}{d_{borg} - d_{crb}} = \frac{H_b - S_l - H_x}{d_x - d_{crb}} \quad (9.21)$$

$$H_x = H_b - S_l - \frac{H_b(d_x - d_{crb})}{d_{borg} - d_{crb}}$$

e) Height H_x at diameter d_x if $d_{crb} \geq d_x$

$$\frac{H - H_b}{d_{crb}} = \frac{H - H_x - S_l}{d_x} \quad (9.22)$$

$$H_x = H - S_l - \frac{d_x(H - H_b)}{d_{crb}}$$

f) Height H_x at diameter d_x if $d_{crb} = 0$.

$$H_x = H - S_l - \frac{(H - H_{sto})d_x}{d_{borg}} \quad (9.23)$$

The stem is sampled into different segments. If a segment is analysed ('cutted'), the value S_l is increased by the length of this element and a value of d_b , diameter of the residual stem, is calculated.

The following steps of sampling are realized using the parameters from Table 9-2:

- Stem wood (type ste) which fulfilled the length and diameter requirements:
 - L_{min} – minimum length
 - L_{dmin} – minimum diameter
 - L_{zmin} – minimum diameter at the small end)
- Stem wood segments (type sg1, sg2) of two different length:
 - $L_{ASFIXL1}$ – length 1
 - $L_{ASFIXL2}$ – length 2
 - L_{ASDmin} – minimum diameter 1
 - L_{ASZmin} – minimum diameter 2)

- Industrial wood (type in1, in2) of two different length:
 - I_{FIXL1} – length 1
 - I_{FIXL2} – length 2
 - I_{SDmin} – minimum diameter
 - I_{SZmin} – minimum diameter at the smaller end
- Fuel wood (type fue)

Table 9-2 Parameter [cm] for sorting of harvested and remaining stems into the different groups (forest expert knowledge) according to Frommhold (2001)

	Beech, oak and similar (deciduous hardwood)	Spruce and similar	Pine and similar	Birch and similar (deciduous softwood)
L_{min}	400	400	400	400
L_{dmin}	30	30	30	35
L_{zmin}	20	14	14	20
L_{ASFIXL1}	400	400	400	400
L_{ASFIXL2}	300	300	300	300
L_{ASDmin}	20	15	15	20
L_{ASZmin}	11	11	11	11
I_{FIXL1}	200	200	200	200
I_{FIXL2}	100	100	100	100
I_{SDmin}	10	10	10	10
I_{SZmin}	7	7	7	7

9.6 WPM and SEA

The wood product model is based on the model concept introduced by Karjalainen et al. (1994) and further developed by Eggers (2002). The WPM simulates carbon pools and fluxes in the wood product sector. The parameters are based on aggregated values of the German timber market report 2002 and 2003 (Verbraucherschutz, 2003; Verbraucherschutz, 2004) and parameters according to Eggers (2002). The WPM consists of three main processes, the grading of the harvested timber, the processing of the timber and allocation of timber to wood products, and the retention period of timber in the final product and later on landfills.

9.6.1 **Main processes of the WPM**

Grading of harvested timber

The first step of the WPM is the grading of the harvested timber. The harvested timber is graded according to the German timber classification system. Following timber grades are used in the WPM:

- TG1 - coniferous logs,
- TG2 - non coniferous logs
- TG3 - coniferous partial logs
- TG4 - non coniferous partial logs
- TG5 - industrial wood
- TG6 - fuelwood

Wood defects due to growth anomalies and defects through harvesting are not simulated in 4C. A down grading due to this wood defects is parameterised in the WPM. Actually 40% of the volume of logs or partial logs is classified as industrial wood.

The amount of carbon in different timber grades is calculated for each year with timber harvest (thinning or harvest). Trees which die between two management operations are removed with the next thinning or harvest and are added to the amount of harvested timber.

Timber processing

In the next step the timber is distributed into *industrial lines* which display the different wood industry branches (sawmills, plywood and veneer industry, particle board manufactures and pulp and paper mills). The distribution of the harvested timber into the industrial lines is based on figures of the German timber market report (Verbraucherschutz, 2003; Verbraucherschutz, 2004). The report lists the main consumer of timber and the amount of purchased coniferous timber, deciduous timber and industrial wood. The following industrial lines are differentiated:

- IL1 - coniferous sawn timber
- IL2 - deciduous sawn timber
- IL3 - plywood and veneer
- IL4 - particle board
- IL5 - chemical pulp
- IL6 - mechanical pulp
- IL7 - fuel wood.

The distribution of timber into these industrial lines is described in Appendix WPM, Table 4.

The timber of the industrial lines is further distributed into *product lines*. This distribution reflects the processing of the timber into the main product and by-products. The distribution is based on parameters according to Eggers (2002) Appendix WPM, Table 5, 6, 7.

Timber products

In the third step the timber is distributed into *use categories*. The following use categories are distinguished according to Eggers (2002):

- U1 - building material
- U2 - other buildings
- U3 - structural support
- U4 – furnishing
- U5 - packing material
- U6 - long life paper
- U7 - short life paper.

The distribution of wood from the product lines into the use categories is described in Appendix WPM (Table 8).

The retention period of the timber in the different use categories is defined by a life span function, an extended logistic decay function by Row and B. (1996)

$$f(p_u) = d_{wpm} - \frac{a_{wpm}}{1 + b_{wpm} \cdot e^{-c_{wpm} \cdot t}} \quad (9.24)$$

where p_u is the fraction of products (carbon) in use, a_{wpm} , b_{wpm} , d_{wpm} are parameters, c_{wpm} is the reciprocal of the half-life period [year^{-1}], and t is the time in years.

The lifespan (half-life period) of the used categories is listed in Appendix WPM (Table 9). The timber which is removed from the use categories will to a certain shares be recycled, put on landfills or be burned (Appendix WPM, Table 9). The redistribution of the recycled timber to the use categories is listed in Appendix WPM, Table 10.

9.6.2 Results of the WPM

WPM creates the following general information:

- total harvested timber [t C ha⁻¹] – annually
- use categories [t C ha⁻¹] – annually
- landfill / waste site [t C ha⁻¹] - annually
- burning [t C ha⁻¹] - annually

- atmosphere [t C ha⁻¹] – annually
- atmosphere [t C ha⁻¹] – cumulative.

In addition, more detailed information are provided about

- timber grades [t C ha⁻¹] – annually
- industrial lines [t C ha⁻¹] - annually
- product lines [t C ha⁻¹] - annually
- use categories [t C ha⁻¹] – annually.

9.6.3 **WPM for Brandenburg**

The application of WPM in Brandenburg is shown in Figure 9-2. In the case of Brandenburg it is assumed that the share of timber which goes to pulp mills is purchased by the closest mills. These mills use chemical method to process the wood. Therefore no wood goes to the industrial – and product line 6 (mechanical pulpwood). These parameters should be adapted if the model is used in other regions.

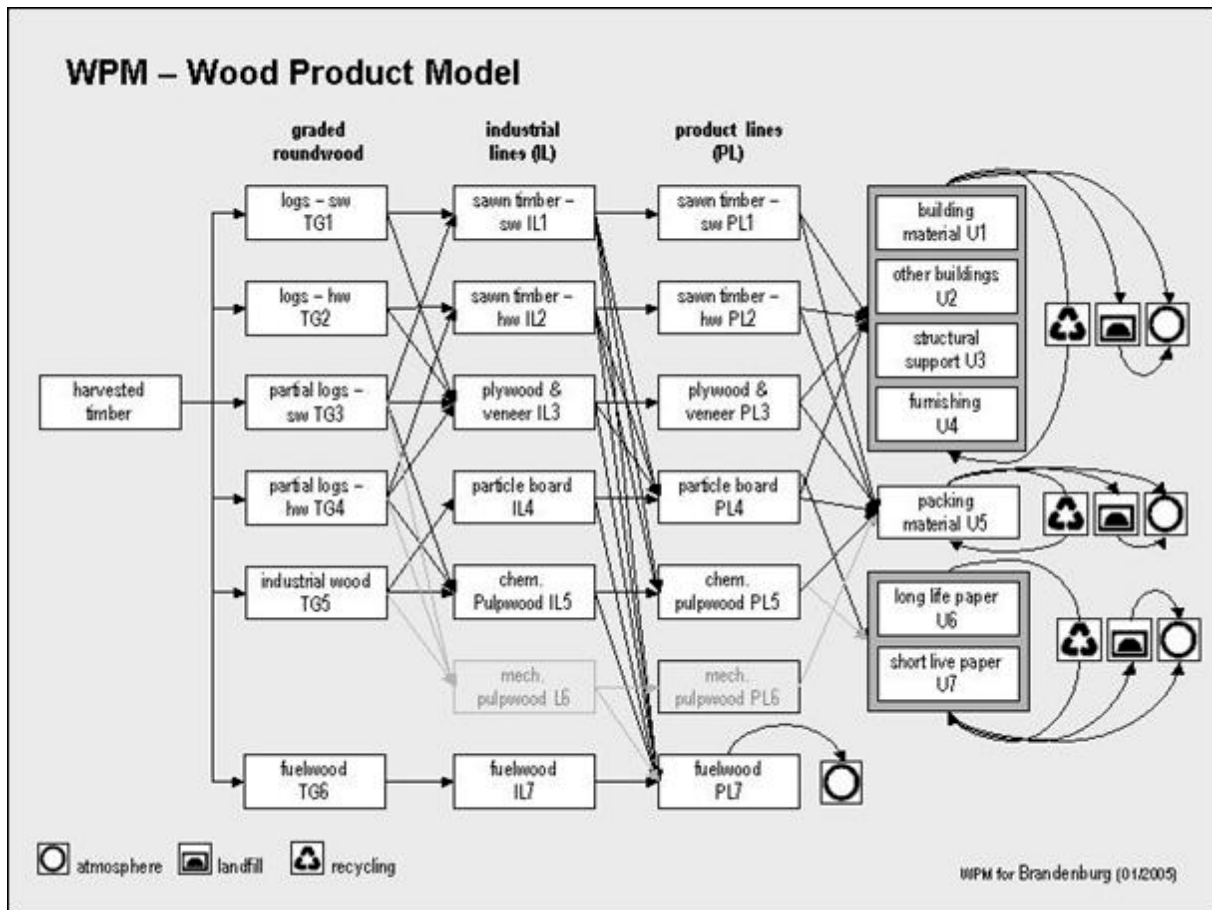


Figure 9-2 Flow chart of the WPM for Brandenburg (Fürstenau, 2008). Abbreviations see Chapter 9.6.1

9.6.4 Spin up for WPM

The spin up calculates the initial amount of carbon in use categories based on average timber production of the study area. The average timber production of the study area has to be simulated by 4C. An example you can find in the Appendix WPM. The time span of the spin up can be chosen.

9.6.5 Socio economic analysis (SEA)

SEA calculates costs, revenues and subsidies of forest management and furthermore the net present value of forest management and the liquidation value of the standing stock.

Timber grades

In the first step of SEA the harvest timber and standing stock is graded according to the German timber classification system. Timber grading after the German timber classification is based on the diameter at the middle of the log and a minimum top diameter of a log. The middle diameter is rounded down to centimetres. Table 9-3 lists the timber grades used in the SEA. Wood defects due to growth anomalies and defects through harvesting are not

simulated in 4C. A down grading due to this wood defects is parameterised in SEA. Actually 40% of the volume of logs or partial logs is classified as industrial wood.

Table 9-3 Timber grades in SEA (o.b. – over bark (diameter including bark), wo.b. – under bark).

Assortment group	Dimension class	Timber grade – German abbreviations	Middle diameter [cm]	Top diameter [cm]	Kind of timber
fuelwood		X		< 7 cm wo.b.	Coniferous and deciduous
Industrial wood		IN		7 cm wo.b.	Coniferous and deciduous
Partial log	1a	L1a	11-14 cm o.b.	11 cm o.b.	pine
Partial log	1b	L1b	15 – 19 cm o.b.	11cm o.b.	Coniferous
Partial log	2a	L2a	20 – 24 cm o.b.	14 cm o.b.	Coniferous and deciduous
Partial log	2b	L2b	25 – 29 cm o.b.	14 cm o.b.	Coniferous and deciduous
Partial log	3a +	L3a	>= 30 cm o.b.	14 cm o.b.	Coniferous and deciduous
Log	2b	L 2b	25 – 29 cm o.b.	14 cm o.b.	Coniferous and deciduous
Log	3a	L 3a	30 – 34 cm o.b.	14 cm o.b.	Coniferous and deciduous
Log	3b +	L 3b	>= 35 cm o.b.	14 cm o.b.	Coniferous and deciduous

Cost, revenues and subsidies

Forest management costs consist of four components: cost of timber harvest including timber hauling, silvicultural costs including regeneration, fencing, and pre-commercial thinning costs, fix costs (e.g. administrative cost and road maintenance) and cost for the assistance of a forest manager in a private owned forest. Revenues of forest management are the prices for the harvested timber. Subsidies of forest management consist of three components: subsidies for silvicultural operation including regeneration, fencing, and pre-commercial thinning, subsidies for fix costs in a private owned forest and subsidies for the cost for the assistance of a forest manager in a private owned forest (Appendix WPM, Table 16). Costs and revenues of timber harvest and pre-commercial thinning are derived from statistics on state forestry in Brandenburg (MLUR 2000, Appendix WPM, Table 13, 14, 15). Regeneration costs (e.g. price of plants, cost for planting) are based on an actual price list of a tree nursery in the region and the practical experience of local forest service personnel (Appendix WPM, Table 15).

Liquidation value and net present value

Two different methods, based on the net present value approach, are applied to investigate the economic impact of forest management. The net present value in general is the difference between the discounted value of the future net cash flow c^f of a certain time span t_{nyear} expected from forest management and the initial investment. In the first case, the initial investment value is assumed to be zero because no investments had to be done since the forest stands are already owned. Therefore, the term of initial investment is neglected. This leads to the calculation of the net present value N_{PV}

$$N_{PV} = \sum_{t_y=1}^{t_{\text{nyear}}} \frac{c^f(t_y)}{(1+p)^{t_y}} \quad (9.25)$$

with the discounting rate p .

The second economic measure, N_{PV}^+ , integrated the value of the standing stock. It was assumed that the investment value is the liquidation value L_1 of the standing stock at the beginning of the simulation. Additionally, the discounted liquidation value of the standing stock at the end of the simulation time $L_{t_{\text{nyear}}}$ was added to the NPV

$$N_{PV}^+ = \sum_{t_y=1}^{t_{\text{nyear}}} \frac{c^f(t_y)}{(1+p)^{t_y}} - L_1 + \frac{L_{t_{\text{nyear}}}}{(1+p)^{t_{\text{nyear}}}} \quad (9.26)$$

Both approaches are calculated with three different interest rates ($p = 0.02, 0.04, 0.06$).

Output

The socio economic analysis provides information about

- timber grades of the harvested timber and standing stock,
- cost, revenues of thinning and harvest per tree species, silvicultural costs, fix cost and subsidies,
- liquidation value, and
- net present value without and with discounting.

10 DISTURBANCES

In 4C two kinds of biotic disturbances are considered. On one hand the model is able to describe the disturbance of pine trees by mistletoe (*Viscum album* L.) and on the other hand it allows to simulate the effect of disturbances by functional groups of insects and pathogens.

10.1 Mistletoe

Infection by mistletoe is implemented in 4C as disturbance on pine trees, starting in the first year of simulation (Kollas et al., 2018).

The mistletoes are considered as an additional cohort. This cohort is initialized before all the tree cohorts with the following values: species-number (number of tree species +2), number of individuals (1), age (10 years), foliage mass (0.0158 kg), sapwood biomass (0), fine root (0), height (20 m), specific leaf area (0), crown area (0.0189 m²), day of bud burst (1). The cohort of mistletoe is associated to the uppermost cohort of trees, as these trees are commonly infected. The height of mistletoe is updated according to the height of that tree cohort. The transpiration of mistletoe is implemented the same way as for trees (see Chapter 5.1.), except that all transpiration demand of mistletoe is added to the demand of the infected tree cohort on the daily time step. Mistletoe photosynthesis is calculated the way it is implemented for trees (see Chapter 4.2.), except that NPP for mistletoe is always calculated without drought (Zweifel et al., 2012) and nitrogen stress and 30 % (Richter and Popp, 1992) of theoretically mistletoe-produced NPP is subtracted from the NPP of the infected tree cohort on the yearly time step.

In the partitioning stem and root compartments of the mistletoe cohort are ignored, only the foliage compartment is being initialized with a standard 10-year old mistletoe individual (0.0158 kg dry weight foliage per infected tree (Pfiz and Kupperts, 2010)). On the yearly time step, foliage is updated by a population growth function, given as external input with the management file. For instance in our paper in Kollas et al. 2017 we chose an exponential function, as this reflects best the expected growth (Noetzli et al., 2003; Pfiz and Kupperts, 2010; Vallauri, 1998). For the evaluated sample stand Berlin-Müggelsee, the following growth function was fitted to measurements used:

$$P_{am} = 0.09 \cdot e^{(0.17t_i)} \quad (10.1)$$

where P_{am} equals the mistletoe photosynthetic active plant area and t_i equals the year after first infection.

There is currently no litter fall, no regeneration, no senescence and no mortality of mistletoe implemented, except for the case that infected trees die. In this case, the corresponding

number of mistletoe is being removed (not placed into the litter-pool) together with the dead trees.

10.2 Pests

Modelling the effects of insects and pathogens in 4C follows a specific framework proposed by Dietze and Matthes (2014). In this framework, insects and pathogens are clustered upon their damaging action and abstracted on the level of functional groups (Table 10-1).

Table 10-1: Implemented functional groups of insects and pathogens as proposed by Dietze and Matthes (2014). The indirect and direct effects on the allocation process of 4C are also listed. NSC = non-structural carbohydrates

Disturbance (biotic)	Impact	Indirect effects on allocation	Direct effects on allocation
Defoliation	% foliage biomass loss	NPP reduction Affect allocation calculations due to changed ratios between biomass pools	Carbon surplus from NSC carbon storage pool at the end of the disturbance year Refilling of NSC carbon storage pool in subsequent years
Xylem clogging	% reduction in water supply rate	NPP reduction due to water stress	Carbon surplus from NSC carbon storage pool at the end of the disturbance year Refilling of NSC carbon storage pool in subsequent years
Hemiparasitic plants	% increase in transpiration and % carbon loss	NPP reduction	If NPP reduction then: Carbon surplus from NSC carbon storage pool at the end of the disturbance year Refilling of NSC carbon storage pool in subsequent years
Phloem feeding	% carbon loss	NPP reduction	Carbon surplus from NSC carbon storage pool at the end of the disturbance year Refilling of NSC carbon storage pool in subsequent years
Root damage	% fine root loss	Affect allocation calculations due to changed ratios between biomass pools	Carbon surplus from NSC carbon storage pool at the end of the disturbance year Refilling of NSC carbon storage pool in subsequent years
Stem rot	% increase in stem mortality	Reduces stem number which changes growing conditions	No direct effects

NSC = non-structural carbohydrates

10.2.1 Defoliation

Foliage biomass loss $M_{f,loss}$ is given by the external input of percentage loss $p_{M_{f,loss}}$ of the foliage biomass M_f^C . The foliage biomass loss is added to the foliage litter pool. The

reduction of the foliage biomass takes place immediately after the day of the year given as an external model input:

$$M_{f,loss} = p_{M_{f,loss}} M_f^c \quad (10.2)$$

10.2.2 Fine root damage

Fine root biomass loss is simulated exactly the same way as foliage biomass loss.

Accordingly, the reduction of the fine root biomass takes place immediately after the day of the year given as an external model input:

$$M_{r,loss} = p_{M_{r,loss}} M_r^c \quad (10.3)$$

10.2.3 Xylem damage

Xylem damage is implemented as percentage loss of xylem conductivity (p_{xcond}) which reduces the transpiration flow by limiting the water uptake by roots. The amount of water uptake calculated by equation (6.4) is therefore reduced by $(1-p_{xcond})$. The reduction of xylem conductivity takes place immediately after the day of the year given as an external model input:

$$W_{upt}^c(t) = \min \left(E_{trd,c}(t), \sum_{i=1}^{n_z} W_{av}(z_i, t) \right) \cdot (1 - p_{xcond}) \quad (10.4)$$

10.2.4 Phloem feeding

Phloem feeding is simulated as percentage carbon loss (p_{pfeed}) by reducing the undisturbed daily net primary production of a tree (f_{NPP}) by $(1-p_{pfeed})$. The carbon loss is given as an input variable to get the disturbed daily net production. The reduction of the daily net primary production takes place immediately after the day of the year given as an external input.

10.2.5 Stem rot

Stem rot is implemented as additional stem mortality by adding the percentage of stem rot caused dead trees p_{srot} to the total mortality rate p_{mort} . The stem rot mortality rate is not allowed to exceed the difference $(1-p_{mort})$:

$$p_{mort} = \max(1, p_{mort} + p_{srot}) \quad (10.5)$$

10.3 Carbon flows from the C-reserve within disturbance simulations

Only in case of simulations with disturbances a NSC-pool (non-structural carbohydrates including starch and sugars) of is activated and the carbon amount for the allocation will be enhanced by carbon from the NSC-pool as a C-reserve of the tree. Due to the fact that the

NSC-pool has been implemented after the formulation of the general allocation process described in section 4.4, the depleting and refilling of the NSC-pool does not affect the determination of the partitioning coefficients λ_i ($i=s,f,r$). The processes described in the following are executed after the determination of the partitioning coefficients and before the allocation of the biomass. The NSC-pool consists of three compartments allocated to the biomass compartments sapwood (s), branch/twigs (tb) wood, and coarse root wood (crt). Leaf and fine root pools are currently not accounted for a NSC-pool because of their phenology and following much more complex NSC flows. The maximum size of the NSC-pools of sapwood and branches, separated for coniferous and deciduous trees, based on data reported by (Hoch et al., 2003). The coarse root values were set equal to the branch value due to lack of information (Table 10-2).

Table 10-2: Relative (p_i^{NSC} , $i=\{tb,s,crt\}$) maximum size of the NSC-pool (starch and sugar) for the three implemented compartments. Maximum size is relative to dry matter mass of the specific compartment biomass ($M_{i,c}$, $i=\{tb,s,crt\}$).

Compartment	Deciduous [% of dry weight]	Coniferous [% of dry weight]
Branch wood $M_{tb,c}$	12.5	6.5
Sapwood $M_{s,c}$	4.2	1.8
Coarse roots ($M_{crt,c}$)	12.5	6.5

The carbon costs of the biosynthesis of NSC compounds for storage are also included by a fix value of 12.8% of the amount used for the refilling of the NSC-pools (Chapin et al., 2011; Eglin et al., 2008). These costs were also subtracted from the annual net primary production and added to the maintenance respiration.

The work flow of the NSC-pools and the carbon surplus is given as follows. At the beginning of the simulation the maximum size equals the actual size of the NSC-pools, which are initialized based upon the biomass of the three considered compartments and the relative shares given in Table 10-2.

$$\begin{aligned}
 C_{\max,i}^{NSC} &= C_{act,i}^{NSC} \\
 &= M_{i,c} p_i^{NSC} \quad \text{with } i = \{tb, s, crt\}
 \end{aligned}
 \tag{10.5}$$

At the end of every simulation year, this maximum is updated (percentage values of Table 10-2) due to the growth of the related biomass pools. Every year it is checked if the actual NSC-pool size is lower than the maximum size. In this case, the NSC-pool will be refilled with carbon from the net primary production of the actual year. Hereby, the amount of carbon

available for the refilling is limited to 50 percent of the net primary production before the refilling process.

$$f_{NPP,ar} = \max \left(\begin{array}{l} 0.5 f_{NPP,br} , \\ f_{NPP,br} - \sum_{i=tb,s,crt} \left((C_{max,i}^{NSC} - C_{act,i}^{NSC}) + 0.128 (C_{max,i}^{NSC} - C_{act,i}^{NSC}) \right) \end{array} \right) \quad (10.5)$$

Where $f_{NPP,ar}$ is the net primary production after the refilling process and $f_{NPP,br}$ the net primary production before the refilling process.

If the simulation year includes a disturbance due to phloem feeding, xylem damage, defoliation or fine root loss, the current net primary production can be increased with carbon from the NSC-pool C_{plus}^{NSC} . The maximum amount which can be taken is either equal to the amount of carbon which is lost by the disturbances (if size of the NSC-pool is greater than the losses by the disturbances) or equal to the size of the NSC-pool (if size of the NSC-pool is less than the losses by the disturbances). The surplus of carbon for the allocation is only available at the end of the disturbance year and is added to the net primary production $f_{NPP,ar}$ which is further used for the allocation process of Equation (4.26).

$$C_{plus}^{NSC} = \min \left[\begin{array}{l} M_{f,loss} + M_{r,loss} + f_{NPP,ar} \cdot (1 - p_{xcond}) + f_{NPP,ar} \cdot (1 - p_{pfeed}), \\ \sum_{i=tb,s,crt} C_{act,i}^{NSC} \end{array} \right] \quad (10.5)$$

11 CLIMATIC AND RISK INDICES

11.1 Forest Fire Index (Käse)

The forest fire index $I_{C,d}$ according to Käse (1969) indicates a potential forest fire risk for the actual day. It depends on the temperature sum up to this day of the year, the vapour pressure deficit, the previous precipitation and the actual phenological data of the corresponding year and is calculated for each day t by

$$I_{C,d}(t) = k_p(t) \cdot I_{C,d}(t-1) + k_{phen}(t) \cdot (T_{max}(t) + 10) \cdot \delta_{13} \quad (11.1)$$

with $46 \leq t \leq 274$. The maximum daily air temperature T_{max} is added with 10 to avoid negative values. The air vapour pressure deficit at 13 h δ_{13} is defined as the difference between the saturated vapour pressure at 13 h P_{sat}^{13} and the vapour pressure at 13 h P_{vap}^{13} by Equation (3.13).

The modifier k_p is determined by the precipitation P_d of the actual day t or the number of snow days n_{snow}

$$k_p(t) = \begin{cases} 0 & P_d(t) \geq 10 & \text{or } n_{snow} > 2 \\ 0.25 & 5 \leq P_d(t) < 10 & \text{or } n_{snow} = 2 \\ 0.5 & 1 \leq P_d(t) < 5 & \text{or } n_{snow} = 1 \\ 1 & \text{otherwise} \end{cases} \quad (11.2)$$

The modifier k_{phen} varies for each day t with phenology and precipitation

$$k_{phen}(t) = \begin{cases} 0.5 & 227 < t & \text{and } P_d(t) \geq 5 \\ 1.0 & d_{BB}^{rob} < t < 227 & \text{and } P_d(t) \geq 5 \\ 2.0 & d_{BB}^{birch} < t < d_{BB}^{rob} & \text{and } P_d(t) < 5 \\ 3.0 & t < d_{BB}^{birch} \end{cases} \quad (11.3)$$

The day of bud burst for birch d_{BB}^{birch} is calculated according to the 4C approach (Schaber, 2002a). The day of bud-burst for Robinia d_{BB}^{rob} is determined with a simple temperature sum model: The bud-burst is reached, when the temperature sum T_{sum} is above a critical value $T_{crit} = 537$ degree days. T_{sum} is calculated as the sum of the daily air temperature T_a from the first day of the year until the day of bud-burst d_{BB}^{rob} :

$$T_{sum} = \sum_{t=1}^{d_{BB}^{rob}} T_a(t) \quad (11.4)$$

Finally, the daily fire hazard level is calculated according to Table 11-1.

Table 11-1 Fire hazard level definition

Fire hazard level (international)	Fire alert level (German)	Condition
1	0	$I_{C,d} \leq 500$
2	1	$500 < I_{C,d} \leq 2000$
3	2	$2000 < I_{C,d} \leq 4000$
4	3	$4000 < I_{C,d} \leq 7000$
5	4	$7000 < I_{C,d}$

Annual fire risk index calculated as average of the daily fire hazard levels (Mid-February through October).

11.2 Bruscek-Index

Bruscek (1994) investigated the relation between the number of forest fires and the climatic conditions in Brandenburg (Germany), represented by the number of summer days n_{summer} from April to September and the precipitation sum of this period. He found a strong correlation and defined an annual index I_A for forest fire risk by

$$I_A = \frac{1}{n_{summer}} \sum_{t=91}^{274} P_d(t) \quad (11.5)$$

with daily precipitation P_d .

11.3 Nesterov-Index

The simple fire danger rating index I_N developed by Nesterov (1949) describes the daily ignition risk of the forest floor in dependence of the maximum day temperature T_{max} and dew point temperature T_{dew} . The index is calculated for days t with $60 < t < 275$, $T_{max} > 0$ °C, and without snow cover. I_N^{val} is the cumulative sum for periods of consecutive days with precipitation less than 3 mm. If the precipitation is greater than 3 mm, the index is set to zero and the process starts again. The Nesterov-Index is defined by

$$I_N^{val}(t_i) = \sum_{i=1}^n (T_{max}(t_i) - T_{dew}(t_i)) \cdot T_{max}(t_i) \quad (11.6)$$

with

n - number of consecutive days with precipitation less than 3 mm

t_i - day of the year with precipitation less than 3 mm.

The dew point temperature T_{dew} is the temperature at which the actual water vapour corresponds to 100 % relative humidity and the actual vapour pressure P_{vap} is equal to the saturated vapour pressure. It is less or equal than the actual air temperature and does not depend on it. The calculation follows DVWK (1996)

$$T_{dew} = a \cdot \frac{\ln P_{vap} - c}{b - \ln P_{vap}} \quad (11.7)$$

with a , b , c – parameters (see Table 11-2).

Table 11-2 Parameters of calculation of dew point temperature (DVWK, 1996) in dependence on air temperature T_a

Scope of application	a	b	c
$T_a \geq 0^\circ\text{C}$	243.12	19.43	1.81
$T_a < 0^\circ\text{C}$	272.20	24.27	1.81

Because of the cumulative addition over the days since last precipitation the value of the index I_N^{val} increases each day of the considered period. For each day the Nesterov-index as a fire danger level will be determined (see Table 11-3).

Table 11-3 Fire danger levels of Nesterov-Index

Value of I_N^{val}	Fire danger	Level of I_N
$I_N^{val} \leq 300$	minimal	1
$300 < I_N^{val} \leq 1000$	moderate	2
$1000 < I_N^{val} \leq 4000$	high	3
$I_N^{val} > 4000$	extreme	4

11.4 Nun moth risk index

The model 4C calculates an index for the risk of nun moth (*Lymantria monacha* L.) mass outbreaks according to Zwölfer (1935). The nun moth risk index I_{NT} describes the annual risk of appearance or mass outbreaks of nun moth (*Lymantria monacha* L.). Zwölfer (1935) developed a thermal index on the basis of experiments about the influence of hydrothermal conditions on the survival and reproduction ability of nun moth. He investigated the impact of temperature on the different life stages of nun moth and determined three parameters for each life stage whereas the nine life stages were split into thirteen phases according to the relation between month and life stage.

The general used formula for the development time D_{time} [days] of a life stage is:

$$D_{time} = \frac{p_{nun}}{T_m - T_0} \quad (11.8)$$

with the monthly mean temperature T_m , the development zero point T_0 [$^\circ\text{C}$], and the parameter p_{nun} . The parameters are given in Table 11-4.

Table 11-4 Parameters of the nun moth life stages; T_m – related monthly mean temperature for the calculation of T_{sum} , T_4, \dots, T_9 - monthly mean temperature from April to September

Life Stage	Phase	p_{nun}	minimum temperature of the stage ($^{\circ}\text{C}$) T_0	number of days of the phase r	Month	T_m
Egg (hatching period)	1	65	4.9	30	IV	T_4
	2	65	4.9	3	V	T_5
Larva I	3	217	3.2	17	V	T_5
Larva II	4	84	5.7	8	V	T_5
Larva III	5	84	7.2	3	V	T_5
	6	84	7.2	6	VI	T_6
Larva IV	7	90	7.6	10	VI	T_6
Larva V	8	132	7.8	14	VI	T_6
Larva VI	9	197	6.0	18	VII	T_7
Pupa	10	130	8.4	13	VII	T_7
	11	130	8.4	2	VIII	T_8
Egg (embryo of next generation)	12	240	6.8	29	VIII	T_8
	13	240	6.8	30	IX	T_9
Sum		1239				

For the first stage, egg (hatch period), Zwölfer (1935) calculated under wet saturated atmosphere (relative humidity of 100 %) $p = 65$ and $T_0 = 4.9$. He assumed for the life stage larva I no clear influence of the relative humidity within the range 40 – 100%. The data for the following stages (larva II, III, IV, V) were collected for a relative humidity of 70 – 80% (Table 11-4). Therefore, the index does not allow statements under dry climate conditions. A thermal constant T_{tot} of the whole life stage was derived from these data as a sum of the parameters p of the different life stages. Zwölfer (1935) stated

$$T_{tot} = 1240 \pm 40 \quad (11.9)$$

From the observations of the phenology of the life stages of nun moth he defined for each phase a mean number of days r (Table 11-4). Using the local monthly means of temperature for the period April until September T_i ($i=4, \dots, 9$) which are assigned to the 13 phases $T_m(j)$

($j=1, \dots, 13$) (Table 11-4) a local annual temperature sum T_{sum}^a is calculated in the following way:

$$T_{sum}^a = \sum_{j=1}^{13} r(j) \cdot (T_m(j) - T_0(j)) \quad (11.10)$$

T_m – related monthly mean temperature [°C]

The annual nun moth risk index I_{NMR} is defined as following:

$$I_{NMR} = \frac{T_{sum}^a}{T_{tot}} \quad (11.11)$$

Zwölfer (1935) stated that if I_{NMR} is less than one, the required temperature sum for the whole life cycle is not available. If the value $I_{NMR} = 1$ is reached, then the minimum temperature limited distribution area is given. The index allows the presentation of the northern horizontal distribution border but also of the vertical border. The southern distribution border is estimated for a I_{NMR} value of 1.5 – 1.6. The distribution area of nun moth is characterised by I_{NMR} values less than 1.6 and greater than 1.0. Typical areas for mass outbreaks of nun moth are characterised by I_{NMR} values varying from 1.1 to 1.4 as long-term mean.

11.5 Climatic and continentality indices

In 4C a variety of climatic and continentality indices are calculated only for considering climate change effects. Short descriptions are given in the following chapters.

11.5.1 Index according to Coutagne

This index is calculated according to Coutagne (1935) on monthly scale from the monthly mean temperature and the monthly precipitation sum

$$I_{cm} = \frac{12 P_{mon}}{T_{mon} + 10} \quad (11.12)$$

and on annual scale as the mean of the monthly indices

$$I_{cout} = \frac{1}{12} \sum_{m=1}^{12} I_{cm} \quad (11.13)$$

If I_{cm} is less than 20 aridity is indicated.

11.5.2 Index according to Wissmann

This index is calculated according to Wissmann (1939) on monthly time scale and summarised on annual scale

$$I_{wiss,m} = \frac{12 P_{mon}}{T_{mon} + 7} \quad (11.14)$$

$$I_{wiss} = \sum_{i=1}^{12} I_{wiss,m}$$

If I_{wiss} is less than 20 aridity is indicated.

11.5.3 Index according to De Martonne

This index is calculated according to De Martonne (1941) on annual time scale

$$I_{mart} = \frac{P_{ann}}{T_{ann} + 10} \quad (11.15)$$

If it holds $T_{ann} < -9.9$ for the annual mean temperature the index I_{mart} is set to 100. The index can be classified according to Table 11-5.

Table 11-5 Index de Martonne

I_{mart}	Classification
> 60	perhumid
60 - 30	humid
30 - 20	subhumid
20 - 15	semiarid
15 - 5	arid(Steppe)
5 - 0	extrem arid (desert)

11.5.4 Aridity Index

This index I_{arid} is calculated on annual time scale as the quo tient

$$I_{arid} = \frac{P_{ann}}{E_{pot}} \quad (11.16)$$

according to UNEP (1992). The index is classified as given in Table 11-6.

Table 11-6 Aridity Index

I_{arid}	Classification
< 0.05	hyperarid
0.05 < AI < 0.2	arid
0.2 < AI < 0.5	semi-arid
0.5 < AI < 0.65	dry subhumid

11.5.5 Climatic water balance

The climatic water balance I_{cwb} is defined as

$$I_{cwb} = P_{ann} - E_{pot} \quad (11.17)$$

and is calculated annually.

11.5.6 Index according to Emberger

This index (called also 'quotient pluviothermique') is calculated on an annual time scale and uses the average temperatures of the warmest and coldest month T_{wm} and T_{cm} respective

$$I_{emb} = \frac{100 P_{ann}}{2 \left[\left(\frac{T_{wm} + T_{cm}}{2} \right) \cdot (T_{wm} - T_{cm}) \right]} \quad (11.18)$$

$$= \frac{100 P_{ann}}{(T_{wm}^2 - T_{cm}^2)}$$

It can be classified with Table 11-7.

Table 11-7 Emberger Index

I_{emb}	Classification
>90	humid
90-50	subhumid
50-30	semiarid
<30	arid

11.5.7 Index according to Lang

This index is calculated annually according to Lang (1915) as the quotient of annual precipitation sum and annual mean air temperature

$$I_{lang} = \frac{P_{ann}}{T_{ann}} \quad (11.19)$$

It can be classified with Table 11-8.

Table 11-8 Lang Index

I_{lang}	Classification
>160	humid
160-100	wet temperate
100-60	warm temperate
60-40	semiarid
<40	arid

11.5.8 Reichel Index

The index I_{reich} was introduced by Reichel (1928) (see also Mitscherlich (1949), Mitscherlich (1950a) and Mitscherlich (1950b)) and is calculated from annual mean temperature T_{ann} , the annual precipitation sum, and the number of days n_{dr} with rain > 0.1 mm

$$I_{reich} = \frac{P_{ann} n_{dr}}{180 (T_{ann} + 10)} \quad (11.20)$$

It can be classified according to Table 11-9.

Table 11-9 Reichel Index

I_{reich}	Classification
Pine	26 - 44
Oak	30 (northeast Germany) - 55 (Nordspessart)
Beech (growing area)	30 (northeast Germany) - >60 (Südschwarzwald)

11.5.9 Weck Index

This index I_{weck} was defined by Weck (1954) on the basis of the mean temperature T_{mj} from May to July, the precipitation sum P_{mj} , and the number of days with precipitation n_{mj} of the same period as well as the number of days without frost n_{wof} ($T_{min} > 0^{\circ}\text{C}$)

$$I_{weck} = \frac{P_{mj} n_{mj} (n_{wof} - 60)}{9200 (T_{mj} + 10)} \quad (11.21)$$

The index is calculated annually.

11.5.10 Budyko radiation index

The index I_{bud} is calculated annually according to Nikol'skii et al. (2006) as an indicator of dryness from the annual net radiation sum R_{nets} and the annual precipitation

$$I_{bud} = \frac{R_{nets}}{1000 \lambda P_{ann}} \quad (11.22)$$

with $\lambda = 2.51 \text{ MJ kg}^{-1}$ (enthalpy of evaporation). It is classified by Table 11-10.

Table 11-10 Budyko Index

I_{bud}	Characteristics	Geobotanical characteristics
< 0.45	excessive wet	arctic desert, tundra, forest tundra, alpine grassland
0.45 -1.0	wet	forest
1.0 – 3.0	insufficient wet	forest steppe, steppe, xerophyt. subtropic vegetation
> 3.0	dry	desert

11.5.11 Seljaninov Index

The Seljaninov coefficient I_{shc} defines the degree of climatic dryness or wetness in months when the mean temperature is equal to or greater than 10°C . It is also used as indicator for outbreaks of pine-tree lappet (*Dendrolimus pini*). This index (or hydrothermal coefficient) is implemented according to Ray et al. (2016) and calculated annually as follows:

$$I_{shc} = \frac{10 \sum_{T_{mon} \geq 10} P_{mon}}{\sum_{T_{mon} \geq 10} T_{mon}} \quad (11.23)$$

It can be classified according to Table 11-11.

Table 11-11 Classification of index I_{shc}

I_{shc}	Characteristics
<0.5	extremely dry
0.5 – 0.7	very dry
0.7 – 0.9	dry
1.0 – 1.3	insufficiently wet
1.3 – 1.5	moderately wet
1.5 – 2.0	wet
2.0 – 3.0	very wet
3.0	extremely wet
– 1.5	optimum climatic conditions for outbreaks of <i>Dendrolimus pini</i>
1.2	area with most serious outbreaks
>1.5	too humid for outbreaks
<1.0	too dry for outbreaks

11.5.12 **Continental Index according to Gorczyński**

This index I_{gor} is defined by Gorczyński (1920). In addition to the monthly mean temperature of the warmest and coldest month, the latitude X_{lat} is also taken into account

$$I_{gor} = 1.7 \frac{(T_{wm} - T_{cm})}{\sin(0.5 \pi \frac{X_{lat}}{90})} - 20.4 \quad (11.24)$$

11.5.13 **Continental Index according to Currey**

This index I_{cur} is introduced by Currey (1974) and calculated annually as follows

$$I_{cur} = \frac{T_{wm} - T_{cm}}{\left(1 + \frac{1}{3} X_{lat}\right)} \quad (11.25)$$

Its classification is given by Table 11-12.

Table 11-12 Currey Index

I_{cur}	Classification
0-0.6	hyperoceanic
0.6 – 1.1	oceanic
1.1 – 1.7	subcontinental
1.7 -2.3	continental
2.3 – 5.0	hypercontinental

11.5.14 **Continental Index according to Conrad**

This index is calculated according to Conrad (1946) and defined as follows:

$$I_{con} = 1.7 \cdot \frac{T_{wm} - T_{cm}}{\sin(f(X_{lat} + 10))} - 14 \quad (11.26)$$

Its classification is given by Table 11-13.

Table 11-13 Conrad Index

I_{con}	Classification
-20 - 20	hyperoceanic
20 - 40	oceanic
40 - 60	subcontinental
60 - 80	continental
80 - 120	hypercontinental

11.6 Late frost danger indices

The late frost danger index I_{lf} is based on Czajkowski and Bolte (2006) and is calculated for a time period (the simulation time period). Five different values are calculated for the time period:

- I_{lf1} : mean number of days with a frost event (minimum temperature less than 0°C according to Anandhi et al. (2013) after starting the vegetation period (mean temperature greater than 10°C) or
- I_{lf1_sp} : mean number of days with a frost event (minimum temperature less than 0°C) after starting bud burst (deciduous tree species)
- I_{lf2} : mean minimum may temperature

- I_{lf3} : minimum May temperature of the whole time period
- I_{lf4} : mean date of the last late frost event
- I_{lf5} : date of the last late frost event of the period.

Each of the 5 indicators is classified according to Table 11-14 and gets values from 1 to 6. They are aggregated by averaging over all indicators for the time period to a single indicator I_{lf} .

Table 11-14 Classification scheme for the late frost danger index I_{lf}

risk	level	I_{lf1} or I_{lf1_sp} [d]	I_{lf2} [°C]	I_{lf3} [°C]	I_{lf4} [date/DOY]	Ind I_{lf5} [date/DOY]
very low	1	< 2.5	<1.5	>-5	< 10.5./130	< 5.6./156
low	2	2.6-3.5	-1.6- -2.0	> -6	< 15.5./135	<10.6./161
medium	3	3.6-4.5	-2.1 - -2.5	> -6	16.-20.5./135-140	11.-15.6./162-166
moderate high	4	4.6 -5.0	-2.6- 3.0	> -7	21.-25.5./141-145	16.-20.6./167-171
high	5	5.1-5.5	-3.1- -3.5	> -8	21.5.-25.5./141-145	21.-25.6./172-176
very high	6	>5.5	<-3.5	< -8	> 25.5./145	>25.6./176

A variety of annual indicators are defined to characterize late frost risk per year, see Table 11-15.

Table 11-15 Annual late frost indices in 4C

Indicator	Description
F_{day}	Number of days with late frost risk ($T_{min} < 0^{\circ}C$) after starting the vegetation period ($T_a > 10^{\circ}C$)
F_{day_sp}	Number of days with late frost risk ($T_{min} < 0^{\circ}C$) after starting of bud burst (deciduous species)
L_{frost}	Date of the year of the last late frost event after bud burst or start of the vegetation period
$L_{frostitot}$	Date of the year of the last late frost event of the year

11.7 Climatic characteristics

For each year further characteristic climatic data are calculated, see Table 11-16.

Table 11-16 Characteristic climatic values

Indicator	Description
n_{dry}	Number of days without precipitation

Indicator	Description
n_{hot}	Number of hot days, $T_{max} \geq 30^{\circ}\text{C}$
n_{rain}	Number of days with heavy rain, $P_d > 10\text{mm}$
n_{ice}	Number of ice days, $T_{max} < 0^{\circ}\text{C}$
n_{snow}	Number of days with snow cover
n_{summer}	Number of summer days, $T_{max} \geq 25^{\circ}\text{C}$
T_{gdd}	Annual growing degree day, $T_{gdd} = \sum_{t=1}^{366} T_a(t) \quad \text{with} \quad T_a(t) > T_{gdd,0} \quad \text{and}$ threshold $T_{gdd,0} = 5^{\circ}\text{C}$

12 REFERENCES

- Anandhi, A. et al., 2013. Past and future changes in frost day indices in Catskill Mountain region of New York. *Hydrological Processes*, 27(21): 3094-3104.
- Badeck, F.W. et al., 2007. Parametrisierung, Kalibrierung und Validierung von Modellen des Kohlenstoffumsatzes in Waldökosystemen und deren Böden, Bayerische Landesanstalt für Wald und Forstwirtschaft (LWF), Institut für Bodenkunde und Waldernährung der Universität Göttingen (IBW), Landesforstanstalt Eberswalde (LFE), Leibniz-Zentrum für Agrarlandschaftsforschung (ZALF), Nordwestdeutsche Forstliche Versuchsanstalt (NW-FVA), Potsdam-Institut für Klimafolgenforschung (PIK).
- Barigah, T.S., Saugier, B., Mousseau, M., Guittet, J. and Ceulemans, R., 1994. Photosynthesis, Leaf-Area and Productivity of 5 Poplar Clones During Their Establishment Year. *Annales Des Sciences Forestieres*, 51(6): 613-625.
- Binkley, D., Stape, J.L., Ryan, M.G., Barnard, H.R. and Fownes, J., 2002. Age-related decline in forest ecosystem growth: An individual- tree, stand-structure hypothesis. *Ecosystems*, 5(1): 58-67.
- Bond-Lamberty, B., Wang, C. and Gower, S.T., 2002. Aboveground and belowground biomass and sapwood area allometric equations for six boreal tree species of northern Manitoba. *Canadian Journal Of Forest Research-Revue Canadienne De Recherche Forestiere*, 32(8): 1441-1450.
- Borys, A., 2015. Kohlenstoffspeicherung in Abhängigkeit von Waldpflege, Klimawandel und Ökonomie. Doctoral Thesis Thesis, Universität Potsdam, Potsdam, 180 pp.
- Borys, A. et al., 2015. Ökonomische Analyse der Kohlenstoffsequestrierung in Buchenbeständen im Kontext von Waldpflege und Klimawandel. *Allg. Forst- u. J. Ztg.*, 186(3/4): 72-84.
- Borys, A., Lasch, P., Suckow, F. and Reyer, C., 2013. Kohlenstoffspeicherung in Buchenbeständen in Abhängigkeit von Waldpflege und Klimawandel. *Allg. Forst- u. J.-Ztg.*, 184(1/2): 26-35.
- Borys, A., Suckow, F., Reyer, C., Gutsch, M. and Lasch-Born, P., 2016. The impact of climate change under different thinning regimes on carbon sequestration in a German forest district. *Mitig Adapt Strateg Glob Change*, 21(6): 861-881.
- Botkin, D.B., Janak, J. and Wallis, J., 1972. Some ecological consequences of a computer model of forest growth. *J. Ecol.*, 60: 849-872.

- Bruschek, G.J., 1994. Waldgebiete und Waldbrandgeschehen in Brandenburg im Trockensommer 1992. In: H.-J. Schellnhuber, Enke, W., Flechsig, M (Editor), Extremer Nordsommer 1992. PIK-Report. PIK, Potsdam, pp. 265-298.
- Bugmann, H., 1994. On the ecology of mountainous forests in a changing climate: A simulation study. Ph.D. Thesis Thesis, ETH Zürich, Switzerland, 258 pp.
- Bugmann, H., Grote, R., Lasch, P., Lindner, M. and Suckow, F., 1997. A new forest gap model to study the effects of environmental change on forest structure and functioning. In: G.M.J. Mohren, K. Kramer and S. Sabate (Editors), Impacts of Global Change of Tree Physiology and Forest Ecosystem. Proceedings of the International Conference on Impacts of Global Change on Tree Physiology and Forest Ecosystems, held 26-29 November 1996, Wageningen. Forestry Science. Kluwer Academic Publisher, Dordrecht, pp. 255-261.
- Campbell, G.S., 1985. Soil physics with basic : transport models for soil-plant systems. Developments in soil science. Elsevier, Amsterdam [u.a.].
- Cannell, M.G.R. and Smith, R., 1983. Thermal time, chill days and prediction of budburst in *Picea sitchensis*. J. Appl. Ecol., 20: 951-963.
- Chapin, F.S., Chapin, M.C., Matson, P.A. and Vitousek, P., 2011. Principles of Terrestrial Ecosystem Ecology. Springer New York.
- Chen, C.W., 1993. The response of plants to interacting stresses: PGSM Version 1.3 Model Documentation. TR-101880, Electric Power Res. Inst., Palo Alto, USA.
- Chertov, O.G. and Komarov, A.S., 1997. SOMM: A model of soil organic matter dynamics. Ecol. Modell., 94(2-3): 177-189.
- Collatz, G.J., Ball, J.T., Grivet, C. and Berry, J.A., 1991. Physiological and Environmental-Regulation of Stomatal Conductance, Photosynthesis and Transpiration - a Model That Includes a Laminar Boundary-Layer. Agric. For. Meteorol., 54(2-4): 107-136.
- Conrad, V., 1946. Methods in Climatology. Harvard University Press: 296-300.
- Coutagne, A., 1935. Comment définir et caractériser le degré d'aridité d'une region et sa variation saisonnière. Météorologie: 141-151.
- Currey, D.R., 1974. Continentality of extratropical climates. Annals of the Association of American Geographers, 64(2): 268-280.
- Czajkowski, T. and Bolte, A., 2006. Frosttoleranz deutscher und polnischer Herkunft der Buche (*Fagus sylvatica* L.) und ihre Beeinflussung durch Trockenheit. Archiv f. Forstwesen u. Landsch.ökol., 40(3): 119-126.
- Davidson, R.L., 1969. Effect of root/leaf temperature differentials on root/shoot ratios in some pasture grasses and clover. Ann. Bot., 33: 561-569.
- De Martonne, E., 1941. Nouvelle carte mondiale de l'indice s'aridité. Météorologie: 3-26.
- de Vries, P.A., 1963. Thermal properties of soils. In: W.R. van Wijk (Editor), Physics of plant environment. North-Holland Publishing Company, Amsterdam, pp. 211-235.
- Dietze, M.C. and Matthes, J.H., 2014. A general ecophysiological framework for modelling the impact of pests and pathogens on forest ecosystems. Ecol. Lett., 17(11): 1418-1426.
- Dohrenbusch, A., 1997. Die natürliche Verjüngung der Kiefer (*Pinus sylvestris* L.) im nordwestdeutschen Pleistozän. 123, Institut für Waldbau der Universität Göttingen, Göttingen.
- DVWK, 1996. Ermittlung der Verdunstung von Land- und Wasserflächen. DVWK - Merkblätter zur Wasserwirtschaft, 238/1996. Wirtschafts- und Verlagsgesellschaft Gas und Wasser mbH Bonn, Bonn, 134 pp.
- Dyck, S. and Peschke, G., 1989. Grundlagen der Hydrologie. Verlag für Bauwesen, Berlin, 408 pp.
- Eggers, T., 2002. The impacts of manufacturing and utilization of wood products on the European carbon budget. 9, European Forest Institute, Joensuu.
- Eglin, T. et al., 2008. Biochemical composition is not the main factor influencing variability in carbon isotope composition of tree rings. Tree Physiol., 28(11): 1619-1628.
- Farquhar, G.D., Caemmerer, S.V. and Berry, J.A., 1980. A Biochemical-Model of Photosynthetic CO₂ Assimilation in Leaves of C-3 Species. Planta, 149(1): 78-90.

- Flint, A.L. and Childs, S.W., 1991. Use of the Priestley-Taylor evaporation equation for soil water limited conditions in a small forest clearcut. *Agric. For. Meteorol.*, 56(3): 247-260.
- Franko, U., 1990. C- und N-Dynamik beim Umsatz organischer Substanz im Boden. Dissertation B Thesis, Akademie der Landwirtschaftswissenschaften der DDR, Berlin.
- Freytag, H.E. and Lüttich, M., 1985. Zum Einfluss der Bodenfeuchte auf die Bodenatmung unter Einbeziehung der Trockenraumdichte. *Archiv für Acker und Pflanzenbau und Bodenkunde - Archives of Agronomy and Soil Science*, 29: 485-492.
- Frommhold, H., 2001. Kommentar zu „Rohholzaushaltung Rohholzverkauf“ (Handelsklassensortierung, HKS Brandenburg), MLUR Brandenburg, Potsdam.
- Fürstenau, C., 2008. The impact of silvicultural strategies and climate change on carbon sequestration and other forest ecosystem functions, Universität Potsdam, Potsdam, 137 pp.
- Fürstenau, C. et al., 2007. Multiple-use forest management in consideration of climate change and the interests of stakeholder groups. *European Journal of Forest Research*, 126(2): 225-239.
- Gerold, D., 1990. Modellierung des Wachstums von Waldbeständen auf der Basis der Durchmesserstruktur. Dissertation B Thesis, Technische Universität Dresden, Dresden, 174 pp.
- Gerstengarbe, F.-W. et al., 2003. Studie zur klimatischen Entwicklung im Land Brandenburg bis 2055 und deren Auswirkungen auf den Wasserhaushalt, die Forst- und Landwirtschaft sowie die Ableitung erster Perspektiven. 83, PIK, Potsdam.
- Gerstengarbe, F.W. and Welzer, H., 2013. Zwei Grad mehr in Deutschland: Wie der Klimawandel unseren Alltag verändern wird. Fischer Taschenbuch, Frankfurt am Main, 320 pp.
- Glugla, G., 1969. Berechnungsverfahren zur Ermittlung des aktuellen Wassergehaltes und Gravitationswasserabflusses im Boden. *Albrecht-Thaer-Archiv*, 13: 371-376.
- Gorczyński, W., 1920. Sur le calcul du degré de continentalisme et son application dans la climatologie. *Geografiska Annaler*, 2: 324-331.
- Goto, N., Sakoda, A. and Suzuki, M., 1994. Modelling of soil carbon dynamics as a part of carbon cycle interrestrial ecosystems. *Ecol. Modell.*, 74: 183-204.
- Grote, R. and Erhard, M., 1999. Simulation of tree and stand development under different environmental conditions with a physiologically based model. *Forest Ecology & Management*, 120(1-3): 59-76.
- Gutsch, M. et al., 2015. Uncertainty of biomass contributions from agriculture and forestry to renewable energy resources under climate change. *Meteorologische Zeitschrift*, 24(2): 1-11.
- Gutsch, M., Lasch, P., Suckow, F. and Reyer, C., 2011. Management of mixed oak-pine forests under climate scenario uncertainty. *Forest Systems*, 20(3): 453-463.
- Hänninen, H., 1995. Effects of climatic-change on trees from cool and temperate regions - an ecophysiological approach to modeling of bud burst phenology. *Canadian Journal of Botany-Revue Canadienne De Botanique*, 73(2): 183-199.
- Haude, W., 1955. Zur Bestimmung der Verdunstung auf möglichst einfache Weise. *Mitteilungen des Deutschen Wetterdienstes*, 11: 1-22.
- Hauskeller-Bullerjahn, K., 1997. Wachstum junger Eichen unter Schirm. Bd. 147, Forschungszentrum Waldökosysteme der Universität Göttingen, Göttingen.
- Haxeltine, A. and Prentice, I.C., 1996a. BIOME3: An equilibrium terrestrial biosphere model based on ecophysiological constraints, resource availability and competition among plant functional types. *Global Biogeochemical Cycles*, 10(4): 693-709.
- Haxeltine, A. and Prentice, I.C., 1996b. A general model for the light-use efficiency of primary production. *Functional Ecology*, 10(5): 551-561.
- Heide, O.M., 1993a. Daylength and thermal time responses of budburst during dormancy release in some northern deciduous trees. *Physiol. Plant.*, 88(4): 531-540.
- Heide, O.M., 1993b. Dormancy release in beech buds (*Fagus sylvatica*) requires both chilling and long days. *Physiol. Plant.*, 89(1): 187-191.
- Hoch, G., Richter, A. and Körner, C., 2003. Non-structural carbon compounds in temperate forest trees. *Plant, Cell & Environment*, 26(7): 1067-1081.

- Hotopp, I.S., 2014. Nitrifikation und Denitrifikation im Boden in Abhängigkeit von Sauerstoff und mikrobieller Aktivität. Entwicklung, Analyse, Parametrisierung und Anwendung eines gekoppelten Simulationsmodells, Universität Osnabrück, Osnabrück, 161 pp.
- IPCC, 2013. Summary for Policymakers. In: T.F. Stocker et al. (Editors), *Climate Change 2013: The Physical Science Basis. Contribution of Working Group I to the Fifth Assessment Report of the Intergovernmental Panel on Climate Change*. Cambridge University Press, Cambridge, United Kingdom and New York, NY, USA.
- Jackson, R.B. et al., 1996. A global analysis of root distributions for terrestrial biomes. *Oecologia*, 108(3): 389-411.
- Jansson, P.-E., 1991. Simulation model for soil water and heat conditions. Description of the SOIL model. Report, 165. Swedish University of Agricultural Sciences, Department of Soil Sciences, Division of Agricultural Hydrotechnics, Uppsala.
- Johnson, I.R. and Thornley, J.H.M., 1985. Temperature dependence of plant and crop processes. *Annals of Botany*, 55: 7-24.
- Johnsson, H., Bergström, L. and Jansson, P.E., 1987. Simulated nitrogen dynamics and losses in a layered agricultural soil. *Agriculture, Ecosystems and Environment*, 18: 333-356.
- Karjalainen, T., S., K. and A., P., 1994. Role of wood-based products in absorbing atmospheric carbon. *Silva Fennica*, 28(2): 67-80.
- Kartschall, T., Döring, P. and Suckow, F., 1990. Simulation of Nitrogen, Water and Temperature Dynamics in Soil. *Syst. Anal. Model. Simul.*, 7(6): 33-40.
- Käse, H., 1969. Ein Vorschlag für eine Methode zur Bestimmung und Vorhersage der Waldbrandgefährdung mit Hilfe komplexer Kennziffern. Nr. 94, Band XII, Berlin.
- Keane, R.E., Morgan, P. and Running, S.W., 1996. FIRE-BGC - A mechanistic ecological process model for simulating fire succession on coniferous forest landscapes of the northern Rocky Mountains. INT-RP-484, United States Department of Agriculture, Forest Service, Intermountain Research Station, Ogden, UT.
- Kellomäki, S. and Leinonen, S.E., 2005. Management of European Forests under Changing Climatic Conditions. Final Report of the Project "Silvicultural Response Strategies to Climatic Change in Management of European Forests" funded by the European Union under the Contract EVK2-2000-00723 (SilviStrat). 163, University of Joensuu, Faculty of Forestry, Joensuu.
- King, D.A., 1995. Equilibrium analysis of a decomposition and yield model applied to *Pinus radiata* plantations on sites of contrasting fertility. *Ecol. Modell.*, 83: 349-358.
- Kint, V., Lasch, P., Lindner, M. and Muys, B., 2009. Multipurpose conversion management of Scots pine towards mixed oak-birch stands--A long-term simulation approach. *For. Ecol. Manage.*, 257(1): 199-214.
- Klößing, B., 1991. Ein Modell zur Beschreibung des Wasser-, Wärme- und Stickstoffhaushaltes im Boden unter besonderer Berücksichtigung des Winterzeitraumes. Dissertation A Thesis, Akademie der Landwirtschaftswissenschaften der DDR, Berlin.
- Koitzsch, R., 1977. Schätzung der Bodenfeuchte aus meteorologischen Daten, Boden- und Pflanzenparametern mit einem Mehrschichtmodell. *Z. f. Meteor.*, 27(5): 302-306.
- Koitzsch, R. and Günther, R., 1990. Modell zur ganzjährigen Simulation der Verdunstung und der Bodenfeuchte landwirtschaftlicher Nutzflächen mit und ohne Bewuchs. *Arch. Acker- Pflanzenbau Bodenkd*, 34(12): 803-810.
- Kollas, C., Gutsch, M., Hommel, R., Lasch-Born, P. and Suckow, F., 2018. Mistletoe-induced growth reductions at the forest stand scale. *Tree Physiol*, 38(5): 1-10.
- Kollas, C., Lasch, P., Rock, J. and Suckow, F., 2009. Bioenergy potential in Germany - assessing spatial patterns of biomass production with aspen short-rotation coppice. *International Agrophysics*, 23(4): 343-352.
- Kopp, D. and Schwanecke, W., 1994. Standörtlich-naturräumliche Grundlagen ökologischer Forstwirtschaft. Deutscher Landwirtschaftsverlag Berlin GmbH, Berlin, 248 pp.
- Kramer, K., 1994. Selecting a model to predict the onset of growth of *Fagus sylvatica*. *J. Appl. Ecol.*, 31: 172-181.

- Krebs, C.J., 1994. Ecology - The experimental analysis of distribution and abundance. Harper & Row, New York, 801 pp.
- Landsberg, J.J. and Waring, R.H., 1997. A Generalised Model of Forest Productivity Using Simplified Concepts of Radiation-Use Efficiency, Carbon Balance and Partitioning. *Forest Ecology & Management*, 95(3): 209-228.
- Lang, R., 1915. Versuch einer exakten Klassifikation der Böden in klimatischer und geologischer Hinsicht. *Intern. Mitt. f. Bodenkunde*, 5: 312-346.
- Lasch-Born, P. et al., 2015. Forests under climate change: potential risks and opportunities. *Meteorologische Zeitschrift*, 24(2): 157-172.
- Lasch, P., Badeck, F.W., Suckow, F., Lindner, M. and Mohr, P., 2005. Model-based analysis of management alternatives at stand and regional level in Brandenburg (Germany). *For. Ecol. Manage.*, 207(1-2): 59-74.
- Lasch, P., Kollas, C., Rock, J. and Suckow, F., 2010. Potentials and impacts of short-rotation coppice plantation with aspen in Eastern Germany under conditions of climate change. *Reg Environ Change*, 10(2): 83-94.
- Lasch, P., Lindner, M., Erhard, M., Suckow, F. and Wenzel, A., 2002. Regional impact assessment on forest structure and functions under climate change - the Brandenburg case study. *For. Ecol. Manage.*, 162(1): 73-86.
- Lindner, M., 1998. Wirkung von Klimaveränderungen in mitteleuropäischen Wirtschaftswäldern. 46, Potsdam Institute for Climate Impact Research, Potsdam.
- Lindner, M., 2000. Developing adaptive forest management strategies to cope with climate change. *Tree Physiol.*, 20(5-6): 299-307.
- Loehle, C. and LeBlanc, D., 1996. Model-based assessments of climate change effects on forests: a critical review. *Ecological Modelling*, 90: 1-31.
- Mailly, D. and Kimmins, J.P., 1997. Growth of *Pseudotsuga menziesii* and *Tsuga heterophylla* seedlings along a light gradient: resource allocation and morphological acclimation. *Canadian Journal Of Botany-Revue Canadienne De Botanique*, 75(9): 1424-1435.
- Mäkelä, A., 1986. Implications of the pipe model theory on dry matter partitioning and height growth trees. *Journal of Theoretical Biology*, 123: 103-120.
- Mäkelä, A., Sievänen, R., Lindner, M. and Lasch, P., 2000. Application of volume growth and survival graphs in the evaluation of four process-based forest growth models. *Tree Physiol.*, 20: 347-355.
- Medhurst, J.L. et al., 1999. Allometric relationships for *Eucalyptus nitens* (Deane and Maiden) Maiden plantations. *Trees-Struct. Funct.*, 14(2): 91-101.
- Meinshausen, M. et al., 2011. The RCP greenhouse gas concentrations and their extensions from 1765 to 2300. *Clim. Change*, 109(1-2): 213-241.
- Meiwes, K.-J. et al., 2007. Kohlenstoffumsatz in Waldökosystemen und deren Böden. Parametrisierung, Kalibrierung und Validierung von Modellen. *AFZ / Der Wald*(20/2007): 1076-1078.
- Menzel, A., 1997. Phänologie von Waldbäumen unter sich ändernden Klimabedingungen - Auswertung der Beobachtungen in den Internationalen Phänologischen Gärten und Möglichkeiten der Modellierung von Phänodaten. *Forstliche Forschungsberichte*, 164. Universität München, München, 150 pp.
- Mitscherlich, G., 1949. Über den Einfluß der Wuchsgebiete auf das Wachstum von Kiefernbeständen. *Forstwissenschaftliches Centralblatt*, 68(4): 194 - 216.
- Mitscherlich, G., 1950a. Die Bedeutung der Wuchsgebiete für das Bestandeswachstum von Buche, Eiche, Erle und Birke. *Forstwissenschaftliches Centralblatt*, 69(4): 184-211.
- Mitscherlich, G., 1950b. Die Bedeutung der Wuchsgebiete für das Bestandeswachstum von Fichte und Douglasie. *Forstwissenschaftliches Centralblatt*, 69(1): 27 - 51.
- Monteith, J.L., 1995. Accomodation between transpiring vegetation and the convective boundary layer. *Journal of Hydrology*, 166: 251-263.
- Monteith, J.L. and Unsworth, M.H., 1990. Principles of environmental physics. Edward Arnold, London.
- Murray, F.W., 1967. On the computation of saturation vapor pressure. *J. Appl. Meteorol.*, 6: 203-204.

- Nagel, J., 1995. BWERT: Programm zur Bestandesbewertung und zur Prognose der Bestandesentwicklung, Deutscher Verband Forstlicher Forschungsanstalten, Sektion Ertragskunde, Joachimstal, 29. - 31. Mai 1995, pp. 184-198.
- Nagel, J., 2002. Modellfunktionen und Koeffizienten des Forst Simulators BWINPro 7.0. In: N.F. Versuchsanstalt (Editor), pp. 17.
- Nesterov, V.G., 1949 Combustibility of the forest and methods for its determination. USSR State Industry Press., 75 pp.
- Neusypina, T.A., 1979. Raschet teplovo reshima pochvi v modeli formirovaniy uroshaya, Teoreticheskij osnovy i kolichestvennyye metody programmirovaniya uroshaeve, Leningrad, pp. 53-62.
- Nikol'skii, Y.N., Castillo-Alvarez, M., Bakhlaeva, O.S., Roma-Calleros, X.A. and Maslov, B.S., 2006. The influence of the possible global climate change on the properties of Mexican soils. *Eurasian Soil Science*, 39(11): 1164-1169.
- Nitsch, J.P., 1957. Photoperiodism in woody plants. *Proceedings of the Am. Soc. for Horticultural Sciences*, 79: 526-544.
- Noetzli, K.P., Müller, B. and Sieber, T.N., 2003. Impact of population dynamics of white mistletoe (*Viscum album ssp. abietis*) on European silver fir (*Abies alba*). *Annals of Forest Science*, 60(8): 773-779.
- Nutto, L., Spathelf, P. and Selig, I., 2006. MANAGEMENT OF INDIVIDUAL TREE DIAMETER GROWTH AND IMPLICATIONS FOR PRUNING FOR BRAZILIAN *Eucalyptus grandis* Hill ex Maiden. *FLORESTA*, 36(3): 397-413.
- Painter, H.A., 1970. A review of literature on inorganic nitrogen metabolism in microorganisms. *Water Research*, 4(6): 393-450.
- Parton, W.J., Schimel, D.S., Cole, C.V. and Ojima, D.S., 1987. Analysis of factors controlling soil organic matter levels in Great Plains grasslands. *Soil Science Society of America Journal*, 51: 1173-1179.
- Perry, T.O., 1971. Dormancy of trees in winter. *Science*, 171(3966): 29-&.
- Pfiz, M. and Koppers, M., 2010. Dense crowns of the hemiparasitic mistletoe *Viscum album* L. exhibit shrub-like growth and high dry matter turnover. *Flora*, 205(12): 787-796.
- Pretzsch, H., Biber, P. and Dursky, J., 2002. The single tree-based stand simulator SILVA: construction, application and evaluation. *For. Ecol. Manage.*, 162(1): 3-21.
- Priestley, C.H.B. and Taylor, R.J., 1972. On the assessment of surface heat flux and evaporation using large-scale parameters. *Monthly weather review*, 100: 81-92.
- Ranatunga, K., Keenan, R.J., Wulschleger, S.D., Post, W.A. and Tharp, M.L., 2008. Effects of harvest management practices on forest biomass and soil carbon in eucalypt forests in New South Wales, Australia: Simulations with the forest succession model LINKAGES. *For. Ecol. Manage.*, 255(7): 2407-2415.
- Ray, D. et al., 2016. Improved prediction of the climate-driven outbreaks of *Dendrolimus pini* in *Pinus sylvestris* forests. *Forestry*, 89(2): 230-244.
- Reichel, E., 1928. Der Trockenheitsindex, insbesondere für Deutschland. *Ber. Tätigk. Preuß. Meteor. Inst.*: 84-105.
- Reyer, C. et al., 2014. Projections of regional changes in forest net primary productivity for different tree species in Europe driven by climate change and carbon dioxide. *Annals Of Forest Science*, 71(2): 211-225.
- Reyer, C., Lasch, P., Mohren, G.M.J. and Sterck, F.J., 2010. Inter-specific competition in mixed forests of Douglas-fir (*Pseudotsuga menziesii*) and common beech (*Fagus sylvatica*) under climate change - a model-based analysis. *Annals Of Forest Science*, 67(8).
- Richter, A. and Popp, M., 1992. The physiological importance of accumulation of cyclitols in *Viscum album* L. *New Phytologist*, 121(3): 431-438.
- Rogers, R. and Johnson, P.S., 1998. Approaches to Modeling Natural Regeneration in Oak-Dominated Forests. *Forest Ecology & Management*, 106(1): 45-54.

- Row, C. and B., P.R., 1996. Wood carbon flows and storage after timber harvest. In: R.N. Sampson and D. Hair (Editors), *Forest Management Opportunities for Mitigating Carbon Emissions. Forests and Global Change*. American Forests, Washington, DC, pp. 27-58.
- Running, S.W. and Gower, S.T., 1991. FOREST-BGC, A general model of forest ecosystem processes for regional applications II. Dynamic carbon allocation and nitrogen budgets. *Tree Physiol.*, 9: 147-160.
- Schaber, J., 2002a. Phenology in Germany in the 20th century: methods, analyses and models. PhD Thesis, Universität Potsdam, Potsdam, 164 pp.
- Schaber, J., 2002b. Phenology in Germany in the 20th century: methods, analyses and models. 78, PIK, Potsdam.
- Schaber, J. and Badeck, F.-W., 2003. Physiology based phenology models for forest tree species in Germany. *Intern. J. Biometeorol.*, 47(7): 193-201.
- Schall, P., 1998. Ein Ansatz zur Modellierung der Naturverjüngungsprozesse im Bergmischwald der östlichen bayrischen Alpen. Reihe A Bd 155, Forschungszentrum Waldökosysteme, Göttingen.
- Shinozaki, K., Yoda, K., Hozumi, K. and Kira, T., 1964. A quantitative analysis of plant form - the pipe model theory. I. Basic analysis. *Jap. J. of Ecology*, 14: 97-105.
- Shugart, H.H. et al., 2018. Gap models and their individual-based relatives in the assessment of the consequences of global change. *Environmental Research Letters*, 13(3): 033001.
- Sievänen, R., Lindner, M., Mäkelä, A. and Lasch, P., 2000. Volume growth and survival graphs: A method for evaluating process-based forest growth models. *Tree Physiol.*, 20(5/6): 357-365.
- Stape, J.L. et al., 2010. The Brazil Eucalyptus Potential Productivity Project: Influence of water, nutrients and stand uniformity on wood production. *For. Ecol. Manage.*, 259(9): 1684-1694.
- Suckow, F., 1986. Ein Modell zur Berechnung der Bodentemperatur unter Brache und unter Pflanzenbestand. Dissertation Thesis, Akademie der Landwirtschaftswissenschaften der DDR, Berlin.
- Suckow, F., 1989. Ein Modell zur Berechnung der Bodentemperatur im Rahmen des Basismodells Boden (BAMO), Tag.-Ber. Akad. Landwirtsch.-Wiss. DDR, Berlin, pp. 159-164.
- Suckow, F., Lasch-Born, P., Gerstengarbe, F.-W., Werner, P. and Reyer, C.P.O., 2016. Climate change impacts on a pine stand in Central Siberia. *Reg Environ Change*, 16(6): 1671-1683.
- Suckow, F., Lasch, P. and Badeck, F.-W., 2002. Auswirkungen von Klimaveränderungen auf die Grundwasserneubildung. In: U.u.R. Ministerium für Landwirtschaft (Editor), *Funktionen des Waldes und Aufgaben der Forstwirtschaft in Verbindung mit dem Landschaftswasserhaushalt*. Eberswalder Forstliche Schriftenreihe. LFE, Eberswalde, pp. 114.
- Sykes, M.T. and Prentice, I.C., 1996. Carbon storage and climate change in Swedish forests: a comparison of static and dynamic modelling approaches. In: M. Apps and D.T. Price (Editors), *Forest ecosystems, forest management and the global carbon cycle*. NATO ASI Series I: Global Environmental Change. Springer, Berlin Heidelberg New York, pp. 69-78.
- Ter-Mikaelian, M.T. and Korzukhin, M.D., 1997. Biomass equations for sixty-five North American tree species. *For. Ecol. Manage.*, 97(1): 1-24.
- UNEP, 1992. *World Atlas of Desertification*.
- Vallauri, D., 1998. Dynamique parasitaire de *Viscum album* L. sur pin noir dans le bassin du Saignon (préalpes françaises du sud), *Annales des sciences forestières*. EDP Sciences, pp. 823-835.
- van't Hoff, J.H., 1884. *Etudes de dynamique chimique*. Muller, Amsterdam, 214 pp.
- Van Hees, A.F.M., 1997. Growth and Morphology of Pedunculate Oak (*Quercus Robur* L) and Beech (*Fagus Sylvatica* L) Seedlings in Relation to Shading and Drought. *Annales des Sciences Forestieres*, 54(1): 9-18.
- van Wijk, W.R., 1963. *Physics of plant environment*, Amsterdam.
- Vegis, A., 1973. Dependence of growth processes on temperature. In: H. Precht, J. Christophersen, H.Hensel and W. Larcher (Editors), *Temperature and life*. Springer-Verlag, Berlin, pp. 145-169.
- Verbraucherschutz, B.f., 2003. Holzmarktbericht 2002, Bundesministerium für Verbraucherschutz, Bonn.
- Verbraucherschutz, B.F., 2004. Holzmarktbericht 1/2003, Bundesministerium Für Verbraucherschutz, Bonn.

- Wang, J.Y., 1960. A critique of the heat unit approach to plant response studies. *Ecology*, 41: 785-790.
- Wareing, P.F., 1956. Photoperiodism in woody plants. *Annual Review of Plant Physiology and Plant Molecular Biology*, 7: 191-214.
- Weck, J., 1954. Untersuchungen über das Ertragspotenzial der deutschen Waldlandschaften. *AFJZ*, 125: 153-159.
- Weimann, H., 1980. Berechnung von Langholzmengen und -stärken für Eichen-, Buchen-, Fichten- und Kiefernbestände. *Forstarchiv*, 51: 5-10.
- Wenk, G. and Gerold, D., 1996. Dynamics of the diameter distribution. In: G. Wenk (Editor), Conference on effects of environmental factors on tree and stand growth. IUFRO S4.01, Berggießhübel/Dresden, pp. 283-289.
- Wissmann, H.v., 1939. Die Klima- und Vegetationsgebiete Eurasien. *Z. Ges. Erdk.*: 1-14.
- Zweifel, R., Bangerter, S., Rigling, A. and Sterck, F.J., 2012. Pine and mistletoes: how to live with a leak in the water flow and storage system? *Journal of Experimental Botany*, 63(7): 2565-2578.
- Zwölfer, W., 1935. Die Temperaturabhängigkeit der Entwicklung der Nonne (*Lymantria monacha* L) und ihre bevölkerungswissenschaftliche Auswertung. *Zeitschrift für Angewandte Entomologie*, XXI(3): 333-384.

APPENDIX

Appendix 1 List of variables

Variable	Definition	Dimension
α_c	ratio of sum of twigs, branches and coarse roots to sapwood	-
α_h	growth rate depends on relative light regime in the middle of the canopy	-
α_m	Priestley-Taylor coefficient	-
α_{PT}	Priestley-Taylor coefficient	-
α_r	auxiliary variable of partitioning functions	-
α_{refl}	albedo of the canopy	-
α_s	auxiliary variable of partitioning functions	cm ⁻¹
α_{wint}	mortality parameter	-
$\alpha_{wstress}$	mortality parameter	-
β	Average sun inclination angle between DOY 120 and 280	rad
β_r	auxiliary variable of partitioning functions	-
γ_{aom}	C/N-ratio of active organic matter per layer	-
γ_p	modified psychrometric constant	hPa K ⁻¹
γ_{pom}	C/N-ratio of primary organic matter per layer	-
$\gamma_{pom}^{fol,j}$	C/N-ratio of foliage litter pool per species j	-
Δ	slope of vapour pressure curve against temperature	hPa K ⁻¹
δ	saturation vapour pressure deficit of air	hPa
δ_{13}	saturation vapour pressure deficit at noon	hPa
δ_H	standard deviation of height of plants	-

Variable	Definition	Dimension
η_R	factor of conversion from global radiation [J cm^{-2}] to photosynthetically active radiation [mol m^{-2}]	-
η_s	foliage to sapwood area relationship	kg cm^{-2}
κ_N^s	slope of photosynthesis response to N-limitation	-
λ_v	latent heat of vaporization	J g^{-1}
λ	optimum ratio of c_i (internal partial pressure of CO_2) to c_a (ambient partial pressure of CO_2)	-
λ_f	partitioning coefficient leaf	-
λ_r	partitioning coefficient fine roots	-
λ_s	partitioning coefficient sapwood	-
λ_i	thermal conductivity of soil components i =air, ice, water, quartz, clay, silt, stone, humus	$\text{J cm}^{-1} \text{s}^{-1} \text{K}^{-1}$
λ_T	thermal conductivity	$\text{J cm}^{-1} \text{s}^{-1} \text{K}^{-1}$
λ_w	lambda parameter for percolation	-
λ_{wint}	lambda parameter of Weibull distribution/ intrinsic mortality	-
$\lambda_{wstress}$	lambda parameter of distribution / stress mortality	-
ρ_a	mean air density at constant pressure	g cm^{-3}
ρ_s	sapwood density	kg cm^{-3}
σ_f	leaf activity rate	$\text{kg kg}^{-1} \text{DW a}^{-1}$
σ_H	standard deviation of height	-
σ_r	root activity rate (N uptake) per year	$\text{kg N kg}^{-1} \text{DW a}^{-1}$
ψ	psychrometric constant	K^{-1}

Variable	Definition	Dimension
a	tree age	years
a_0	parameter of the height curve after Kuleschis, in Gerold1991	-
a_1	parameter of the height curve after Kuleschis, in Gerold1991	-
a_2	parameter of the height curve after Kuleschis, in Gerold1991	-
A_{bs}	base area of a stem	cm ²
A_c	optimum gross assimilation rate per tree	kg DW d ⁻¹ patch ⁻¹
a_c	parameter for calculation of crown area	m cm ⁻¹
a_{cr}^c	projected crown coverage area	m ²
a_{cs}	scaling factor CSM	-
A_{dt}	net daytime assimilation rate per tree	g C m ⁻² d ⁻¹
A_{hb}	cross sectional area of heartwood at stem base	cm ²
A_{hc}	cross sectional area of heartwood at crown base	cm ²
a_{max}	species specific maximum tree age	years
a_{ring}^{max}	cambial age of the innermost ring	-
A_{net}	realized net daily assimilation rate	kg DW d ⁻¹ patch ⁻¹
a_{ring}	current age of ring	-
A_s	tree sapwood cross sectional area	cm ²
A_{sp}	specific gross photosynthesis per tree	g C m ⁻² d ⁻¹

Variable	Definition	Dimension
A_{SWring}	sapwood area of a given ring	cm ²
A_{tot}	total cross sectional area	cm ²
b_0	parameter of the height curve after Kuleschis, in Gerold1991	-
b_1	parameter of the height curve after Kuleschis, in Gerold1991	-
b_2	parameter of the height curve after Kuleschis, in Gerold1991	-
b_c	parameter for calculation of crown radius	m cm ⁻¹
b_{cs}	scaling factor CSM	-
c	identification of a cohort	-
C	sum of all crown projection areas in layer j	m ²
c_1	crown base height calculation (Nagel 1995)	-
c_2	crown base height calculation (Nagel 1995)	-
C_a	atmospheric CO ₂ content	mol mol ⁻¹
C_{air}	specific heat capacity of air	J g ⁻¹ K ⁻¹
	parameter for calculation of crown area	m
$c_c(j)$	fraction of the patch covered by the crown projection area of cohort c in crown layer j	-
C_{chill}	counter of 'chill days', phenology model CSM	-
C_{int}^c	interception capacity parameter per LAI	mm m ⁻²
C^f	sum of management costs	€
C_{health}	number of years without stress	-

Variable	Definition	Dimension
C_{int}	potential interception capacity of the whole canopy per LAI	mm m^{-2}
C_{mass}	molar mass of carbon	g mol^{-1}
C_n	fraction of the patch that will be covered by a new cohort	-
$C_{act,crt}^{NSC}$	actual C-amount of coarse root NSC-pool	kg C / tree
$C_{act,s}^{NSC}$	actual C-amount of sapwood NSC-pool	kg C / tree
$C_{act,tb}^{NSC}$	actual C-amount of twigs and branch NSC-pool	kg C / tree
$C_{max,crt}^{NSC}$	maximum C-amount of coarse root NSC-pool	kg C / tree
$C_{max,s}^{NSC}$	maximum C-amount of sapwood NSC-pool	kg C / tree
$C_{max,tb}^{NSC}$	maximum C-amount of twigs and branch NSC-pool	kg C / tree
C_{plus}^{NSC}	carbon available for NPP allocation after disturbance	kg DW/tree
$C_P(j)$	fraction of the patch NOT covered by cohort (LM2-4)	-
C_{part}	part of C in biomass	-
C_{pom}	whole C-content of dead biomass per layer without stems	g C m^{-2}
C_{frac}	part of twigs and branches of the coarse wood fraction (twigs, branches and coarse roots)	-
C_s	specific heat capacity of soil	$\text{J g}^{-1} \text{K}^{-1}$
C_{stress}	number of stress years	years
C_T	heat capacity	$\text{J cm}^{-3} \text{K}^{-1}$
C_W	heat capacity of soil water	$\text{J cm}^{-3} \text{K}^{-1}$
d_b	diameter at base of the stem segment	cm
d_{BB}^{birch}	bud break birch	d

Variable	Definition	Dimension
d_{BB}^{rob}	bud break black locust	d
d_{bh}	diameter at breast height	cm
d_{bs}	diameter at forest floor	-
$d_c(j)$	number of trees without leaves in canopy layer j	-
d_{cb}	diameter at crown base	cm
d_g	quadratic mean diameter	cm
d_{inc}	annual diameter increment	cm
d_l	photoperiod of actual day	h
d_{limf}	drought factor limiting the assimilation rate	-
D_{time}	development time (nun moth risk index)	d
E_{trd}^c	potential transpiration demand of a tree	mm d ⁻¹
E_{int}	actual evaporation of intercepted water	mm d ⁻¹
E_{pot}	daily potential evaporation rate	mm d ⁻¹
E_{tr}	actual canopy transpiration	mm d ⁻¹
E_{trd}	potential canopy transpiration demand	mm d ⁻¹
f_c	Light Model 1-3: fraction of I_{PAR} absorbed by each layer j per crown coverage area per cohort c [-] Light Model 4: fraction of I_{PAR} absorbed until each layer l per patch per cohort c [-]	-
f_{tot}^c	total fraction of I_{PAR} absorbed by a cohort	-
F_{day}	number of days with late frost risk after starting the vegetation period	-

Variable	Definition	Dimension
F_{day_sp}	number of days with late frost risk after starting bud burst (deciduous species)	-
f_i	volume fraction of soil components, i=air, ice, water, quartz, clay, silt, stone, humus	-
$f_{mres,r}$	fine root maintenance respiration per day	kg DW d ⁻¹
$f_{mres,sw}$	sapwood maintenance respiration per day	kg DW d ⁻¹
f_{NPP}	NPP per tree of a cohort	kg DW a ⁻¹
$f_{s,f}$	senescence rate foliage	kg a ⁻¹
$f_{s,r}$	senescence rate fine roots	kg a ⁻¹
$f_{s,s}$	senescence rate sapwood	kg a ⁻¹
F_t	fraction of total radiation absorbed at a given height in a given layer j (LM1)	-
G	basal area	m ² ha ⁻¹
g_a^i	shape factor of soil particles, i=ice, quartz, clay, silt, stone	-
g^c	unstressed stomatal conductance of a tree	mol m ⁻² d ⁻¹
g_{max}	maximum stomatal conductance of the canopy	mol m ⁻² d ⁻¹
g_{min}	minimum stomatal conductance of the canopy	mol m ⁻² d ⁻¹
g_{tot}	unstressed stomatal conductance of the canopy	mol m ⁻² d ⁻¹
H	tree height	cm
H_b	bole height	cm
H_c	sapling height	cm
H_{dbh}	breast height for inventory measurement	cm

Variable	Definition	Dimension
H_g	height of the tree with diameter D_g	m
H_{thr}	height threshold for saplings	cm
H_p	specific mean height of plants	cm
H_p^{min}	minimum sapling height	cm
h_r	relative humidity of actual day	%
H_s	sapwood height	cm
I_A	fire index of Bruscheck	-
I_{arid}	aridity index	-
I_{bud}	dryness index Buidyko	-
$i_c(j)$	relative incident light intensity at the top of canopy layer j and cohort c (LM3, LM4)	-
$I_{c,d}$	forest fire indicator east of Käse	-
I_{drps}^c	daily drought index	-
I_{cm}	monthly aridity index Coutange	-
I_{con}	continentality index Conrad	-
I_{cout}	annual aridity index Coutange	-
I_{cur}	continentality index Currey	-
I_{cwb}	climatic water balance	mm
I_{dral}	drought index for allocation calculation (cumulative)	-
I_{drps}	drought index for photosynthesis calculation (cumulative)	-
I_{emb}	aridity index Emberger	-
I_{gor}	continentality index Gorczynski	-
I_{lang}	aridity index Lang	-

Variable	Definition	Dimension
I_{lf}	late frost index	-
I_{marta}	aridity index Martonne annual	-
I_{martvp}	aridity index Martonne vegetation period	-
I_N	fire danger rating index of Nesterov	-
I_{NMR}	nun moth risk index	-
I_N^{val}	cumulative sum of ignition index of Nesterov	-
$I_P(j)$	relative light intensity in the pool (LM3,4)	-
I_{PAR}	photosynthetically active radiation	mol m^{-2}
I_{phen}	depending on phenology model: inhibitor or chill days	-
I_{reich}	aridity index Reichel	-
I_{relcan}	relative light regime in the middle of the cohort's canopy	-
I_{shc}	hydrothermal coefficient Seljaninov	-
I_{weck}	aridity index Weck	-
I_{wiss}	aridity index Wissmann	-
k	light extinction coefficient	-
k_a	coefficients of the Campbell-equation (calculation of thermal conductivity)	-
k_{aom}	mineralization constant of humus	d^{-1}
k_b	coefficients of the Campbell-equation (calculation of thermal conductivity)	-
k_c	coefficients of the Campbell-equation (calculation of thermal conductivity)	-
k_{c0}	parameter of the height curve after Kuleschis, in erold1991	-

Variable	Definition	Dimension
k_{c1}	parameter of the height curve after Kuleschis, in erold1991	-
k_{c2}	parameter of the height curve after Kuleschis, in erold1991	-
k_d	coefficients of the Campbell-equation (calculation of thermal conductivity)	-
k_i	weighting factor of soil components i=air, ice, water, quartz, clay, silt, stone, humus; in case of the continuous medium air and water resp.	-
k_{pom}	species specific mineralization constant of litter *=fol (foliage), tb (twigs and branches), stem (stem wood), frt (fine roots), crt (coarse roots)	d ⁻¹
k_s	daily correction coefficient	-
K_s^i	coefficients of soil surface temperature calculation, i=0, 1, 2	-
k_{syn}	species specific synthesis coefficient of litter *=fol (foliage), tb (twigs and branches), stem (stem wood), frt (fine roots), crt (coarse roots)	d ⁻¹
k_{ua}	Parameter of the height curve after Kuleschis	-
k_{ub}	Parameter of the height curve after Kuleschis	-
k_{uc}	parameter of the height curve after Kuleschis	-
L	cumulated leaf area index at a given height down to layer j	-
L_1	liquidation value of the standing stock at the beginning of the simulation	€ ha ⁻¹
L_a	leaf area at given layer j over all cohort height	m ²
$l_{a,c}$	array of leaf area per layer j and cohort c	m ²
L_{AI}	leaf area index of the whole patch	m ² m ⁻²

Variable	Definition	Dimension
$l_c(j)$	side length of the cuboid of cohort c in layer j	m
L_{frost}	date (DOY) of the last late frost event after bud burst or start of the vegetation period	-
$L_{frosttot}$	date (DOY) of the last late frost event of the year	-
L_T	capping limit	cm
L_{tyear}	liquidation value of the standing stock at the end of the simulation	€ ha ⁻¹
L_{UE}	light use efficiency	g C μmol ⁻¹
M_{bio}	total stem biomass	Kg DW
$M_{f,c}$	foliage biomass per tree	kg DW
M_r^c	fine root biomass per tree	kg DW
M_r^{c*}	fine root biomass of a single tree per soil layer	kg DW
$M_{f,loss}$	lost fine root biomass due to root disturbance	kg DW
M_{hw}	heartwood biomass per tree	kg DW
$M_{r,loss}$	lost fine root biomass due to root disturbance	kg DW
M_s	sapwood biomass per tree	kg DW
M_{seed}	seed mass	g DW
M_{tbc}	twigs, branches, and coarse roots biomass	Kg DW
N_{aom}	total N content of humus in the soil profile at the end of the year	g N m ⁻²
n_c	actual number of cohort	-
n_a^c	number of alive trees per cohort, $c=1 - n_c$	-

Variable	Definition	Dimension
n_d^c	number of dead trees per cohort	-
n_s^c	number of saplings per cohort	-
N_{dem}^c	cumulative N demand per tree	g N d^{-1}
$N_{upt}^{c,d}$	daily N uptake per tree	$\text{g N m}^{-2} \text{d}^{-1}$
$N_{dem}^{c,d}$	daily N demand per tree	g N d^{-1}
N_{upt}^c	cumulative N uptake per tree and year	g N a^{-1}
n_{cl}	number of height classes	-
n_{dr}	number of days with rain > 0.1 mm	-
n_{dry}	number of days without precipitation	-
$N_{mov}^{NH_4}$	ammonium transport into next layer	g N m^{-2}
$N_{mov}^{NO_3}$	nitrate transport into next layer	g N m^{-2}
n_{hot}	number of hot days	-
n_{hrain}	number of days with heavy rain	-
n_{ice}	number of ice days	-
n_l	number of the highest layer in the stand	-
n_{mj}	number of days with precipitation May-July	-
n_{pl}	number of planted saplings	-
N_{PV}	net present value	€ ha^{-1}
N_{PV}^+	net present value with liquidation values	€ ha^{-1}
n_r	number of rooting layers	-
n_s	number of soil components	-

Variable	Definition	Dimension
N_{dem}^s	cumulative N demand per species and year	g N m^{-2}
n_{seed}^{max}	specific seed rate	$\text{m}^{-1} \text{a}^{-1}$
n_{seed}	annual potential seed rate	-
n_{snow}	number of days with snow	-
n_{summer}	number of summer days	-
N_{upt}^s	cumulative N uptake per species and year	g N m^{-2}
N_{upt}	yearly total N uptake	gN m^{-2}
n_{wof}	number of days without frost ($T_{min} > 0^\circ\text{C}$)	-
n_z	number of soil layers	-
ρ	Interest rate	-
ρ_1, ρ_4	scaling factor of phenology model PIM	-
ρ_{sat}^{13}	saturated vapour pressure at 13 h	-
P_2	inhibitor scaling factor of phenology model PIM	-
ρ_3	promotor scaling factor of phenology model PIM	-
P_a	patch area	m^2
ρ_{ab}	internal parameter for sapling growth	-
P_{act}	air pressure of actual day	hPa
P_{ann}	annual sum of precipitation	mm
P_d	precipitation of actual day	mm
ρ_h	height growth rate	cm kg^{-1}
ρ_{h1}	species-specific parameter for height-shoot biomass relation of seedlings	-

Variable	Definition	Dimension
ρ_{h2}	species-specific parameter for height-shoot biomass relation of seedlings	-
ρ_{h3}	species-specific parameter for height-shoot biomass relation of seedlings	-
ρ_{hv1}	height growth parameter 1 for nonlinear foliage height relationship	-
ρ_{hv2}	height growth parameter 2 for nonlinear foliage height relationship	-
ρ_{hv3}	height growth parameter 3 for nonlinear foliage height relationship	-
ρ_{int}	yearly intrinsic death rate	-
$\rho_{Mr,loss}$	percentage loss of foliage biomass	-
P_{mj}	sum of precipitation May-July	mm
P_{mon}	monthly precipitation sum	mm
ρ_{mort}	total mortality of a cohort	-
$\rho_{Mr,loss}$	percentage loss of fine root biomass	-
ρ_{NC}	N/C ratio of biomass	kg kg ⁻¹
ρ_{nun}	parameter of calculation of nun moth index	-
ρ_{pfeed}	percentage loss of carbon	-
P_{phen}	promotor of the phenology model PSM	-
ρ_{rg}	growth respiration per day	-
ρ_{sa}	species-specific parameter for shoot-foliage relationship of seedlings	-
P_{sat}	saturated vapour pressure of actual day	hPa

Variable	Definition	Dimension
ρ_{sb}	species-specific parameter for shoot-foliage relationship of seedlings	-
ρ_{srot}	Percentage loss of stems	-
ρ_{st}	shade tolerance class (1-5)	-
ρ_{stress}	stress induces mortality rate	-
P_{vap}	vapour pressure	hPa
ρ_{xcond}	Percentage loss of xylem conductivity	-
ρ_{wint}	yearly intrinsic species-specific death rate	-
Q_{10}^{min}	Q10 coefficient of van't Hoff's rule	-
Q_{10}^{nit}	Q10 coefficient of van't Hoff's rule	-
r_a	surface aerodynamic resistance for water vapour	$s\ m^{-1}$
$r_{fr}^c(z_i)$	relative part of fine root mass of tree per soil layer i	-
$r_{Mr}^c(z_i)$	relative part of fine root mass of cohort of total layer fine root mass per soil layer i	-
R_N^c	photosynthesis nitrogen reduction factor for each cohort	-
r_{co}	respiration coefficient - fraction of gross production respired by the plant	-
r_{cum}	cumulative root fraction of trees	-
R_{dc}	leaf respiration rate	$kg\ DW\ d^{-1}\ patch^{-1}$
R_{ds}	specific leaf respiration	$g\ C\ m^{-2}\ d^{-1}$
r_{fr}	root fraction per soil layer	-
R_g	global radiation of actual day	$J\ cm^{-2}\ d^{-1}$

Variable	Definition	Dimension
$r_{m,r}$	specific fine root maintenance respiration rate per day	$\text{kg kg}^{-1} \text{d}^{-1}$
$r_{m,sw}$	specific sapwood maintenance respiration rate per day	$\text{kg kg}^{-1} \text{d}^{-1}$
R_p^{min}	reduction of mineralization depending on pH-value	-
R_T^{min}	reduction of mineralization depending on soil temperature	-
R_W^{min}	reduction of mineralization depending on soil water content	-
R_n	net radiation	J cm^{-2}
R_{nets}	annual radiation sum	J cm^{-2}
R_T^{nit}	reduction of mineralization depending on soil temperature	-
R_W^{nit}	reduction of mineralization depending on soil water content	-
R_p^{nit}	reduction of nitrification depending on pH-value	-
r_c	canopy surface resistance	s m^{-1}
r_{sap}	describes the fraction of wood which is sapwood	-
R_N^S	tree specific photosynthesis nitrogen reduction factor	-
S_a	change in SLA for a 100% drop in relative quantum flux density = slope of SLA - quantum flux relationship	$\text{m}^2 \text{kg}^{-1} \text{DW}$
$S_{av,c}$	average specific one-side leaf area per cohort	$\text{m}^2 \text{kg}^{-1} \text{DW}$
S_{min}^c	minimum specific one-side leaf area (SLA of sun leaves)	$\text{m}^2 \text{kg}^{-1} \text{DW}$
S_f	specific foliage senescence rate per year	$\text{kg kg}^{-1} \text{a}^{-1}$
S_l	length of the stem segment	cm

Variable	Definition	Dimension
$S_{max,c}$	maximum specific one-side leaf area per cohort (SLA of shade leaves)	$m^2 kg^{-1} DW$
S_r	specific fine roots senescence rate per year	$kg kg^{-1} a^{-1}$
S_s	specific sapwood senescence rate per year	$kg kg^{-1} a^{-1}$
t	actual day of simulation	day
T_0	development zero point	$^{\circ}C$
T_a	average air temperature of actual day	$^{\circ}C$
T_{ann}	yearly mean temperature	$^{\circ}C$
T_b	base temperature CSM	$^{\circ}C$
T_b	base temperature TSM	$^{\circ}C$
T_c	chilling base temperature CSM	$^{\circ}C$
T_{cm}	average temperature of the coldest month	$^{\circ}C$
T_{crit}	required temperature sum for bud burst	$^{\circ}C$
T_{crit}	critical temperature sum TSM	$^{\circ}C$
T_{dew}	dew point temperature	$^{\circ}C$
T_{gdd}	annual growing degree day	$^{\circ}C$
$T_{gdd,0}$	threshold for growing degree day calculation	$^{\circ}C$
$T_{I,max}$	inhibitor maximum temperature of phenology model PIM)	$^{\circ}C$
$T_{I,min}$	inhibitor minimum temperature of phenology model PIM	$^{\circ}C$
$T_{I,opt}$	inhibitor optimum temperature of phenology model PIM	$^{\circ}C$
T_m	monthly mean temperature	$^{\circ}C$
T_{max}	maximum air temperature	$^{\circ}C$

Variable	Definition	Dimension
T_{min}	minimum air temperature	°C
T_{mj}	mean temperature May-July	°C
T_{mon}	monthly mean temperature	°C
t_{nyear}	number of simulation years	-
T_{opt}^{min}	optimal temperature for mineralisation	°C
T_{opt}^{nit}	optimal temperature for nitrification	°C
$T_{P,max}$	promotor maximum temperature of phenology model PIM	°C
$T_{P,min}$	promotor minimum temperature of phenology model PIM	°C
$T_{P,opt}$	promotor optimum temperature of phenology model PIM	°C
T_s	soil temperature per layer	°C
$T_{s,s}$	soil surface temperature	°C
T_{snow}	threshold of air temperature for snow fall	°C
T_{sum}^*	temperature sum for the phenology models CSM, TSM	°C
T_{sum}^a	annual temperature sum	°C
T_{tot}	thermal constant (nun moth risk index)	-
T_{wm}	average temperature of the warmest month	°C
t_y	actual simulation year	-
V_D	stem volume	m ³
$w(j)$	length of the effective shadow cast of canopy layer j	m
W_{av}^c	available soil water per tree cohort c and layer plant available water per layer	mm
W_{upt}^c	supply of soil water to roots of each cohort	mm d ⁻¹

Variable	Definition	Dimension
W_{ev}	water withdrawal by evaporation per layer	mm
w_f	height function according to Weimann	cm
W_{int}	daily interception	mm d ⁻¹
W_{int}^{max}	potential canopy interception storage	mm
W_{int}^{st}	actual canopy interception storage	mm
w_{k1}	height function parameter	-
w_{k2}	Height function parameter	-
W_p	percolation water per layer	mm
w_{ru}	water uptake resistance coefficient of each cohort per layer	-
W_s	water content per layer	mm
W_s^{FC}	field capacity of layer	mm
W_{sn}	snow equivalent	mm
W_{sn}^{pot}	potential water from melting of snow	mm
W_s^{sat}	pore volume of layer equals to saturated water content	mm
W_s^{WP}	wilting point of layer	mm
W_{upt}	cumulative total water uptake by roots	mm
X_{lat}	latitude	radian
y	length of the potential shadow cast	m
Y_s	stress recovery time	years
$Y_{s,i}$	survival age under stress for tolerance class i	year
z	depth of soil layer	cm

Variable	Definition	Dimension
z_{cr}	thickness of a crown layer	cm
z_i	of middle of layer i	cm

For abbreviations see Appendix Abbreviations

Appendix 2 List of model parameters

Variable abbreviatio n	Value	Dimension	Definition
α_m	1.4	-	Priestley-Taylor coefficient for calculation of transpiration demand
α_{refl}	0.2	-	albedo of the canopy
α_{wint}	0.1	-	mortality parameter of intrinsic mortality
$\alpha_{wstress}$	1.5	-	mortality parameter
η_R	0.023	-	factor of conversion from global radiation [J cm ²] to photosynthetically active radiation [mol m ²]
λ	0.7	-	optimum ratio of C_i to C_a
π	3.14159265 36	-	π
ψ	0.000662	hPa K ⁻¹	psychrometer constant
c_{air}	1.005	J g ⁻¹ K ⁻¹	specific heat of air at constant pressure
c_{mass}	12	g mol ⁻¹	molar mass of carbon
C_{part}	0.5	-	part of C in biomass
g_{max}	14000	mol m ⁻² d ⁻¹	maximum stomatal conductance of the canopy (Monteith, 1995)
g_{min}	0	mol m ⁻² d ⁻¹	minimum conductance

Variable abbreviatio n	Value	Dimension	Definition
H_{dbh}	137	cm	breast height for inventory measurements
P_{act}	100	kPa	atmospheric pressure
p_{crt}^{NSC}	0.125	-	fraction of coarse root DW allocated to NSC-Pool for deciduous tree species
p_{crt}^{NSC}	0.065	-	fraction of coarse root DW allocated to NSC-Pool for coniferous tree species
p_s^{NSC}	0.042	-	fraction of sapwood DW allocated to NSC-Pool for deciduous tree species
p_s^{NSC}	0.018	-	fraction of sapwood DW allocated to NSC-Pool for coniferous tree species
p_{tb}^{NSC}	0.125	-	fraction of twigs and branch DW allocated to NSC-Pool for deciduous tree species
p_{tb}^{NSC}	0.065	-	fraction of twigs and branch DW allocated to NSC-Pool for coniferous tree species
Q_{10}^{min}	2.9	-	Q10 coefficient of van't Hoff's rule for mineralisation
Q_{10}^{nit}	2.8	-	Q10 coefficient of van't Hoff's rule for nitrification
$T_{gdd,0}$	5	°C	threshold for growing degree day calculation
T_{snow}	0.2	°C	threshold of air temperature for snow accumulation

Appendix 3 List of Species Parameters

Variable code name	Dimension	Definition
nspecies		number of all species
nspec_tree		number of tree species
species_name		species name
max_age	years	maximum age
yrec	years	stress recovery time
stol	-	shade tolerance class (1-5)
pfext	-	light extinction coefficient
sigman*	kg N kg ⁻¹ DW a ⁻¹	root activity rate (N uptake) per year
respcoeff	-	respiration coeff. - fraction of gross production respired by the plant
prg*	d ⁻¹	growth respiration parameter
prms*		maintenance respiration parameters: sapwood
prmr		maintenance respiration parameters: fine roots
psf*		senescence parameters: foliage,
pss*		sapwood,
psr*		fine roots;
pcnr*	kg N/ kg C	N/C ratio of biomass
ncon_fol		N concentration of folmg / g TM nicht / g C!?!?
ncon_frt	mg/g	N concentration of fine roots
ncon_crt	mg/g	N concentration of coarse roots
ncon_tbc	mg/g	N concentration of twigs and branches
ncon_stem	mg/g	N concentration of stemwood
reallo_fol		reallocation parameter of foliage

Variable code name	Dimension	Definition
reallo_frt		reallocation parameter of fine root
alphac		ratio of coarse wood (twigs, branches, roots) to sapwood
cr_frac		fraction of tbc (twigs, branches, roots) that is coarse roots
prhos*	kg/m ³	sapwood density
pnus	kg/cm ²	foliage mass to sapwood area ratio
pha	cm/kg	height growth paramete
pha_coeff1		height growth parameter coefficient 1
pha_coeff2		height growth parameter coefficient 2
pha_v1		height growth parameter 1 for non linear foliage height relationship
pha_v2		height growth parameter 2 for non linear foliage height relationship
pha_v3		height growth parameter 3 for non linear foliage height relationship
crown_a	m/cm	parameter for crown radius - DBH relation
crown_b	m	parameter for crown radius - DBH relation
crown_c	m	parameter for crown radius - DBH relation
psla_min*	m ² /kg DW	specific one-sided leaf area
psla_a		
phic*	-	efficiency parameter, different for evergreen/deciduous
pnc		N content
kco2_25	Pa	Michaelis constant of temperature (base 25 °C)
ko2_25	kPa	inhibition constant of O ₂

Variable code name	Dimension	Definition
pc_25*		CO ₂ /O ₂ specificity value (base 25 °C)
q10_kco2		Q10 values (acclimated to 25 °C)
q10_ko2		
q10_pc*		
pb		Rd to Vm ratio
Pltmin		Inhibitor minimum temperature PIM
Pltopt		Inhibitor optimum temperature PIM
Pltmax		Inhibitor maximum temperature PIM
Pla		Inhibitor scaling factor PIM
PPtmin		Promotor minimum temperature PIM
PPtopt		Promotor optimum temperature PIM
PPtmax		Promotor maximum temperature PIM
PPa		Promotor scaling factor PIM
PPb		Promotor scaling factor PIM
CSTbC		chilling base temperature CSM
CSTbT		base temperature CSM
CSa		scaling factor CSM
CSb		scaling factor CSM
LTbT		base temperature TSM
LTcrit		critical temperature sum TSM
Lstart		start day after 1.11. TSM
Phmodel		use d pheno model 0: no model, 1: PIM, 2: CSM, 3: TSM
end_bb		leaf shedding / end of vegetation period
fpar_mod		modifying parameter in canopy_geometry

Variable code name	Dimension	Definition
ceppot_spec		interception capacity parameter
Nresp	-	slope of photosynthesis response to N-limitation
regflag		flag for regeneration
seedrate	1/m ²	max. seedling rate
seedmass	g	mass of a single seed
seedsd	g	standard deviation of seed mass
seeda		parameter of allometric relation shoot biomass - foliage bm
seedb		-----"-----
pheight1		parameter of allometric relation shoot biomass - height of seedling
pheight2		-----"-----
pheight3		
pdiam1		parameter of allometric relation shoot biomass - diameter at shoot basis
pdiam2		-----"-----
pdiam3		-----"-----
k_opm_fol		
k_syn_fol		
k_opm_stem		
k_syn_stem		
k_opm_tb		
k_syn_tb		
k_opm_frt		
k_syn_frt		
k_opm_crt		
k_syn_crt		

* marked parameters are sensitive

Species parameter

name	Fagus sylvatica	Picea abies	Pinus sylvestris	Quercus robur	Betula pendula	Pinus contorta	Pinus ponderosa	Populus tremula	Pinus halepensis	Pseudotsugamenziesii	Robinia pseudoacacia	Eucalyptus globulus	Eucalyptus grandis	Ground vegetation	Viscum alba
max_age	430	930	760	1060	220	600	850	160	250	930	200	50	50	5	30
yrec	3	3	3	3	3	3	3	3	3	3	3	3	3	3	3
stol	5	4	1	2	1	1	1	2	1	4	2	1	1	4	1
pfext	0.4	0.6	0.6	0.5	0.54	0.6	0.5	0.872	0.6	0.3	0.46	0.5	0.5	0.5	0.5
sigman	0.032	0.05	0.03	0.03	1.1	0.03	0.03	0.07508	0.03	0.025	0.17617 2	0.025	0.75	1	-99
respcoeff	0.5	0.52	0.52	0.5	0.5	0.71	0.44	0.5	0.52	0.5	0.5	0.53	0.53	0.5	0.5
prg	0.25	0.25	0.2	0.25	0.25	0.2	0.2	0.25	0.32	0.25	-99	0.25	0.25	0.25	0.25
prms	0.0035	0.00043	0.00024	0.0035	0.0035	0.00003 2	0.00024	0.0014	0.00024	-99	-99	0.3	0.3	0.0035	-99
prmr	0.0133	0.0033	0.007	0.01	0.01	0.00338	0.0007	0.0034	0.007	-99	0.1938	-99	-99	0.01	-99
psf	1	0.181	0.31	1	1	0.167	0.24	1	0.5	0.2	1	0.33	0.33	1	0.166

name	Fagus sylvatica	Picea abies	Pinus sylvestris	Quercus robur	Betula pendula	Pinus contorta	Pinus ponderosa	Populus tremula	Pinus halepensis	Pseudotsugamenziesii	Robinia pseudoacacia	Eucalyptus globulus	Eucalyptus grandis	Ground vegetation	Viscum alba
pss	0.026	0.022	0.04	0.05	0.02	0.023	0.05	0.04	0.04	0.05	0.25	0.03	0.03	0.4	-99
psr	0.65	0.5	0.5	0.5	0.5	0.4	0.8	0.5	1.095	0.75	0.67	1	1	0.75	-99
pcnr	0.008	0.0052	0.0079	0.008	0.02	0.0079	0.0212	0.008	0.0079	0.00955	0.0502	0.005	0.005	0.2	-99
ncon_fol	26.01	13.36	13.46	25	25	13.4	10.6	25	13.46	15.22	33.623	12	12	13.4	-99
ncon_frt	7.15	10.77	7.44	8.94	8.9	7.4	7.44	16	7.44	3.67	23.55	9.6	9.6	7.4	-99
ncon_crt	3.03	4.14	1.77	3.71	3.7	1.7	1.77	4	1.77	1.62	17.168	9.6	9.6	1.7	-99
ncon_tbc	4.27	5.24	3.61	6.19	5.4	3.6	3.61	6	3.61	3.62	17.16	3.8	3.8	3.6	-99
ncon_stem	1.54	1.22	1.09	2.1	1.7	1.1	1.09	0.6	1.09	1.035	15.345	1	1	1.1	-99
reallo_fol	0.1	0.1	0.1	0.1	0.1	0.1	0.1	0.6	0.1	0.1	0.1	0.5	0.5	0.1	0.1
reallo_frt	0.1	0.1	0.1	0.1	0.1	0.1	0.1	0.1	0.1	0.1	0.1	0.55	0.55	0.1	-99
alphac	0.48	0.5	0.46	0.56	0.5	0.24	0.46	0.46	0.5	0.54	0.51	0.22	0.22	0.5	-99
cr_frac	0.5	0.6	0.6	0.55	0.42	0.5	0.6	0.328	0.1	0.54	0.86	0.52	0.52	0.5	-99

name	Fagus sylvatica	Picea abies	Pinus sylvestris	Quercus robur	Betula pendula	Pinus contorta	Pinus ponderosa	Populus tremula	Pinus halepensis	Pseudotsugamenziesii	Robinia pseudo-acacia	Eucalyptus globulus	Eucalyptus grandis	Ground vegetation	Viscum alba
prhos	0.00065	0.00042	0.00040 3	0.00056	0.00053 7	0.00042	0.00043 4	0.00040 2	0.00062	0.00040 5	0.00078	0.0005	0.0005	-99	-99
pnus	0.03	0.096	0.05	0.02	0.025	0.046	0.022	0.02	0.043	0.093	0.05	0.04	0.06	0.03	-99
pha	125	40	190	100	150	190	190	150	190	40	-99	-99	-99	-99	-99
pha_coeff1	0.5	0.66666	0.66666	0.5	0.5	0.66666	0.66666	1.0823	0.66666	0.66666	-99	-99	-99	-99	-99
pha_coeff2	0.5	0.33333	0.33333	0.5	0.5	0.33333	0.33333	0.3189	0.33333	0.33333	-99	-99	-99	-99	-99
pha_v1	1089.3	284.8	206	946.7	900	1100	206	900	210	750	500	840	854	-99	-99
pha_v2	0.1351	-0.0151	0.03177	0.299	0.38	0.3	0.03177	0.08	0.08	-0.015	0.8541	-0.02973	-0.2	-99	-99
pha_v3	0.504	0.5039	0.877	0.948	0.9	0.4184	0.877	0.6	0.6	0.35	0.4404	0.29132 3	0.29277	-99	-99
crown_a	0.09571	0.06383	0.05213	0.095	0.0896	0.1437	0.05213	0.06	0.074	0.08128 7	0.0776	0.1249	0.1249	-99	-99
crown_b	0.57732	0.33567	0.48139	0.5	0.5716	0.1081	0.48139	0.4	0.255	0.35548 5	0.7368	0.7879	0.7879	-99	-99

name	Fagus sylvatica	Picea abies	Pinus sylvestris	Quercus robur	Betula pendula	Pinus contorta	Pinus ponderosa	Populus tremula	Pinus halepensis	Pseudotsugamenziesii	Robinia pseudo-acacia	Eucalyptus globulus	Eucalyptus grandis	Ground vegetation	Viscum alba
crown_c	15	12	10	15	6	10	10	6	10	5	4	5.9	5.9	-99	-99
psla_min	12	3.78	4	14	10	7.5	3.1	7.2	4.84	2.82	13.2	15	0.18	20	4.18
psla_a	12	2.4	1	4.7	20	1.2	1	4.4	1	4.87	19.5	13.52	13.52	20	4.18
phic	1	0.8	0.9	1	1	0.9	0.9	1	0.9	0.8	1	1	1	1	0.8
pnc	20	20	20	20	17.9	50	20	24	20	45	33.623	-99	-99	10	-99
kco2_25	30	30	30	30	30	30	30	30	40.4	30	30	30	30	30	30
ko2_25	30	30	60	30	30	60	60	60	24.8	30	30	30	30	30	30
pc_25	3400	2600	3400	3400	3400	3400	3400	3400	3400	2600	3400	3400	3400	3400	3400
Q10_kco2	2.1	2.1	2.1	2.1	2.1	2.1	2.1	2.1	2.1	2.1	2.1	2.1	2.1	2.1	2.1
Q10_ko2	1.2	1.2	1.2	1.2	1.2	1.2	1.2	1.2	1.2	1.2	1.2	1.2	1.2	1.2	1.2
Q10_pc	0.57	0.57	0.57	0.57	0.57	0.57	0.57	0.57	0.57	0.57	0.57	0.57	0.57	0.57	0.57
pb	0.01	0.015	0.01	0.01	0.035	0.01	0.01	0.0143	0.0241	0.015	0.01	0.035	0.035	0.01	0.015

name	Fagus sylvatica	Picea abies	Pinus sylvestris	Quercus robur	Betula pendula	Pinus contorta	Pinus ponderosa	Populus tremula	Pinus halepensis	Pseudotsugamenziesii	Robinia pseudo-acacia	Eucalyptus globulus	Eucalyptus grandis	Ground vegetation	Viscum alba
Pltmin	-10.34	-99	-99	-23.05	-24.96	-99	-99	-10.34	-99	-99	-99	-99	-99	-99	-99
Pltopt	-0.89	-99	-99	-0.3	-10	-99	-99	-0.89	-99	-99	-99	-99	-99	-99	-99
Pltmax	18.11	-99	-99	16.91	15.05	-99	-99	18.11	-99	-99	-99	-99	-99	-99	-99
Pla	0.058326	-99	-99	0.055149	0.030619	-99	-99	0.058326	-99	-99	-99	-99	-99	-99	-99
PPtmin	-10.03	-99	-99	3.46	-7.03	-99	-99	-10.03	-99	-99	-99	-99	-99	-99	-99
PPtopt	28.61	-99	-99	34.55	21.8	-99	-99	28.61	-99	-99	-99	-99	-99	-99	-99
PPtmax	44.49	-99	-99	34.55	25.35	-99	-99	44.49	-99	-99	-99	-99	-99	-99	-99
PPa	0.109494	-99	-99	0.331253	0.064803	-99	-99	0.109494	-99	-99	-99	-99	-99	-99	-99
PPb	0.039178	-99	-99	0.010379	0.045432	-99	-99	0.039178	-99	-99	-99	-99	-99	-99	-99
CSTbC	11.03	-99	-99	18.31	18.42	-99	-99	11.03	-99	-99	-99	-99	-99	-99	-99
CSTbT	6.5	-99	-99	5.58	4.19	-99	-99	6.5	-99	-99	-99	-99	-99	-99	-99

name	Fagus sylvatica	Picea abies	Pinus sylvestris	Quercus robur	Betula pendula	Pinus contorta	Pinus ponderosa	Populus tremula	Pinus halepensis	Pseudotsugamenziesii	Robinia pseudo-acacia	Eucalyptus globulus	Eucalyptus grandis	Ground vegetation	Viscum alba
CSa	3039.76	-99	-99	3451.18	3075.99	-99	-99	3039.76	-99	-99	-99	-99	-99	-99	-99
CSb	-574.49	-99	-99	-631.5	-573.67	-99	-99	-574.49	-99	-99	-99	-99	-99	-99	-99
LTbT	-6.98	-99	-99	0.49	-6.07	-99	-99	-6.98	-99	-99	11.5	-99	-99	-99	-99
LTcrit	664.88	-99	-99	372.49	672.9	-99	-99	664.88	-99	-99	350.9	-99	-99	-99	-99
Lstart	70	-99	-99	70	47	-99	-99	70	-99	-99	70	-99	-99	-99	-99
Phmodel	1	0	0	1	1	0	0	1	0	0	3	-99	-99	0	0
end_bb	282	366	366	287	278	366	366	282	366	366	282	366	366	302	366
fpar_mod	0	0	0	0	0	0	0	0	0	0	0	0	0	0	0
ceppot_spe	0.6	0.8	0.9	0.5	0.5	0.4	0.4	0.3	0.9	0.8	0.5	0.3	0.3	0.5	0.6
Nresp	0.0068	0.0068	0.0062	0.0068	0.0068	0.0062	0.0062	0.0068	0.0062	0.0068	0.0068	0.0068	0.0068	0.006	0.0068
regflag	1	0	0	0	0	0	0	0	0	0	0	0	0	0	0
seedrate	1	1	1	1	1	1	1	1	1.5	1	1	1	1	-99	-99

name	Fagus sylvatica	Picea abies	Pinus sylvestris	Quercus robur	Betula pendula	Pinus contorta	Pinus ponderosa	Populus tremula	Pinus halepensis	Pseudotsugamenziesii	Robinia pseudo-acacia	Eucalyptus globulus	Eucalyptus grandis	Ground vegetation	Viscum alba
seedmass	0.225	0.009	0.006	3.8	0.0002	0.005	0.0055	0.00016	0.019	0.01	0.0228	-99	-99	-99	-99
seedsd	0	0	0.001127	0	0	0.001127	0.001127	0	0.001127	0	0	-99	-99	-99	-99
seeda	0.398	0.8524	0.3927	0.2505	0.313	0.2609	0.3927	0.381	0.5044	1.3217	0.778	-99	-99	-99	-99
seedb	0.947	1.007	0.6786	0.7232	0.8	0.757	0.6786	0.8365	0.6486	1.1288	0.9645	-99	-99	-99	-99
pheight1	2.388	0.443	2.512	1.6947	4.651	1.5	2.512	0.2829	1.3145	5.7278	0.118272	-99	-99	-99	-99
pheight2	0.366	0.23	0.357	0.3896	0.3333	0.7236	0.357	0.57	0.3426	0.2443	0.757755	-99	-99	-99	-99
pheight3	0	0.0134	0	0	0	-99	0	-99	0	-99	-99	-99	-99	-99	-99
pdiam1	-1.637	-1.658	0	0	0	-99	0	-99	0	-99	-99	-99	-99	0.35	-99
pdiam2	0.433	0.386	0	0	0	-99	0	-99	0	-99	-99	-99	-99	0.35	-99
pdiam3	-0.0126	0	0	0	0	-99	0	-99	0	-99	-99	-99	-99	0.3	-99
k_opm_fol	0.02	0.06	0.05	0.015	0.01	0.005	0.015	0.04	0.002	0.08	0.3	0.5	0.5	0.03	0.01

name	Fagus sylvatica	Picea abies	Pinus sylvestris	Quercus robur	Betula pendula	Pinus contorta	Pinus ponderosa	Populus tremula	Pinus halepensis	Pseudotsugamenziesii	Robinia pseudo-acacia	Eucalyptus globulus	Eucalyptus grandis	Ground vegetation	Viscum alba
k_syn_fol	0.3	0.2	0.1	0.4	0.78	0.6	0.8	0.4	0.5	0.2	0.2	0.01	0.01	0.2	0.5
k_opm_frt	0.02	0.05	0.05	0.01	0.00106	0.001	0.009	0.03	0.0004	0.05	0.008	0.001	0.001	0.001	-99
k_syn_frt	0.4	0.1	0.1	0.3	0.3	0.3	0.3	0.4	0.5	0.3	0.3	0.01	0.01	0.3	-99
k_opm_crt	0.0009	0.0009	0.0009	0.0009	0.0009	0.0009	0.0009	0.0009	0.0009	0.0009	0.0009	0.0009	0.0009	0	-99
k_syn_crt	0.1	0.1	0	0.1	0.1	0.1	0	0.1	0	0.1	0.1	0.1	0.1	0.1	-99
k_opm_tb	0.006	0.006	0.006	0.006	0.0009	0.0009	0.0009	0.0009	0.006	0.006	0.0009	0.0009	0.0009	0	-99
k_syn_tb	0.5	0.8	0.5	0.5	0.8	0.5	0.5	0.5	0.5	0.8	0.8	0.8	0.8	0	-99
k_opm_stem	0.0025	0.0005	0.0005	0.0005	0.0005	0.0001	0.00055	0.0001	0.0005	0.0005	0.0005	0.0005	0.0005	0	-99
k_syn_stem	0.1	0.1	0	0.1	0.1	0.1	0	0.1	0	0.1	0.1	0.1	0.1	0	-99
spec_rl	30	15	15	30	30	15	15	30	15	15	30	30	30	60	-99
tbase	5	5	5	5	5	5	5	5	5	5	5	5	5	5	-99
topt	19.4	16.5	16.5	22	16.5	16.5	16.5	16.5	16.5	16.5	16.5	16.5	16.5	16.5	-99

name	Fagus sylvatica	Picea abies	Pinus sylvestris	Quercus robur	Betula pendula	Pinus contorta	Pinus ponderosa	Populus tremula	Pinus halepensis	Pseudotsugamenziesii	Robinia pseudo-acacia	Eucalyptus globulus	Eucalyptus grandis	Ground vegetation	Viscum alba
bdmax_coef	1.55	1.62	1.62	1.55	1.55	1.62	1.62	1.55	1.62	1.62	1.55	1.55	1.55	1.62	-99
porcrit_co	0.4	0.7	0.7	0.4	0.4	0.7	0.7	0.4	0.7	0.7	0.4	0.4	0.4	0.7	-99
ph_opt_max	8.25	5.75	5.75	8.25	8.25	5.75	5.75	8.25	5.75	5.75	8.25	8.25	8.25	8.25	-99
ph_opt_min	4.25	3.75	3.75	4.25	3.75	3.75	3.75	4.25	3.75	3.75	3.75	3.75	3.75	3.5	-99
ph_max	9.25	7.75	7.75	9.25	9.25	7.75	7.75	9.25	7.75	7.75	9.25	9.25	9.25	9.25	-99
ph_min	3.75	2.25	2.25	3.75	2.25	2.25	2.25	3.75	2.25	2.25	2.25	2.25	2.25	2	-99
v_growth	1	1	1	1	1	1	1	1	1	1	1	1	1	5	-99



Appendix 4 Classification of the forest type

The following classification is used in 4C to describe very shortly the simulated forest type

Table 17

Type number	Type description German	Type description English	percentage
10	Fi-Reinbestand	Spruce	
20	Fi-Lh-Mischbestand	Mixed Spruce-Broadleaf	Fi>20%
25	Fi-Nh-Mischbestand	Mixed Spruce-Conifer	Fi>50%
40	Ki-Reinbestand	Pine	
50	Ki-Lh-Mischbestand	Mixed Pine-Broadleaf	Ki>50%
52	Ki-Ei-Mischbestand	Mixed Pine-Oak	Ki>50%
55	Ki-Nh-Mischbestand	Mixed Pine-Conifer	Ki>50%
70	Ta-Bestand	Fir	
75	Ta-Mischbestand	Mixed Fir	
90	sonst. Nh-Bestand	Conifer	
100	Nh-Mischbestand	Mixed Conifer	
110	Bu-Reinbestand	Beech	
120	Bu-Lh-Mischbestand	Mixed Beech-Broadleaf	Bu>50%
122	Bu-Ei-Mischbestand	Mixed Beech-Oak	Bu>50%
125	Bu-Nh-Mischbestand	Mixed Beech-Conifer	Bu>50%
140	Ei-Reinbestand	Oak	
150	Ei-Lh-Mischbestand	Mixed Oak-Broadleaf	Ei>50%
151	Ei-Bu-Mischbestand	Mixed Oak-Beech	Ei>50%
154	Ei-Alh-Mischbestand	Mixed Oak-Other Broadleaf	Ei>50%
155	Ei-Nh-Mischbestand	Mixed Oak-Conifer	Ei>50%
157	Ei-Ki-Mischbestand	Mixed Oak-Pine	Ei>50%
180	Aln-Bestand	Other Broadleaf, lower age	
185	Aln-Mischwald	Mixed other Broadleaf, lower	

		age	
190	Alh-Bestand	Other Broadleaf, higher age	
191	Hartlaub-Auenwald (Ulme-Esche)	Alluvial forest (elm/ ash)	
195	Alh Mischwald	Mixed other Broadleaf, higher age	
200	Lh Mischwald	Mixed Broadleaf	
250	sonst. Mischwald	Mixed Wood	

Alh - Andere Laubhölzer mit hoher Umtriebszeit (z.B. Ahorn, Linde, Esche)/ Other Broadleaf (long-living)

Aln - Andere Laubhölzer mit niedriger Umtriebszeit (z.B. Weide, Aspe, Birke)/ Other Broadleaf

Nh – Nadelholz/ Conifer

Lh – Laubholz/ Broadleaf

Bu – Buche/ beech

Ei – Eiche/ oak

Fi – Fichte/ spruce

Ki – Kiefer/ pine

Ta – Tanne/ fir

Appendix 5 Abbreviations

aom	Active organic matter
BB	Bud burst
C	Carbon
CSM	Cannel and Smith model
DM	Dry mass
DOY	Day of the year
DW	Dry weight
LAI	Leaf area index
LM1	Light model 1
LM2	Light model 2
LM3	Light model 3
LM4	Light model 4
N	Nitrogen
NPP	Net primary production
NSC	Non-structural carbohydrates
PA	Crown projection area
PIM	Promotor-Inhibitor-Model
pom	Primary organic matter
RCP	Representative concentration pathways
SEA	Socio-economic analysis
SLA	Specific leaf area
SRES	Special report on emission scenarios
SSR	Sum of squared residuals
TSM	Temperature sum model
WPM	Wood product model